

Supporting Information

Catalytic Sulfone Upgrading Reaction with Alcohols via Ru(II)

Tomas Vojkovsky,^a Shubham Deolka,^a Saiyyna Stepanova,^a Michael C. Roy^a and Eugene Khaskin^{a}*

a) Okinawa Institute of Science and Technology Graduate University, 1919-1 Tancha, Onna-son, Kunigami-gun, Okinawa, Japan 904-0412
eugenekhaskin@oist.jp

Index

S.N.

1	General Specifications	S2
2	Experimental	S2-S3
3	Substrate Optimization Tables	S4-S9
4	All isolated substrates NMR/HRMS	S10-S56
5	Mechanistic Experiments and Discussion	S58-S63
6	Substrates that were tested but worked poorly	S64-S65
7	References	S66

General Specifications: Reagents and Instrumentation

All solvents and reagents for the reactions were weighed out and dispensed in an inert atmosphere, nitrogen MBraun Unilab pro glovebox unless otherwise stated. Anhydrous toluene was purchased from Kanto Chemical Company with no extra drying or redistilling techniques. Benzyl Phenyl Sulfone and MACHO catalysts were purchased from TCI Chemicals, KHMDS and Ru-SNS (Aldrich No. **746339**) were purchased from Sigma Aldrich. All alcohols and sulfones were purchased from TCI Chemicals, Sigma Aldrich, Alfa Aesar or Oakwood Chemicals with no extra drying or redistilling except for n-butanol and n-hexanol which were distilled. NMR spectra were collected on a JEOL ECZ 600R and JEOL ECZ 400S spectrometer unless otherwise noted. ^1H and ^{13}C chemical shifts are reported referenced to CDCl_3 or CD_3CN peaks. All NMR analysis was performed with MestReNova. GC/MS data was collected on a Shimadzu QP2010-Ultra equipped with an SH-Rxi-1ms 60 meter column with mesitylene standard added after reaction completion. HRMS were obtained on a Thermo LTQ OrbitrapXL with a nanospray interface. Most compounds had both an $[\text{M}]^+$ and $[\text{M}+\text{Na}]^+$ detected. The isolated yield and purity of the products was determined by NMR, after column chromatography. During optimization, yields were calculated from GC/FID results using a GC2014 Shimadzu system equipped with a SH-Rxi-1ms 60meter column, with mesitylene internal standard added after reaction completion.

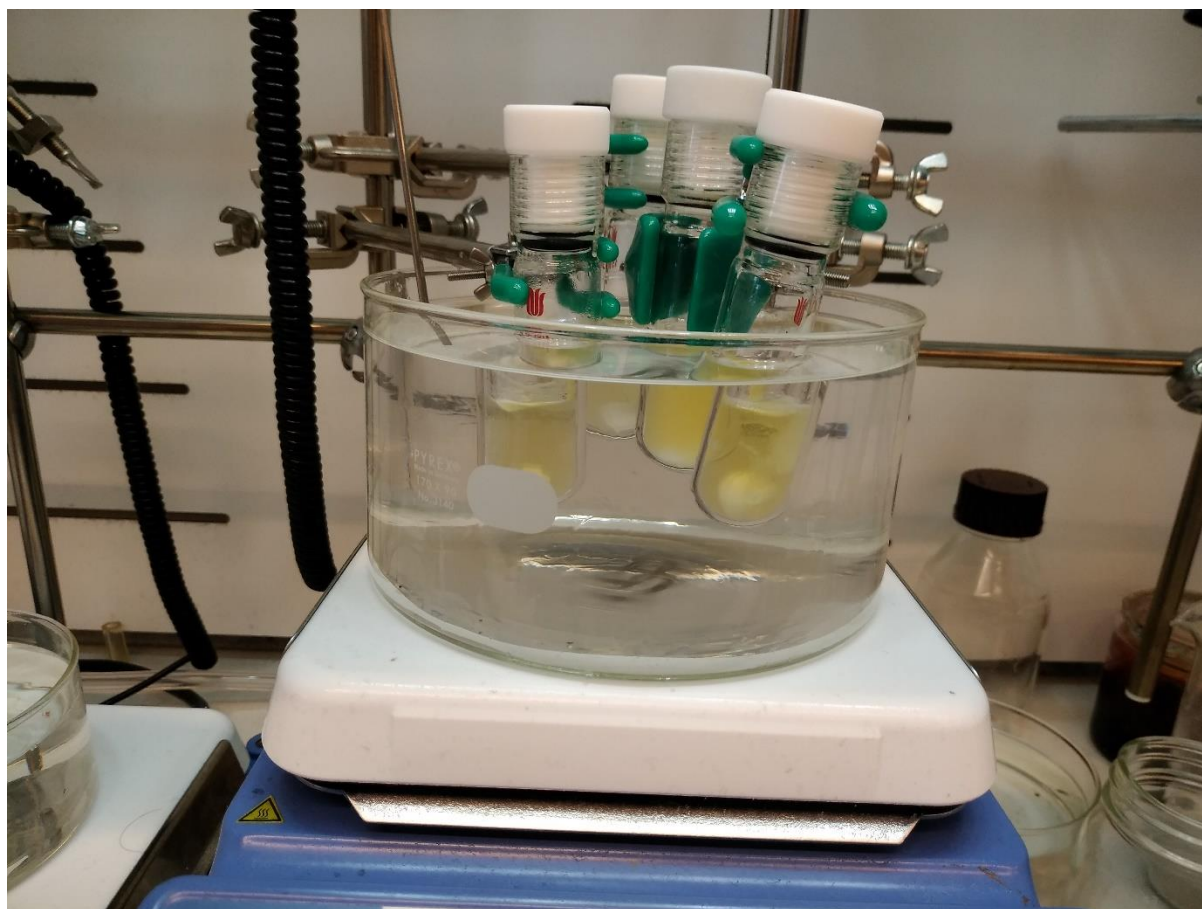
Experimental

Synthesis of linear sulfones; optimized catalytic reaction.

General procedure for closed system (synthesis of pentyl phenyl sulfone used as an amounts example). To an oven dried 15 ml. pressure tube (20 ml. internal volume) under N_2 , typically in the glove box, were added 0.60 mmol of starting sulfone (phenyl methyl sulfone 94 mg.), a 1.1x equivalent of alcohol, 0.66 mol (n-butanol, 60 μl .), 0.45 mmol KHMDS (90 mg.), and 2 mol% or 0.012 mmol (7.0 mg.) of Ru- MACHO-BH catalyst. To the flask, 10 ml. of toluene were added, the flask was tightly closed and placed into an oil bath heated at 90°C for all but the benzylic alcohols, which were reacted at 60°C . The mixture was stirred for 24h. after which time it was filtered through a silica plug with the reaction flask and the silica washed with ~ 100 ml. of EtOAc. The washings and the reaction were added together and concentrated, and then separated by column chromatography. In the case of substrates with amine groups, the silica plug was washed with an aqueous ammonia / methanol / chloroform 1/9/90 mixture and the combined washings were dried under high vacuum before column separation. Typical solvent mixtures for column separation included an increasing polarity gradient of hexane/EtOAc or chloroform/methanol/aqueous ammonia 1/9/90 depending on whether the product contained an amine. The benzylic alcohol substrates were run at 60°C with the other conditions unchanged (See Table S6).

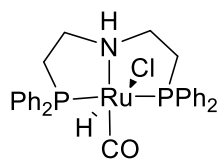
Optimization of the procedure as in tables S1-S6 was carried out in 15mL. long screwcap vials with a PTFE lining. Amount of alcohol to sulfone was 1:1. All the components according to the entry in the table were loaded into the vial under N_2 atmosphere and the vial caps were further wrapped with electric tape. At the conclusion of the reaction 1 equivalent of mesitylene internal standard was added and an aliquot was taken for GC/MS and GC/FID analysis. Amounts for low catalyst loading reactions in Table S5 differ and are noted in the legend of the Table; KO^tBu was used as base for all low catalyst loading reactions.

Figure S1. Typical experimental setup with 15ml (pressure tubes. The pressure tubes were loaded under nitrogen with all the reactants and the solvent. The reactions were heated in an oil bath for the required period of time. Depending on the sulfone, the solution can be heterogenous at the beginning, sometimes becoming more homogenous at the end of the reaction.

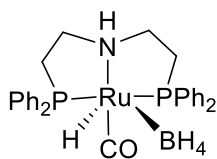


Full Substrate Optimization Tables:

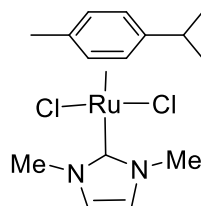
Table S1. Optimization for catalyst



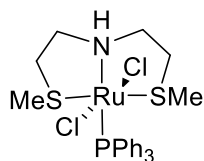
MACHO-Cl



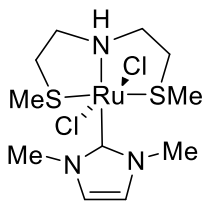
MACHO-BH₄



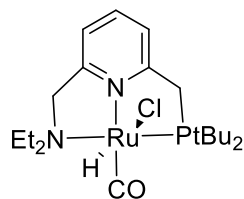
RuCl₂(p-cymene)-NHC



Me-Gusev



Me-Gusev-NHC



Milstein PNN

Entry/ Catalyst	Yield %
1 / MACHO-Cl	90
2 / MACHO-BH ₄	83
3 / Me-Gusev	18
4 / Me-Gusev-NHC	2
5 / Milstein PNN	12
6 / RuCl ₂ (p-cymene)NHC	8
Yield was determined by GC/FID for the linear product only. The selectivity for the MACHO-BH ₄ complex over MACHO-Cl appeared slightly better.	

Table S2. Optimization for linear product based on the amount of base.

<p>1 mol% RuMACHO-BH₄ base KHMDs 0.7-1.2eq. toluene, 90°C concentration 0.125M 24h.</p> <p>linear cyclopropane double addition</p>					
Entry	KHMDs (mol %)	Yield linear %	Yield cyclopropane %	Yield double addition %	Ratio linear/cyclopropane
1	120	73	4.2	0	17
2	110	74	2.6	0.5	28
3	100	87	1.9	1.5	46
4	90	85	2.0	1.1	42
5	80	90	1.6	3.9	55
6	70	91	1.5	5.0	60
7	60	89	1.3	5.8	66
8	50	82	0.9	4.4	96
9	80	88	1.7	2.7	51
10	80	90	1.5	3.8	61
11	70	91	1.5	4.3	60
12	70	88	1.5	4.7	60
<p>Double addition product was not included in the ratio analysis as it's possible to easily separate it chromatographically. However, yields above ~5% are undesirable. Yield determined by GC/FID all products calibrated.</p>					

Table S3. Optimization for linear product based on the amount of catalyst

<p>0.5-3.0 mol% RuMACHO-BH₄ or Cl base KHMDS 0.75eq.. toluene, 90°C, 24h. concentration 0.125M</p> <p>linear cyclopropane double addition</p>						
Entry	Catalyst MACHO XX	Catalyst mol%	Yield linear %	Yield cycloprop ane %	Yield double addition %	Ratio linear/cyclopropane
1	BH ₄	0.5	88	1.5	4.7	60
2	BH ₄	1	89	1.5	3.9	61
3	BH ₄	2	89	0.9	4.5	97
4	BH ₄	3	90	0.9	4.3	99
5	Cl	1	90	1.1	4.6	82
6	Cl	2	89	1.1	4.5	81
7	Cl	3	88	0.9	4.9	103
Double addition product was not included in the ratio analysis as it's possible to easily separate it chromatographically. Yield determined by GC/FID all products calibrated.						

Table S4. Optimization for linear product based on the amount of catalyst

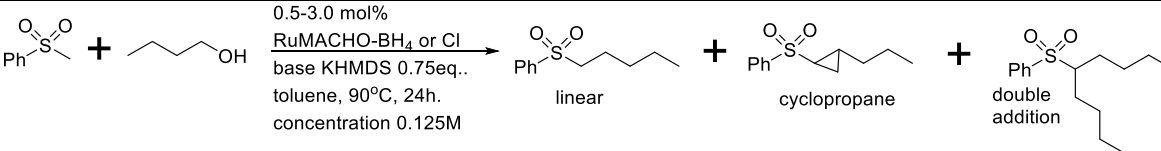
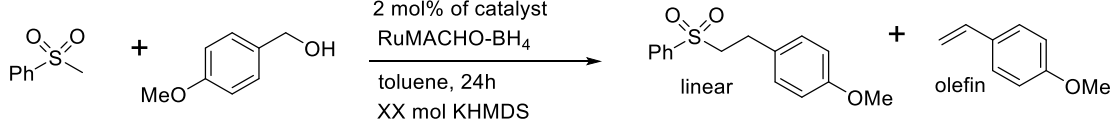
							
Entry	Concentration (M)	Catalyst MACHO XX	Catalyst mol%	Yield linear %	Yield cyclopropane %	Yield double addition %	Ratio linear/cyclopropane
1	0.200	BH ₄	1	83	2.2	5.4	38
2	0.150	BH ₄	1	84	1.7	4.8	50
3	0.125	BH ₄	1	85	1.5	4.2	58
4	0.100	BH ₄	1	85	1.2	3.7	73
5	0.075	BH ₄	1	84	0.9	3.3	95
6	0.050	BH ₄	1	78	0.5	3.0	150
7	0.100	BH ₄	2	88	0.9	3.3	103
8	0.075	BH ₄	2	86	0.7	2.9	125
9	0.060	BH ₄	2	86	0.5	2.8	165
10	0.050	BH ₄	2	85	0.4	2.5	202
11	0.100	Cl	2	88	0.9	3.6	95
12	0.075	Cl	2	85	0.7	3.4	127
13	0.060	Cl	2	85	0.6	2.9	149
14	0.050	Cl	2	85	0.4	2.6	195
Double addition product was not included in the ratio analysis as it's possible to easily separate it chromatographically. Yield determined by GC/FID all products calibrated.							

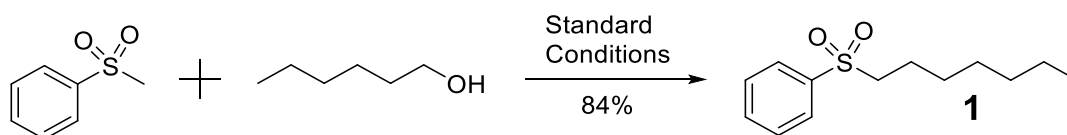
Table S5. Optimization for phenyl pentyl sulfone at low catalyst loading

<p>0.01-0.05 mol% MACHO-BH₄ base KO^tBu toluene, 95°C</p> <p>linear cyclopropane double addition</p>						
Entry	Base mol% (KO ^t Bu)	Catalyst mol%	Yield linear %	Reaction time h.	Concentration (M)	Ratio linear/cyclopropane
1	90	0.01	30	72	1.2	18
2	100	0.01	35	72	1.2	24
3	110	0.01	38	72	1.2	9
4	120	0.01	39	72	1.2	8
5	100	0.05*	76	48	1.3	147
<p>Double addition product was obtained only in trace amounts (<0.1mol% at best) at low catalyst loadings. Yield determined by GC/FID all products calibrated. 781mg of PhSO₂Me (5mmol), 1.45mL (16mmol) of nBuOH, 0.9ml. of toluene, 0.15ml. of mesitylene internal standard; 0.3-1.5 mg catalyst in 15ml. pressure tube. * 0.05mol% catalyst loading reaction done at 90°C.</p>						

Table S6. Optimization for linear product for para-methoxybenzyl alcohol

					
Entry	Concentration (M)	Temperature °C	KHMDS mol%	FID relative peak ratio to standard linear	FID relative peak ratio to standard olefin
1	0.100	90	80	1.356	0.239
2	0.100	80	80	1.374	0.280
3	0.100	70	80	1.457	0.239
4	0.100	60	80	1.470	0.189
5	0.100	60	75	1.502	0.158
6	0.075	60	75	1.542	0.137
7	0.060	60	75	1.586	0.136
8	0.100	60	70	1.483	0.133
9	0.100	60	60	1.450	0.080
10	0.100	50	80	1.398	0.154
<p>Peaks values on the FID are observed only and are uncalibrated. Optimum conditions obtained in run 7 were used for all benzylic substrates and isolated yield was ultimately determined for compounds 29 and 30. No cyclopropane was detected.</p>					

Sulfones obtained with isolated yields and NMR characterization.



Physical State: Colorless oil; solidified to white crystalline solid. Isolated Yield: 84%

^1H NMR (400 MHz, Acetonitrile- d_3) δ 7.91 – 7.85 (m, 2H), 7.75 – 7.69 (m, 1H), 7.65 – 7.59 (m, 2H), 3.18 – 3.06 (m, 2H), 1.66 – 1.54 (m, 2H), 1.42 – 1.10 (m, 8H), 0.85 (t, J = 7.0 Hz, 3H). ^{13}C NMR (101 MHz, Acetonitrile- d_3) δ 140.41, 134.66, 130.32, 128.84, 56.30, 32.14, 29.27, 28.67, 23.45, 23.18, 14.27. HRMS: $[\text{C}_{13}\text{H}_{21}\text{O}_2\text{S}]^+$ Expected 241.1262; Obtained 241.1266.

Figure S2. ^1H NMR of **1**.

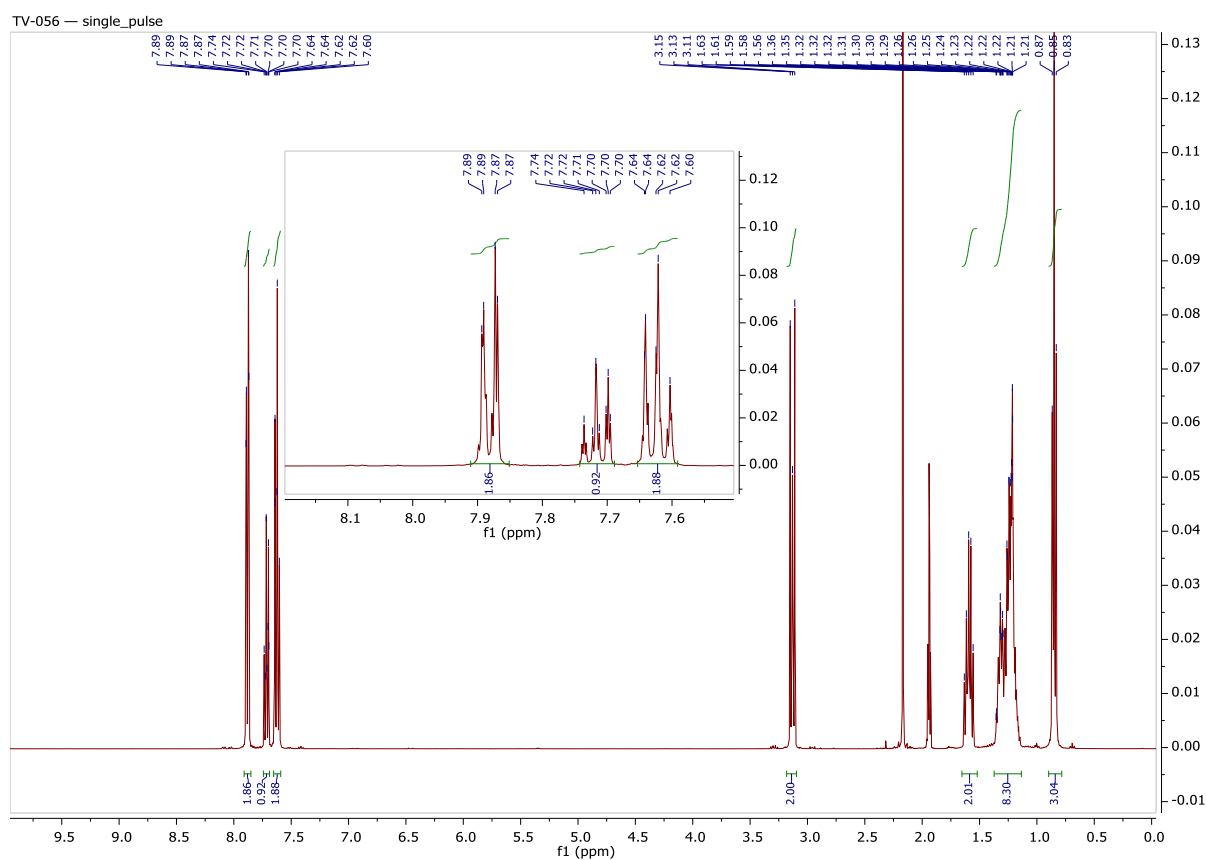
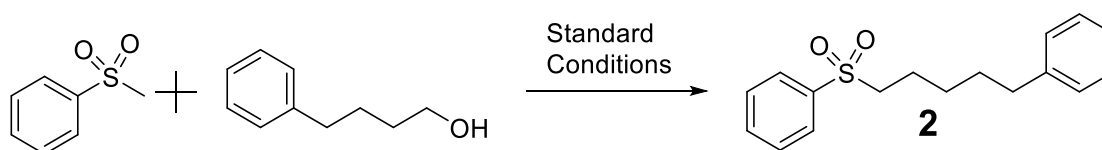
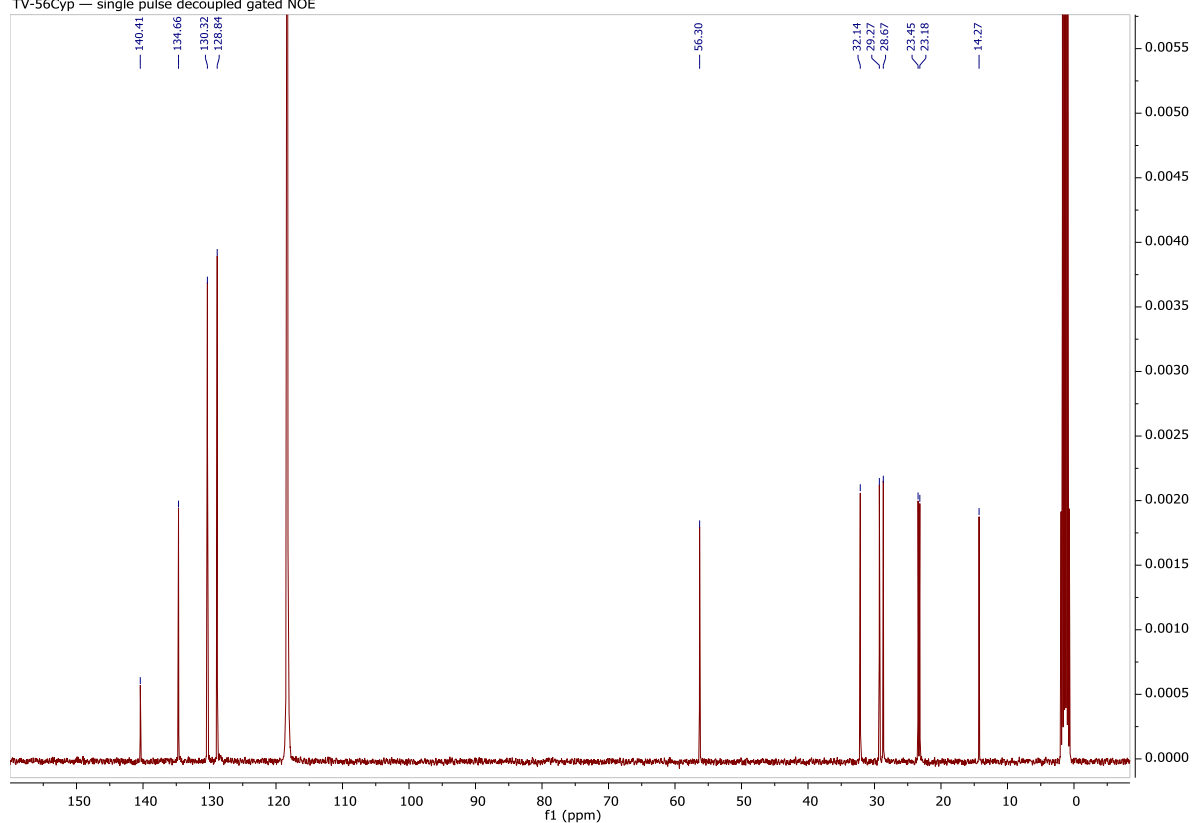


Figure S3. ^{13}C NMR of **1**.

TV-56Cyp — single pulse decoupled gated NOE



Physical State: Colorless oil. Isolated Yield: 89%

^1H NMR (400 MHz, Acetonitrile- d_3) δ 7.89 – 7.81 (m, 2H), 7.69 (t, J = 7.4 Hz, 1H), 7.59 (t, J = 7.5 Hz, 2H), 7.48–7.25 (m, 2H), 7.08–7.15 (m, 3H), 3.17 – 3.04 (m, 2H), 2.55 – 2.47 (m, 2H), 1.65 – 1.56 (m, 2H), 1.57 – 1.47 (m, 2H), 1.37 – 1.27 (m, 2H). ^{13}C NMR (101 MHz, Acetonitrile- d_3) δ 143.43, 140.39, 134.67, 130.33, 129.30, 129.24, 128.84, 126.64, 56.22, 35.98, 31.52, 28.37, 23.32. HRMS: $[\text{C}_{17}\text{H}_{21}\text{O}_2\text{S}]^+$ Expected 289.1262; Obtained 289.1257.

Figure S4. ^1H NMR of **2**.

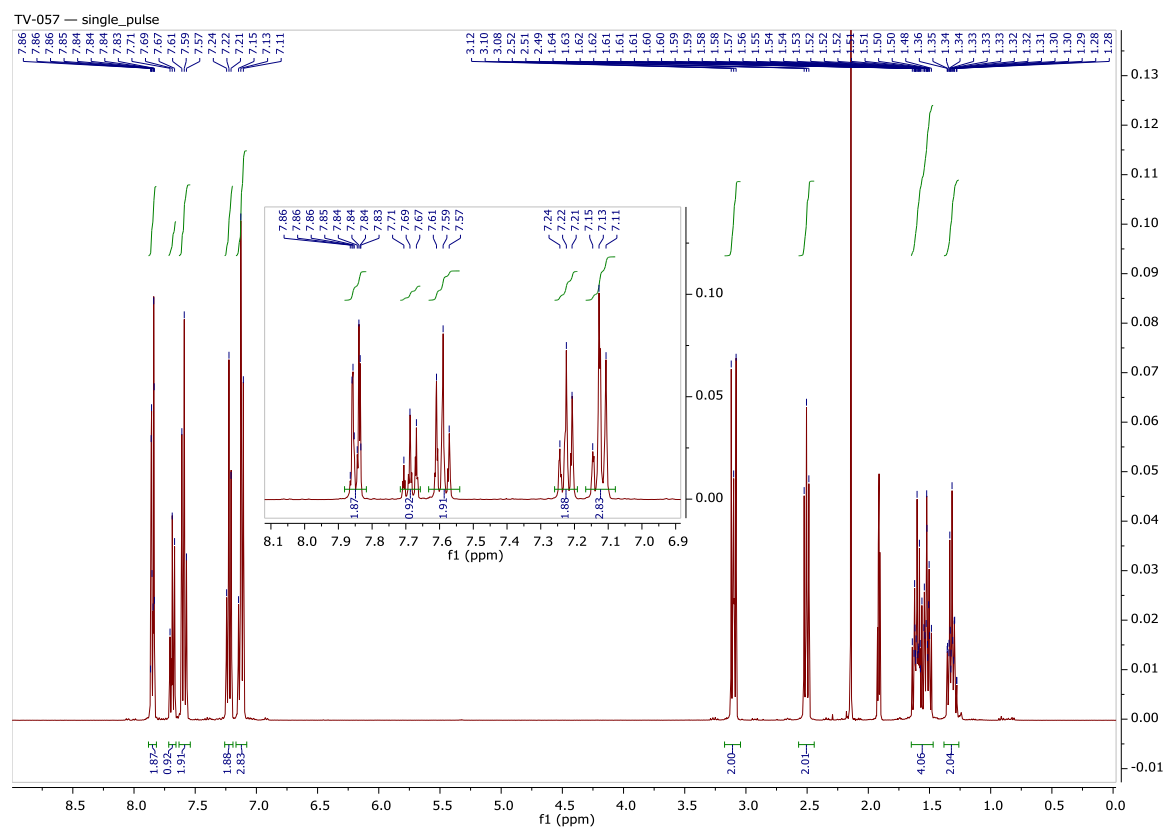
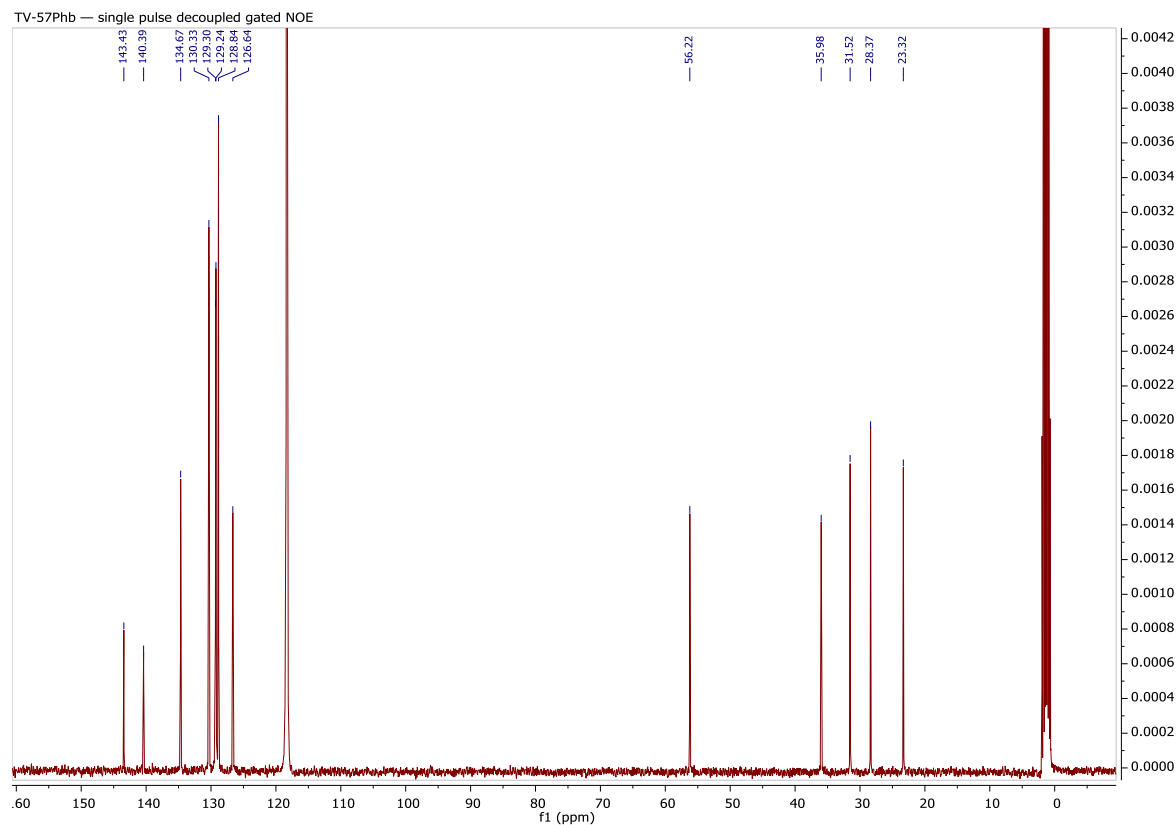
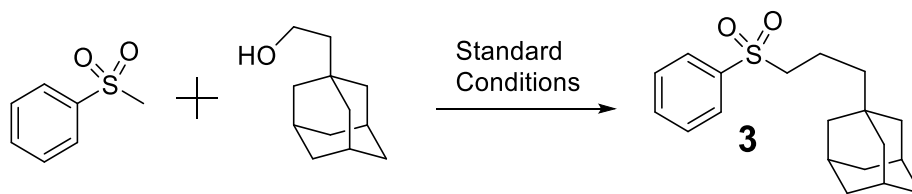


Figure S5. ^{13}C NMR of **2**.





Physical State: White crystalline solid. Isolated Yield: 94%

^1H NMR (400 MHz, Acetonitrile- d_3) δ 7.92 – 7.82 (m, 2H), 7.75 – 7.65 (m, 1H), 7.64 – 7.54 (m, 2H), 3.14 – 2.95 (m, 2H), 1.86 (bs, 3H), 1.76 – 1.63 (m, 3H), 1.62 – 1.47 (m, 5H), 1.38 (bs, 6H), 1.12 – 0.97 (m, 2H). ^{13}C NMR (101 MHz, Acetonitrile- d_3) δ 140.46, 134.67, 130.32, 128.86, 57.15, 43.45, 42.73, 37.67, 32.87, 29.58, 17.07. HRMS: $[\text{C}_{19}\text{H}_{27}\text{O}_2\text{S} ; \text{M}+\text{H}]^+$ Expected 319.1732; Obtained 319.1749.

Figure S6. ^1H NMR of **3**.

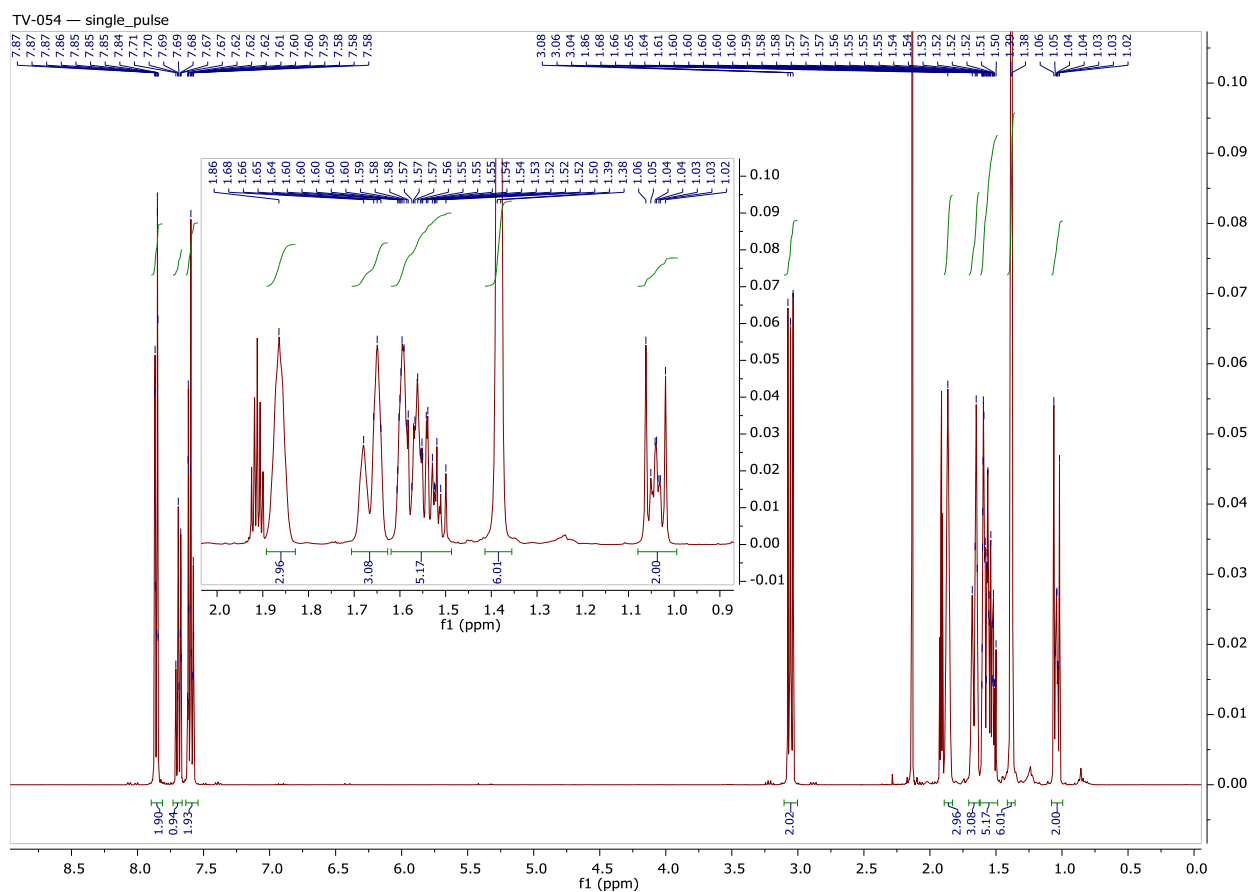
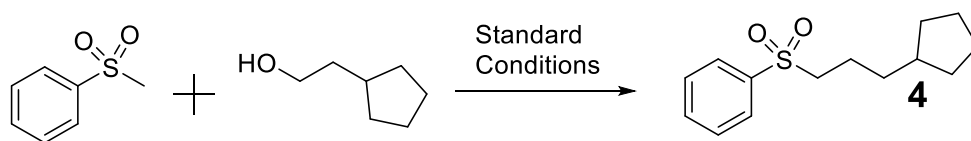
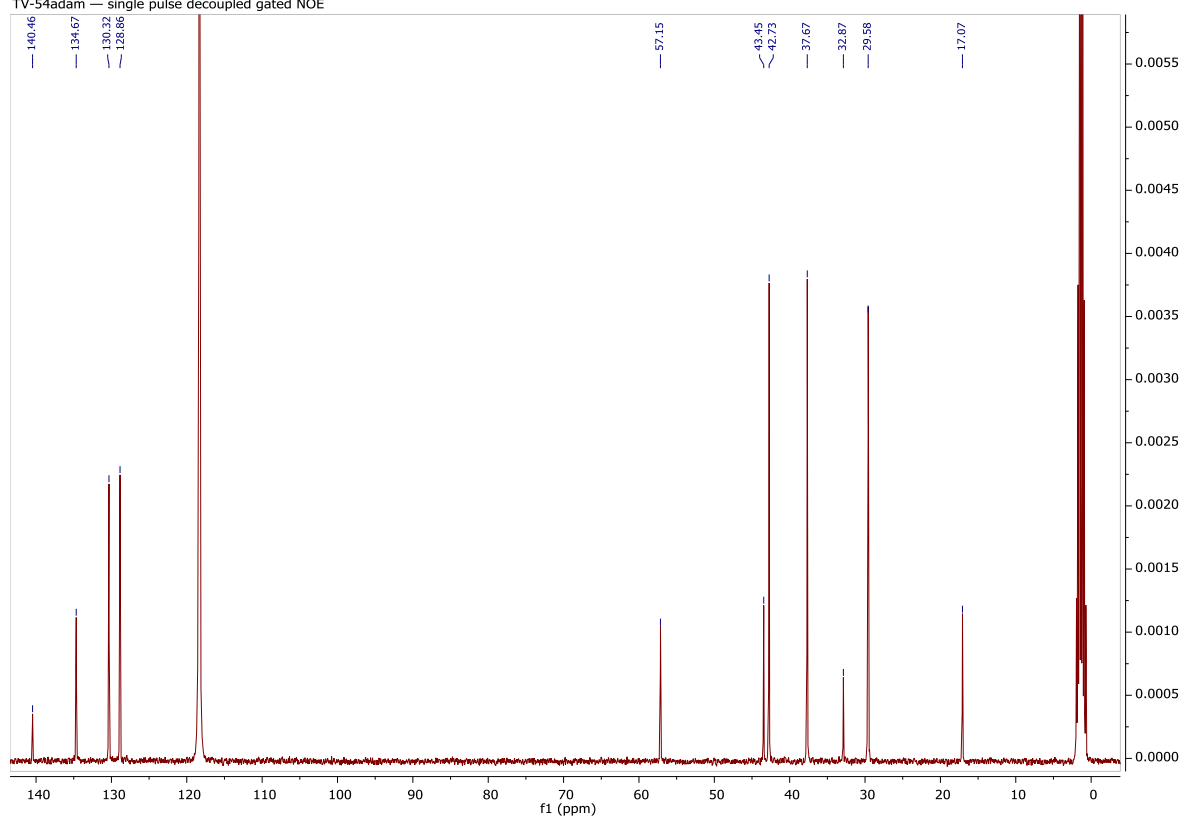


Figure S7. ^{13}C NMR of **3**.

TV-54adam — single pulse decoupled gated NOE



Physical State: Colorless oil. Isolated Yield: 92%

^1H NMR (400 MHz, Acetonitrile- d_3) δ 7.91 – 7.86 (m, 2H), 7.75 – 7.69 (m, 1H), 7.66 – 7.59 (m, 2H), 3.17 – 3.09 (m, 2H), 1.77 – 1.40 (m, 9H), 1.38 – 1.25 (m, 2H), 1.07 – 0.93 (m, 2H). ^{13}C NMR (101 MHz, Acetonitrile- d_3) δ 140.41, 134.66, 130.32, 128.84, 56.44, 40.31, 35.09, 33.04, 25.72, 22.73. HRMS: $[\text{C}_{14}\text{H}_{21}\text{O}_2\text{S}]^+$ Expected 253.1262; Obtained 253.1243.

Figure S8. ^1H NMR of **4**.

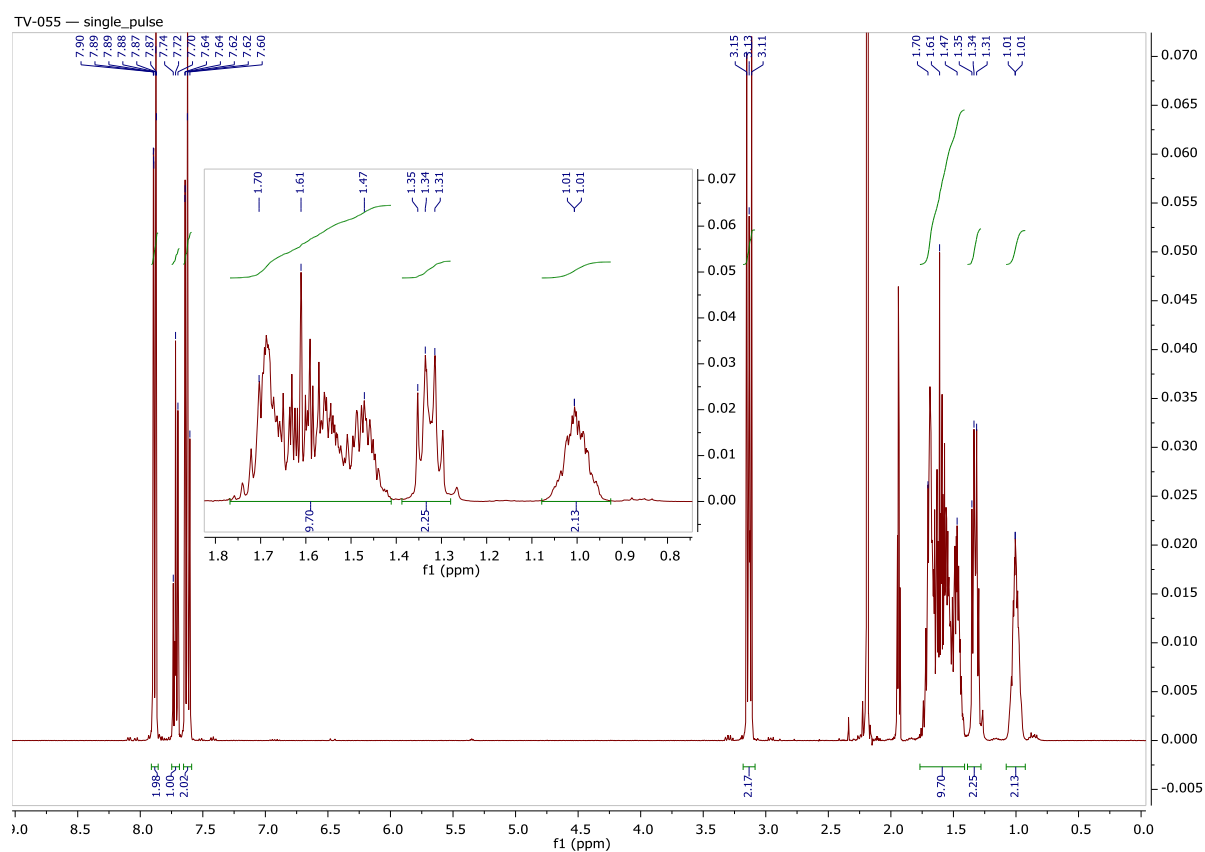
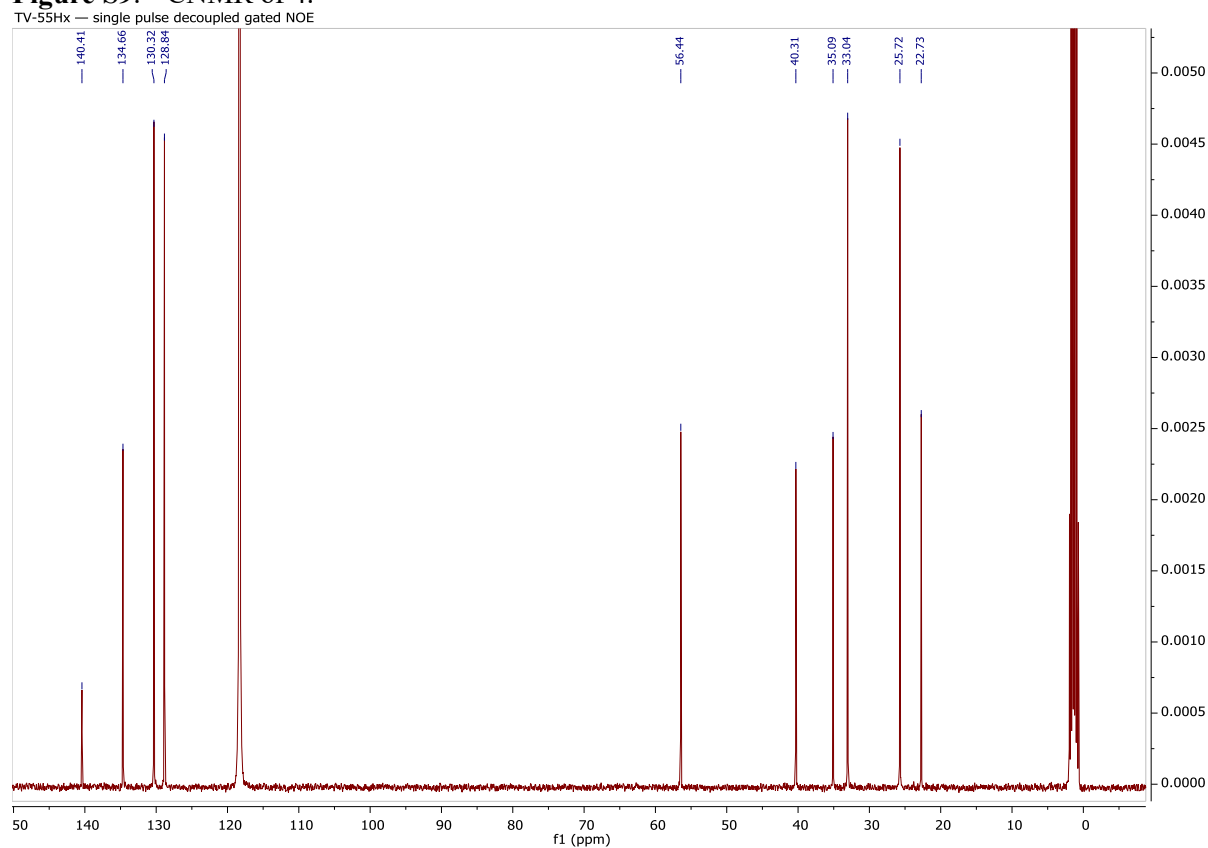
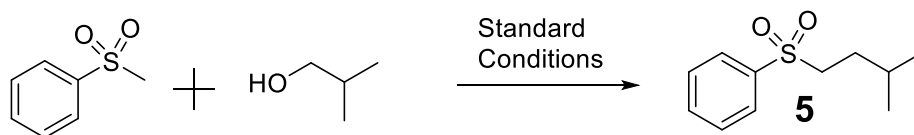


Figure S9. ^{13}C NMR of **4**.





Physical State: Colorless oil. Isolated Yield: 79% (Note: The product gradually evaporates at RT on high vacuum)

^1H NMR (400 MHz, Acetonitrile- d_3) δ 7.89 (d, $J = 7.9$ Hz, 2H), 7.76 – 7.68 (m, 1H), 7.66 – 7.59 (m, 2H), 3.20 – 3.08 (m, 2H), 1.60 (dp, $J = 13.1, 6.6$ Hz, 1H), 1.49 (dt, $J = 11.4, 6.8$ Hz, 2H), 0.84 (d, $J = 6.6$ Hz, 6H). ^{13}C NMR (101 MHz, Acetonitrile- d_3) δ 139.48, 133.77, 129.41, 127.95, 53.89, 31.00, 26.97, 21.32. HRMS: $[\text{C}_{11}\text{H}_{17}\text{O}_2\text{S} ; \text{M}+\text{H}]^+$ Expected 213.0949; Obtained 213.0945.

Figure S10. ^1H NMR of **5**.

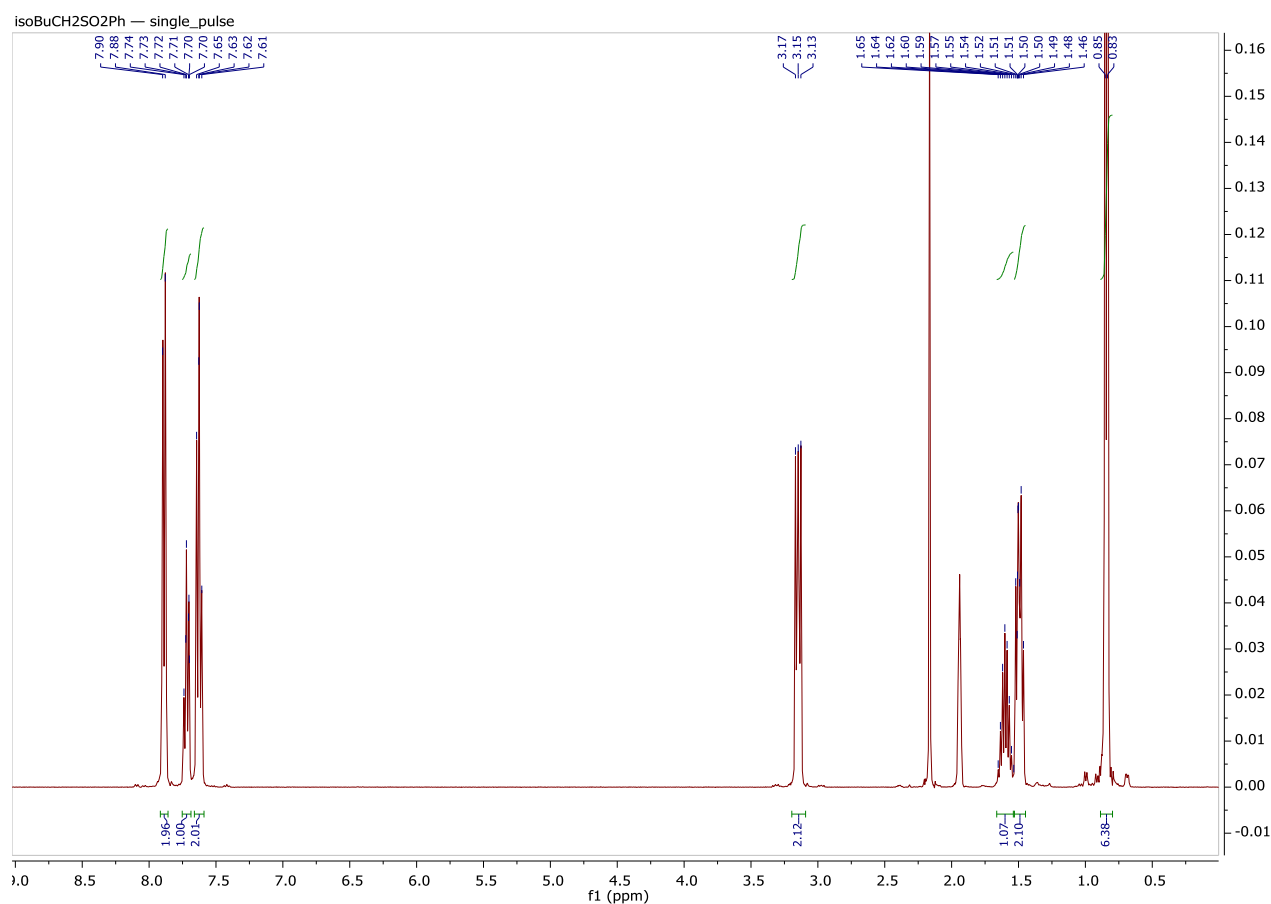
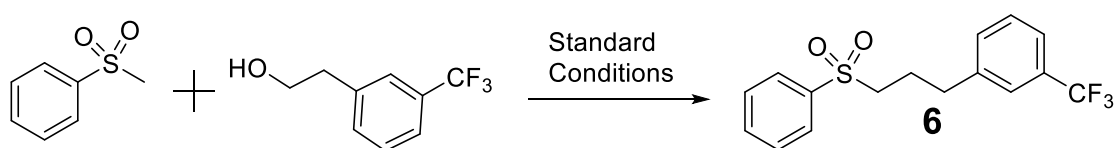
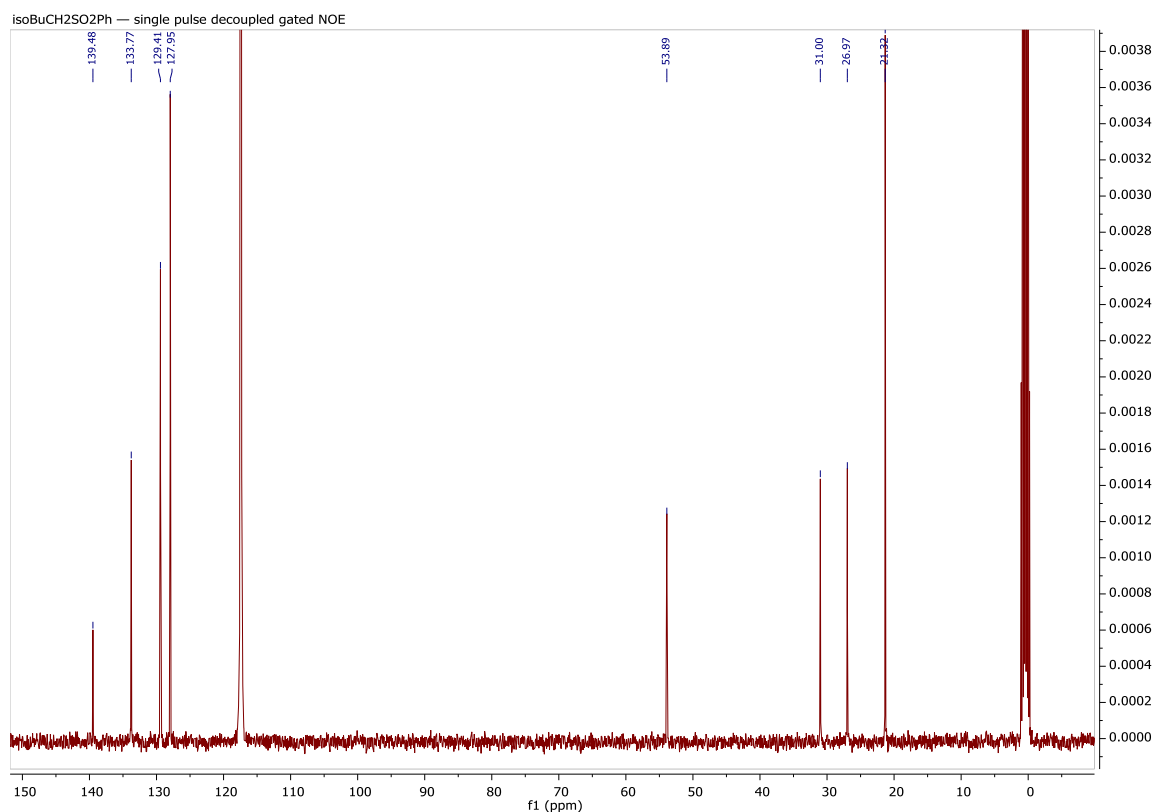


Figure S11. ^{13}C NMR of **5**.



Physical State: White crystalline solid. Isolated Yield: 39%

^1H NMR (400 MHz, Chloroform-*d*) δ 7.94 – 7.85 (m, 2H), 7.72 – 7.63 (m, 1H), 7.61 – 7.53 (m, 2H), 7.47 (d, J = 7.6 Hz, 1H), 7.40 (t, J = 7.7 Hz, 1H), 7.37 – 7.29 (m, 2H), 3.14 – 3.03 (m, 2H), 2.78 (t, J = 7.6 Hz, 2H), 2.15 – 2.01 (m, 2H). ^{13}C NMR (101 MHz, Chloroform-*d*) δ 140.97, 139.11, 133.97, 131.91, 131.07 (d, J_{CF} = 31.9 Hz), 129.52, 129.24, 128.15, 125.19 (q, J_{CF} = 3.9 Hz), 123.54 (q, J_{CF} = 3.9 Hz), 55.35, 33.98, 24.19. CF_3 carbon not observed HRMS: $[\text{C}_{16}\text{H}_{15}\text{O}_2\text{S}_1\text{F}_3\text{Na}]^+$ Expected 351.0643; Obtained 351.0633.

Figure S12. ^1H NMR of **6**.

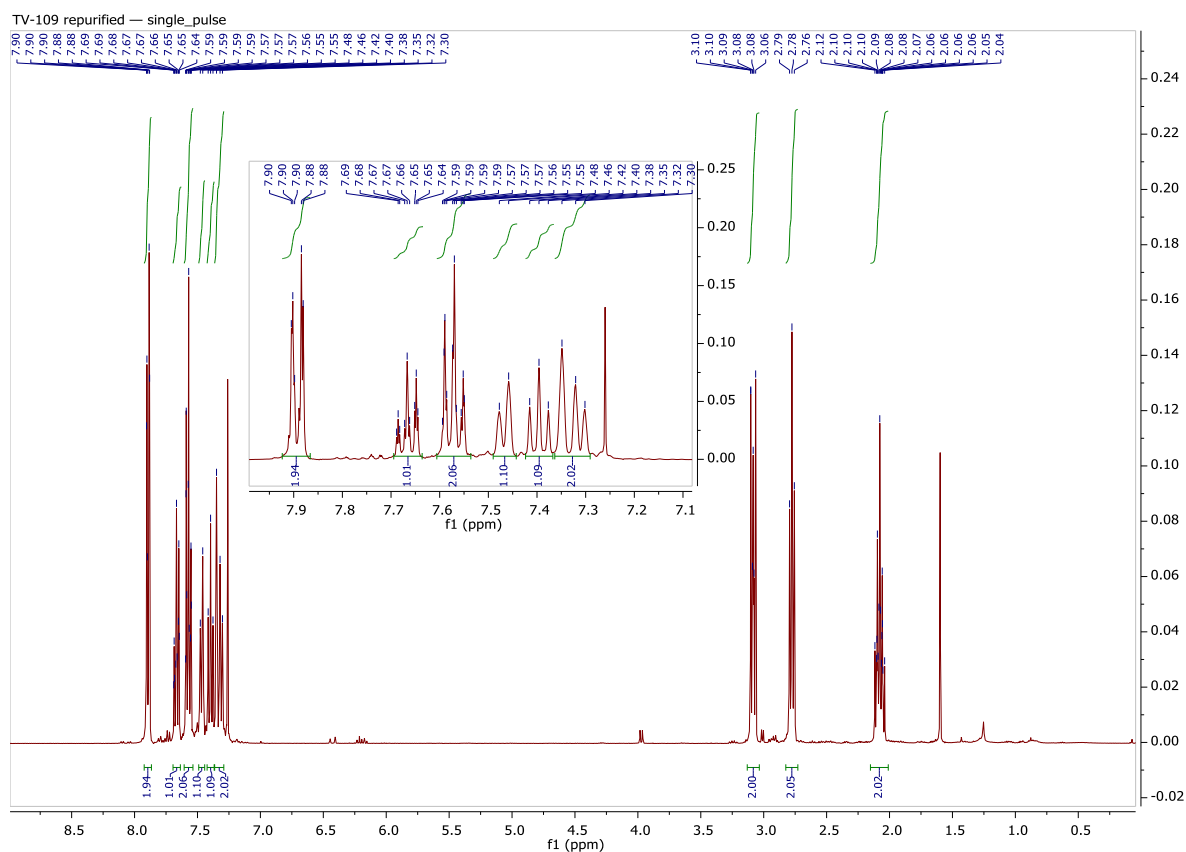
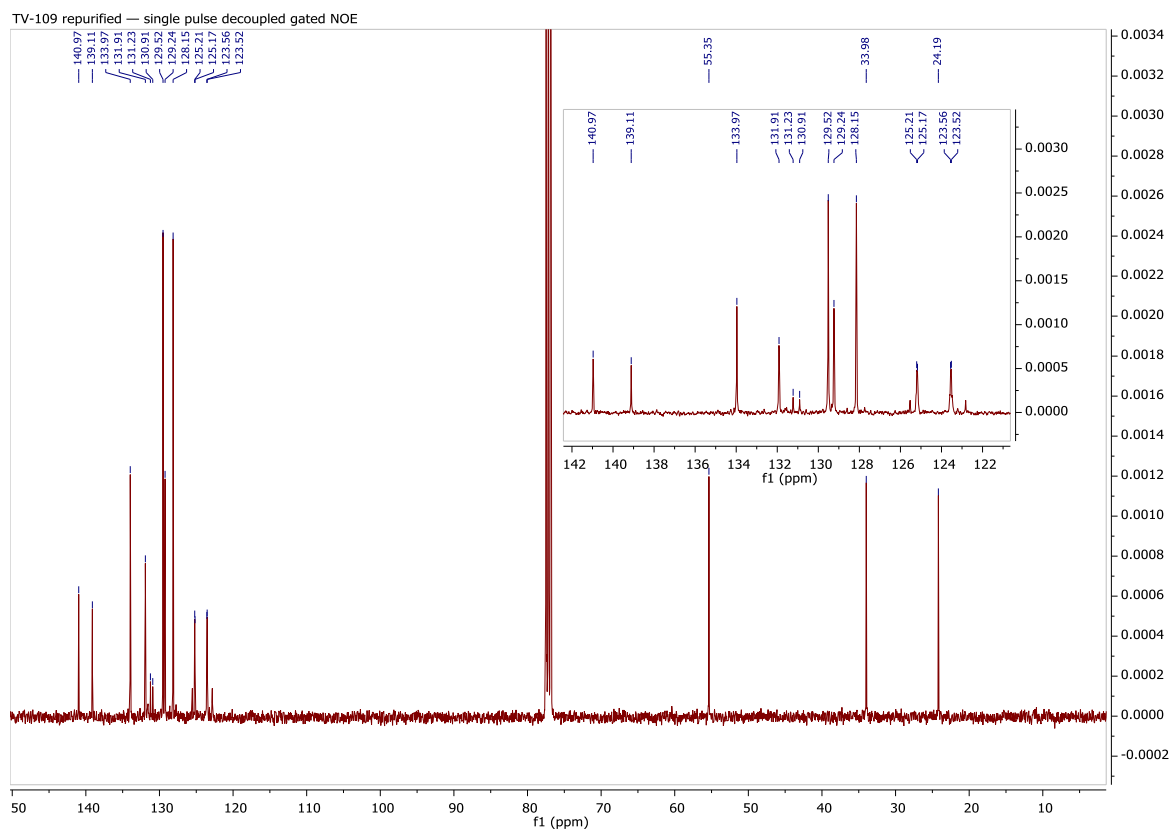
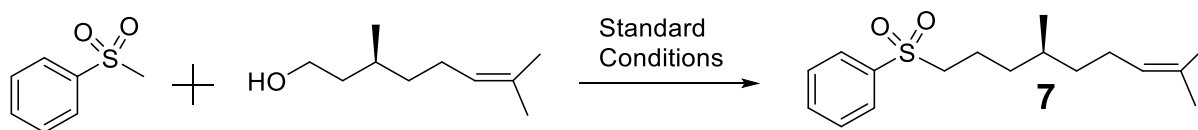


Figure S13. ^{13}C NMR of **6**.





Physical State: Colorless oil. Isolated Yield: 92%

^1H NMR (400 MHz, CDCl_3) δ 7.95 – 7.88 (m, 2H), 7.69 – 7.63 (m, 1H), 7.60 – 7.53 (m, 2H), 5.04 (dddd, $J = 7.1, 5.6, 2.9, 1.4$ Hz, 1H), 3.06 (ddd, $J = 9.0, 6.5, 2.0$ Hz, 2H), 2.03 – 1.84 (m, 2H), 1.82 – 1.63 (m, 5H), 1.57 (bs, 3H), 1.43 – 1.04 (m, 5H), 0.83 (d, $J = 6.5$ Hz, 3H). ^{13}C NMR (101 MHz, Acetonitrile- d_3) δ 140.41, 134.67, 131.99, 130.33, 128.85, 125.63, 56.49, 37.36, 35.71, 32.59, 26.00, 25.80, 21.12, 19.54, 17.70. HRMS: $[\text{C}_{17}\text{H}_{27}\text{O}_2\text{S} ; \text{M}+\text{H}]^+$ Expected 295.1732; Obtained 295.1717.

Figure S14. ^1H NMR of **7**.

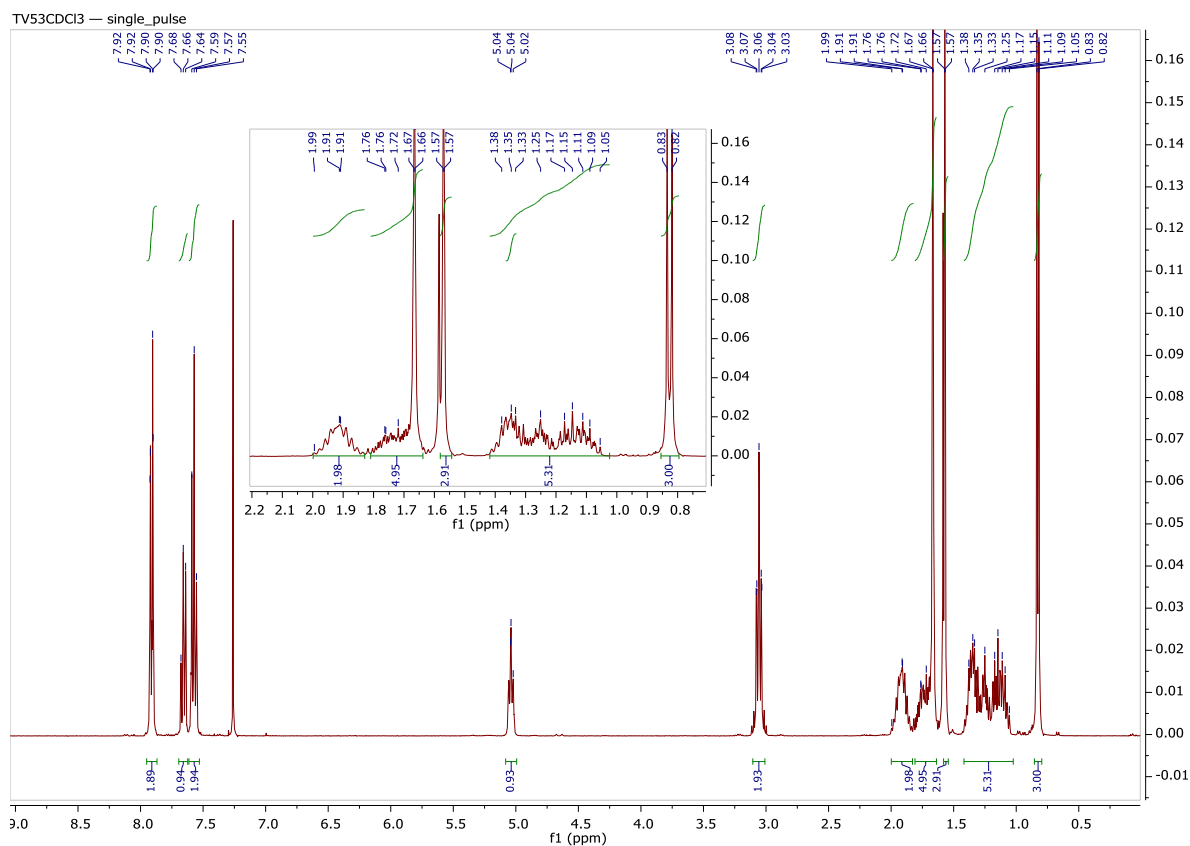
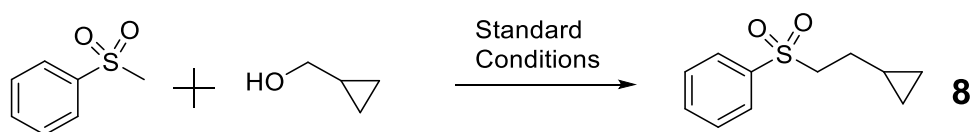
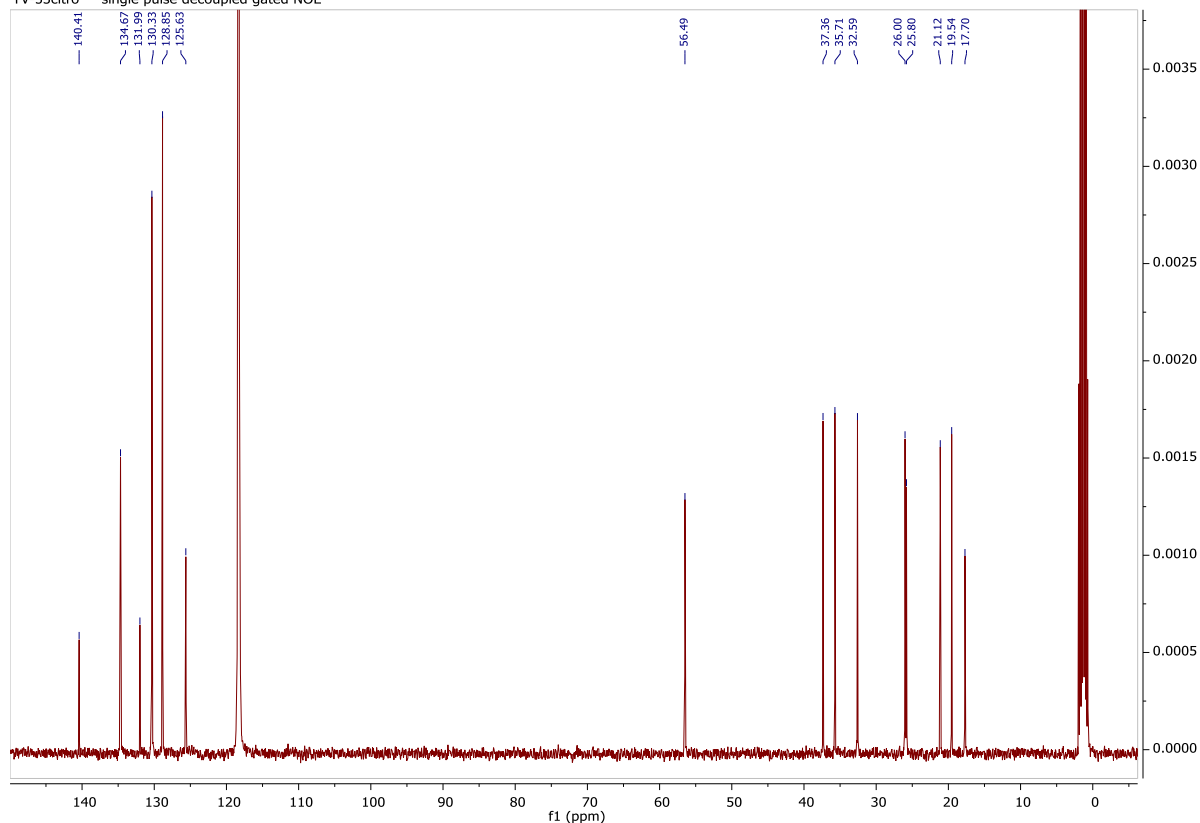


Figure S15. ^{13}C NMR of **7**.

TV-53citro — single pulse decoupled gated NOE



Physical State: Colorless oil. Isolated Yield: 75% (Note: The compound gradually evaporates at RT under high vacuum)

^1H NMR (400 MHz, Chloroform-*d*) δ 7.90 (d, J = 7.1 Hz, 2H), 7.65 (t, J = 7.4 Hz, 1H), 7.56 (t, J = 7.6 Hz, 2H), 3.27 – 3.08 (m, 2H), 1.61 (ddd, J = 11.1, 6.2, 3.7 Hz, 2H), 0.69 (pt, J = 7.4, 4.8 Hz, 1H), 0.53 – 0.33 (m, 2H), 0.04 (q, J = 4.5 Hz, 2H). ^{13}C NMR (101 MHz, Chloroform-*d*) δ 139.35, 133.75, 129.39, 128.14, 56.42, 27.97, 9.78, 4.79. HRMS: $[\text{C}_{11}\text{H}_{15}\text{O}_2\text{S}]^+ ; \text{M}^+ + \text{H}^+$ Expected 211.0793; Obtained 211.0786.

Figure S16. ^1H NMR of **8**.

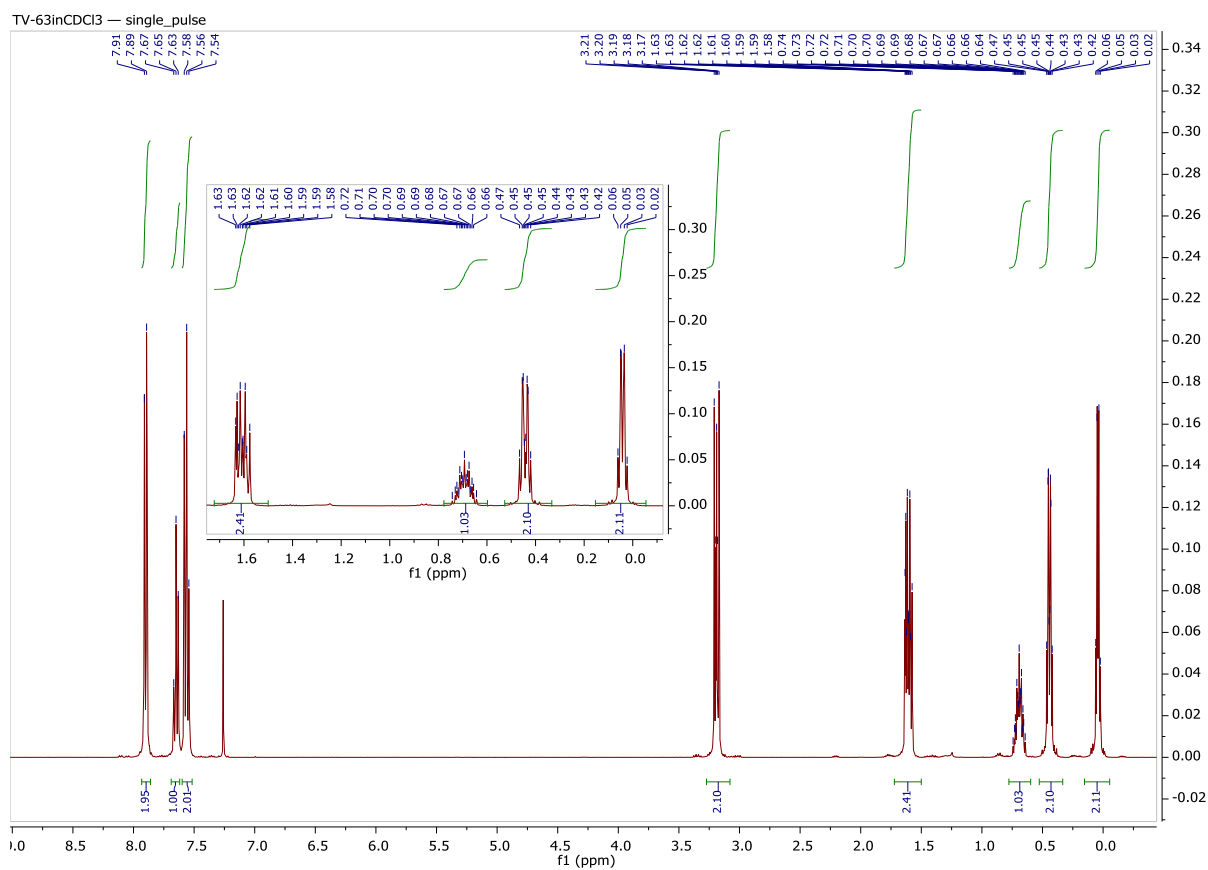
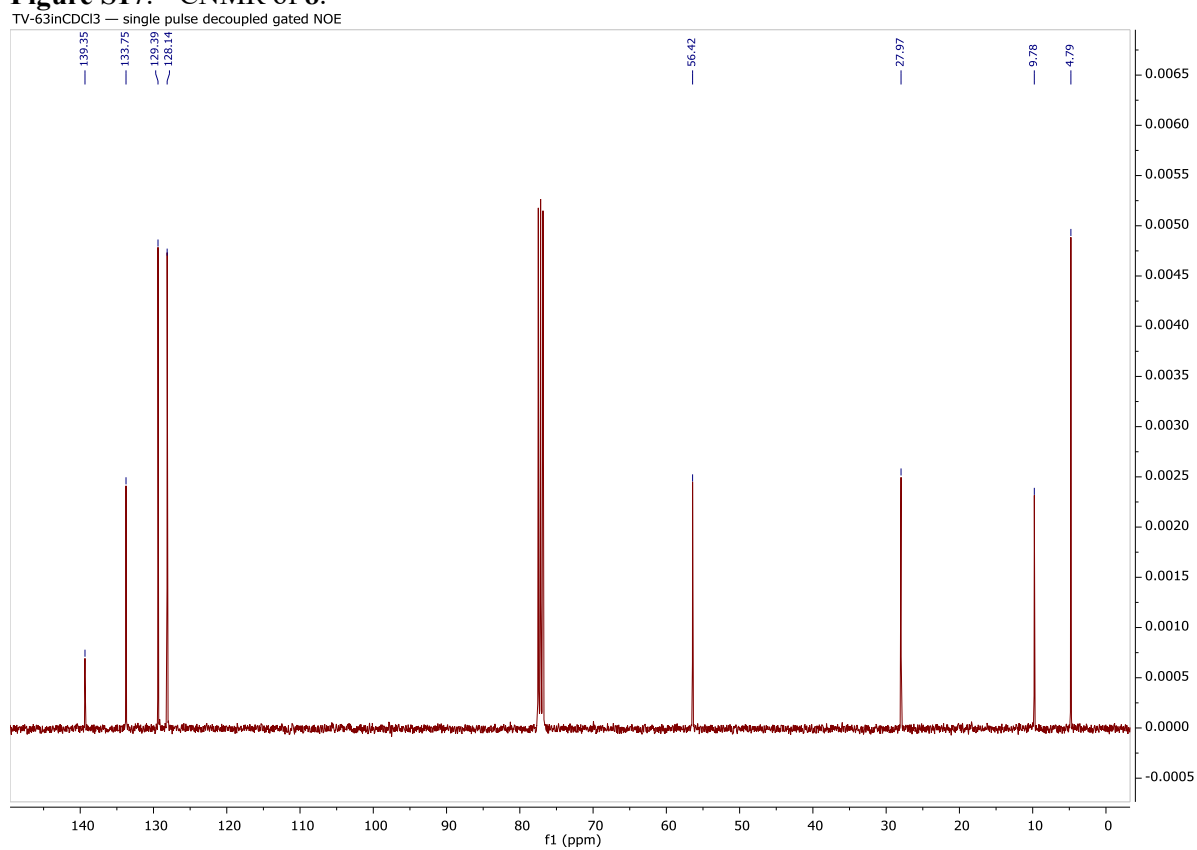
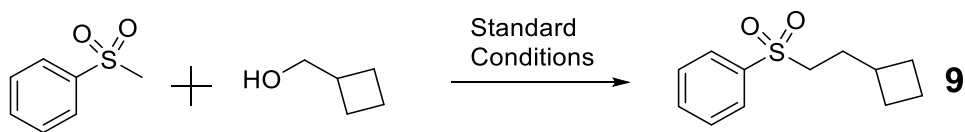


Figure S17. ^{13}C NMR of **8**.





Physical State: White crystalline solid. Isolated Yield: 94%

^1H NMR (400 MHz, Chloroform-*d*) δ 7.93 – 7.87 (m, 2H), 7.69 – 7.62 (m, 1H), 7.60 – 7.54 (m, 2H), 3.09 – 2.87 (m, 2H), 2.33 – 2.20 (m, 1H), 2.06 – 1.95 (m, 2H), 1.89 – 1.73 (m, 4H), 1.63 – 1.50 (m, 2H). ^{13}C NMR (101 MHz, Chloroform-*d*) δ 139.35, 133.74, 129.39, 128.17, 54.41, 34.47, 29.47, 27.78, 18.23. HRMS: $[\text{C}_{12}\text{H}_{17}\text{O}_2\text{S}]^+$; $\text{M}+\text{H}^+$ Expected 225.0949; Obtained 225.0938.

Figure S18. ^1H NMR of **9**.

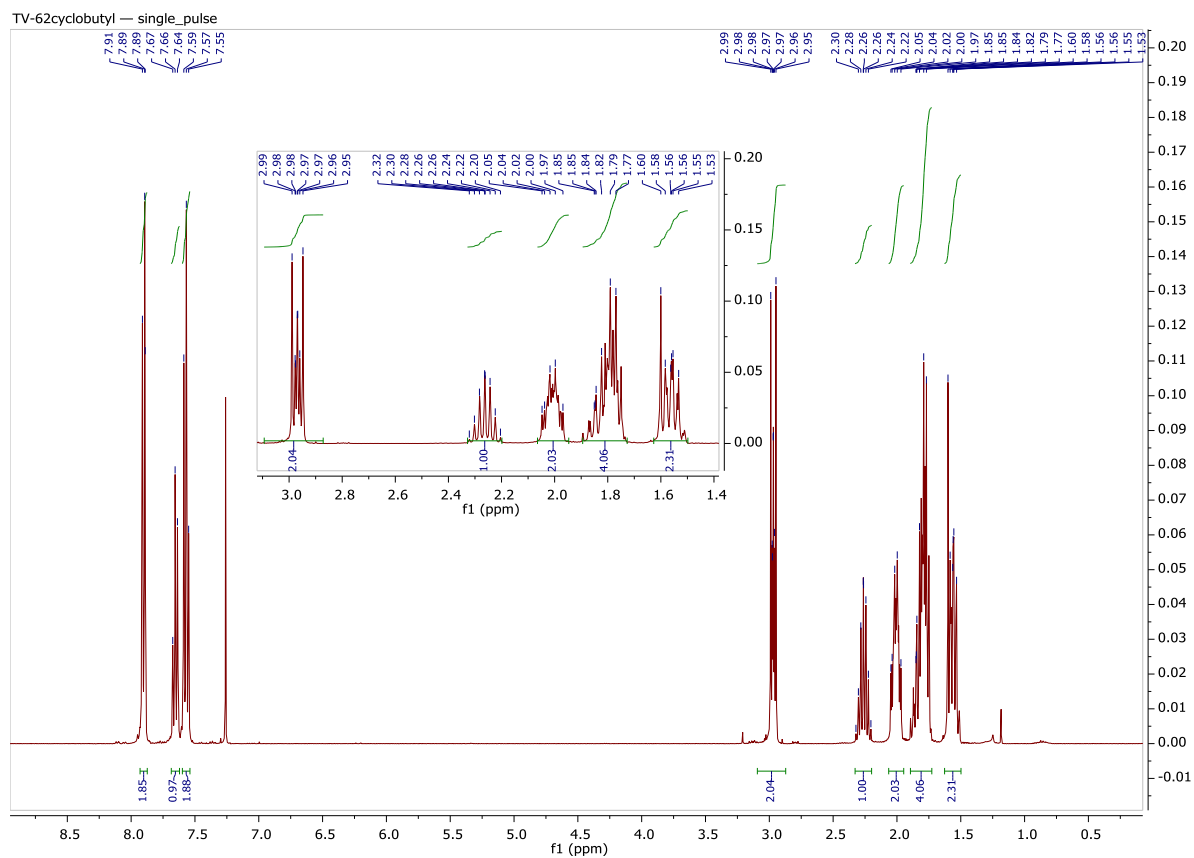
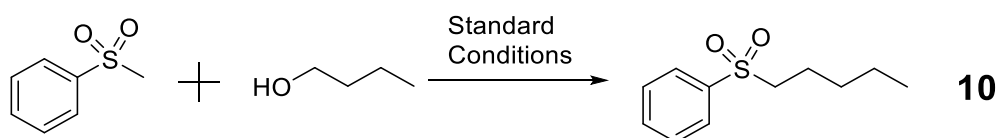
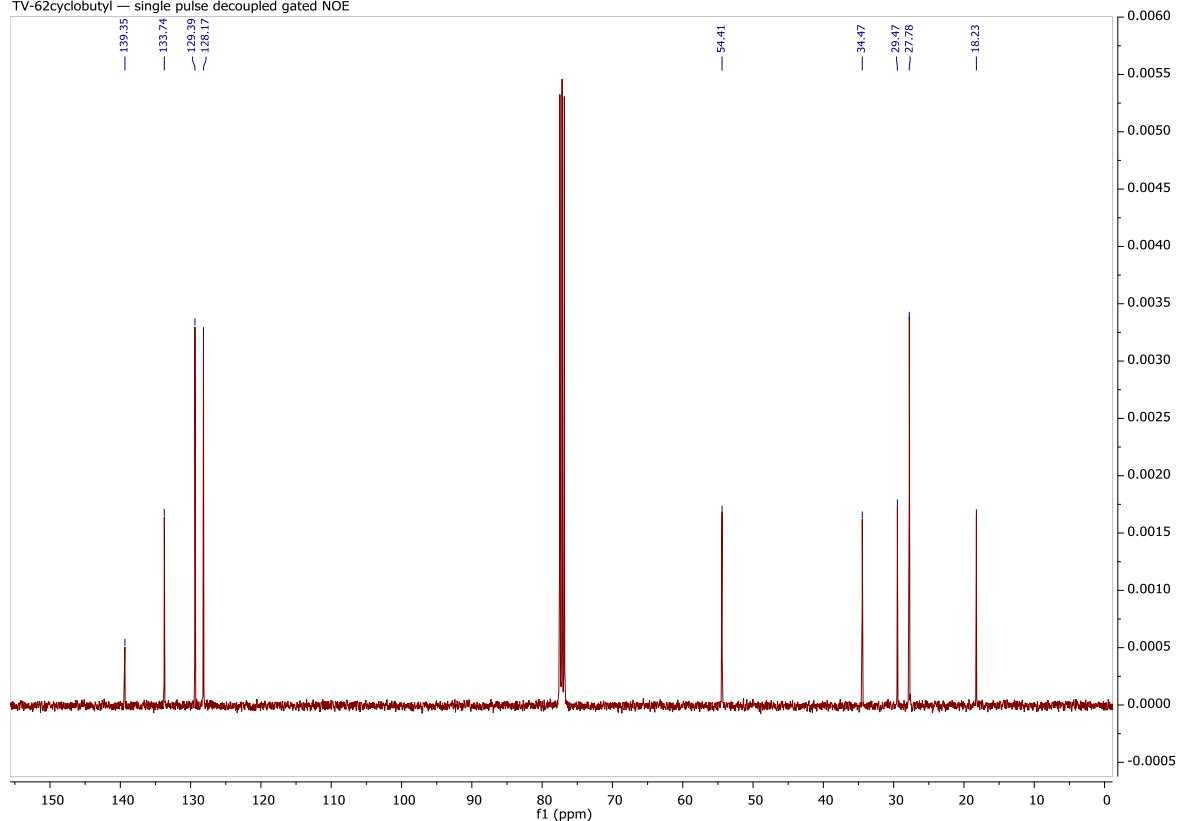


Figure S19. ^{13}C NMR of **9**.

TV-62cyclobutyl — single pulse decoupled gated NOE



Physical State: Colorless liquid that solidified after several months to a white crystalline low-melting solid.

Isolated yield: 83% (Note: the compound gradually evaporates at RT under high vacuum)

^1H NMR (600 MHz, Chloroform-*d*) δ 7.90 (dd, J = 8.4, 1.3 Hz, 2H), 7.68 – 7.62 (m, 1H), 7.57 (t, J = 7.7 Hz, 2H), 3.11 – 3.03 (m, 2H), 1.76 – 1.66 (m, 2H), 1.38 – 1.22 (m, 4H), 0.85 (t, J = 7.2 Hz, 3H).

^{13}C NMR (151 MHz, Chloroform-*d*) δ 139.37, 133.73, 129.38, 128.18, 56.42, 30.47, 22.43, 22.21, 13.80.

HRMS: $[\text{C}_{11}\text{H}_{17}\text{O}_2\text{S}]^+$ Expected 213.0949; Obtained 213.0929.

Figure S20. ^1H NMR of **10**.

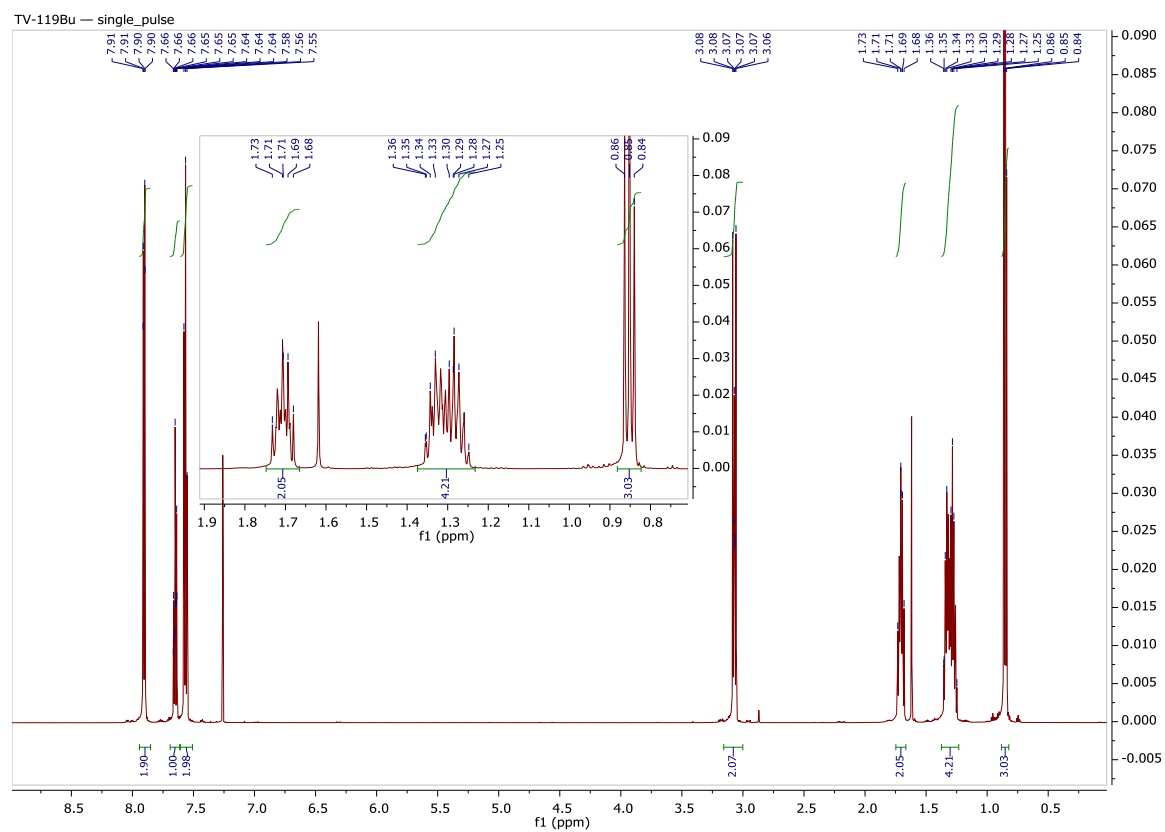
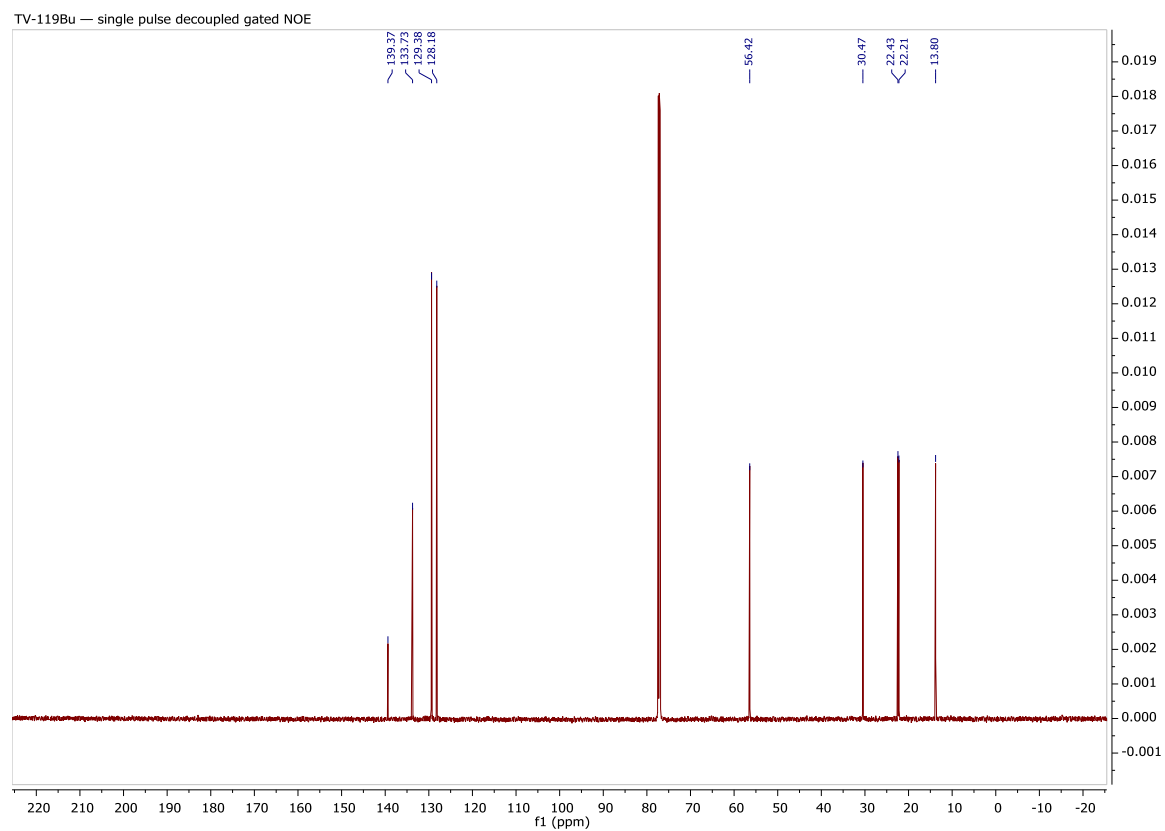


Figure S21. ^{13}C NMR of **10**.



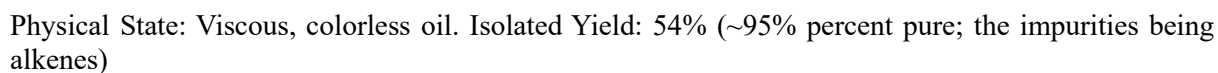


Figure S22. ^1H NMR of **11**.

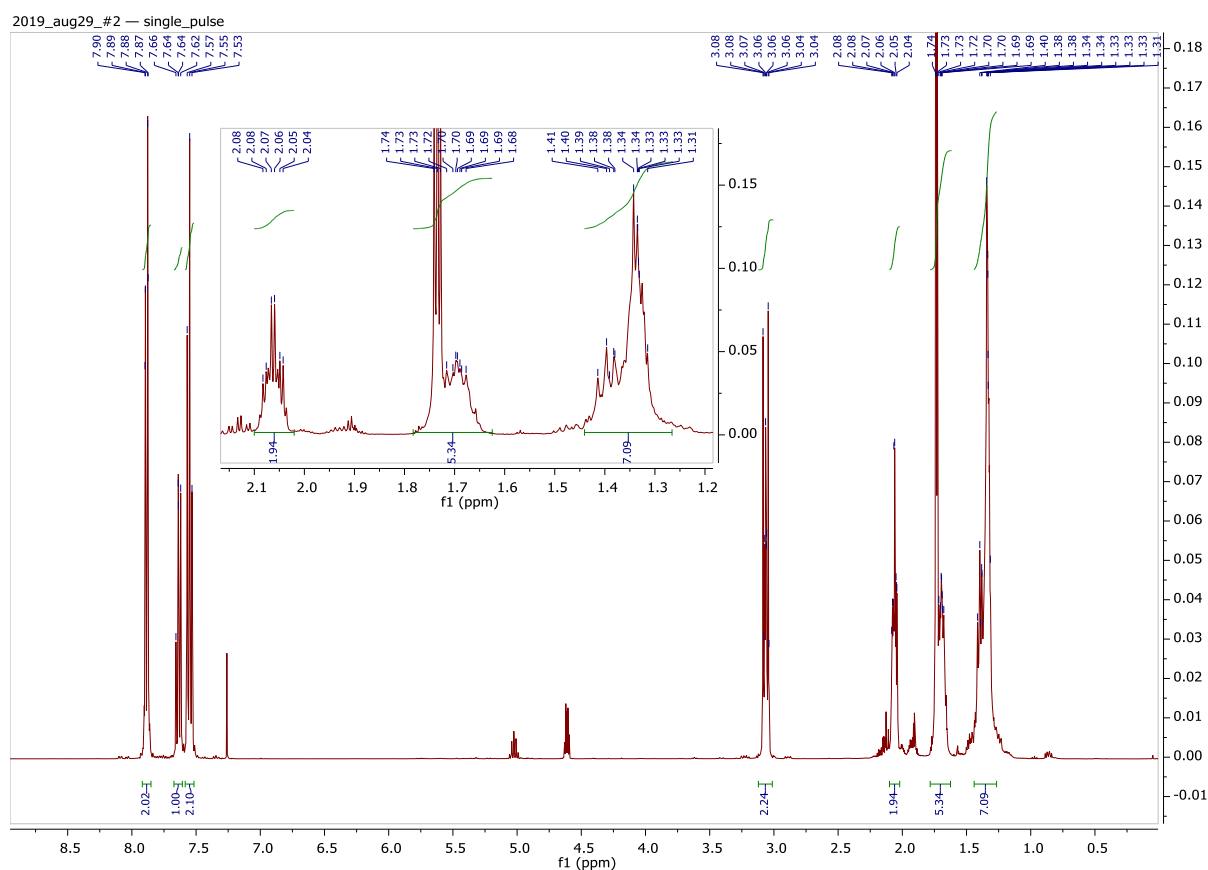
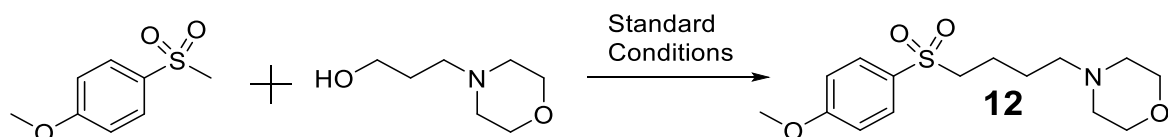
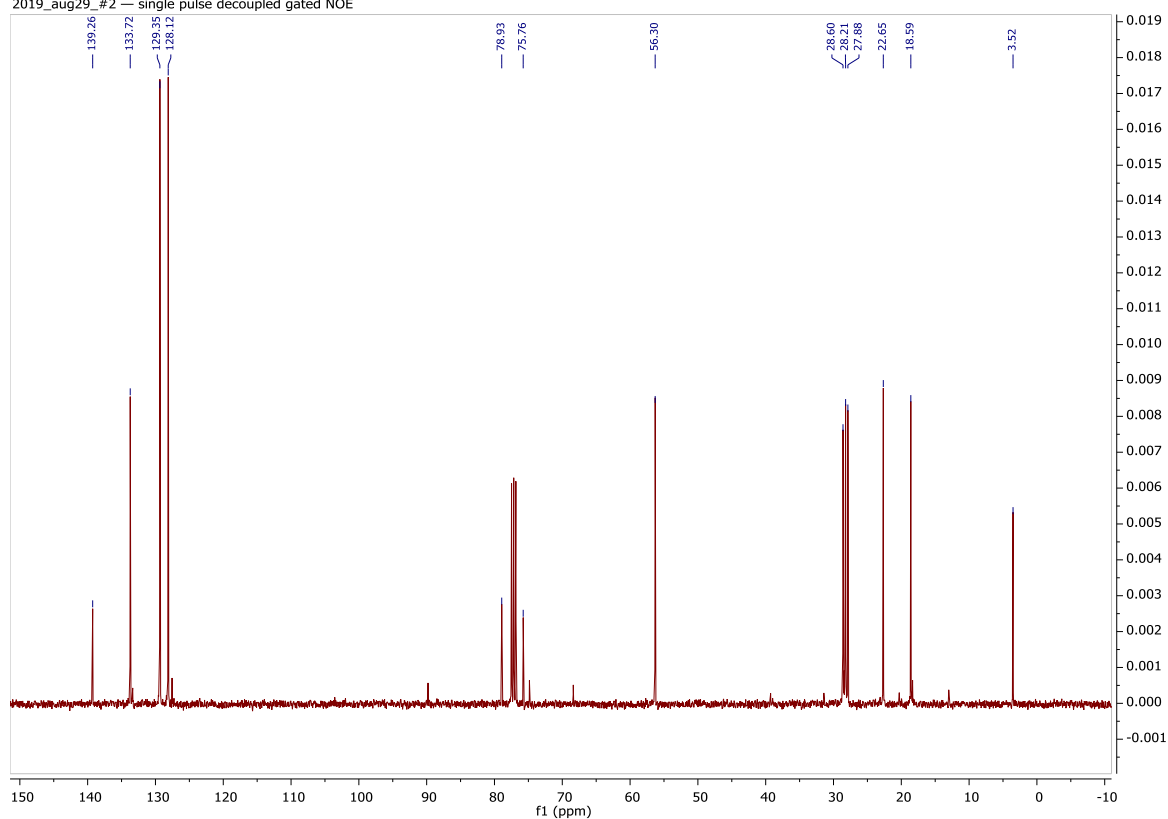


Figure S23. ^{13}C NMR of **11**.

2019_aug29_#2 — single pulse decoupled gated NOE



Physical State: Yellowish oil. Isolated Yield: 85%

^1H NMR (400 MHz, Chloroform-*d*) δ 7.80 (d, J = 8.3 Hz, 2H), 7.00 (d, J = 8.4 Hz, 2H), 3.87 (s, 3H), 3.65 (t, J = 4.7 Hz, 4H), 3.12 – 3.03 (m, 2H), 2.35 (t, J = 4.7 Hz, 4H), 2.31 – 2.23 (m, 2H), 1.72 (tt, J = 8.1, 6.3 Hz, 2H), 1.59 – 1.48 (m, 2H). ^{13}C NMR (101 MHz, Chloroform-*d*) δ 163.81, 130.74, 130.30, 114.54, 66.99, 58.10, 56.40, 55.80, 53.71, 25.12, 20.95. HRMS: $[\text{C}_{15}\text{H}_{24}\text{N}_1\text{O}_4\text{S}_1; \text{M}+\text{H}]^+$ Expected 314.1426; Obtained 314.1429.

Figure S24. ^1H NMR of **12**.

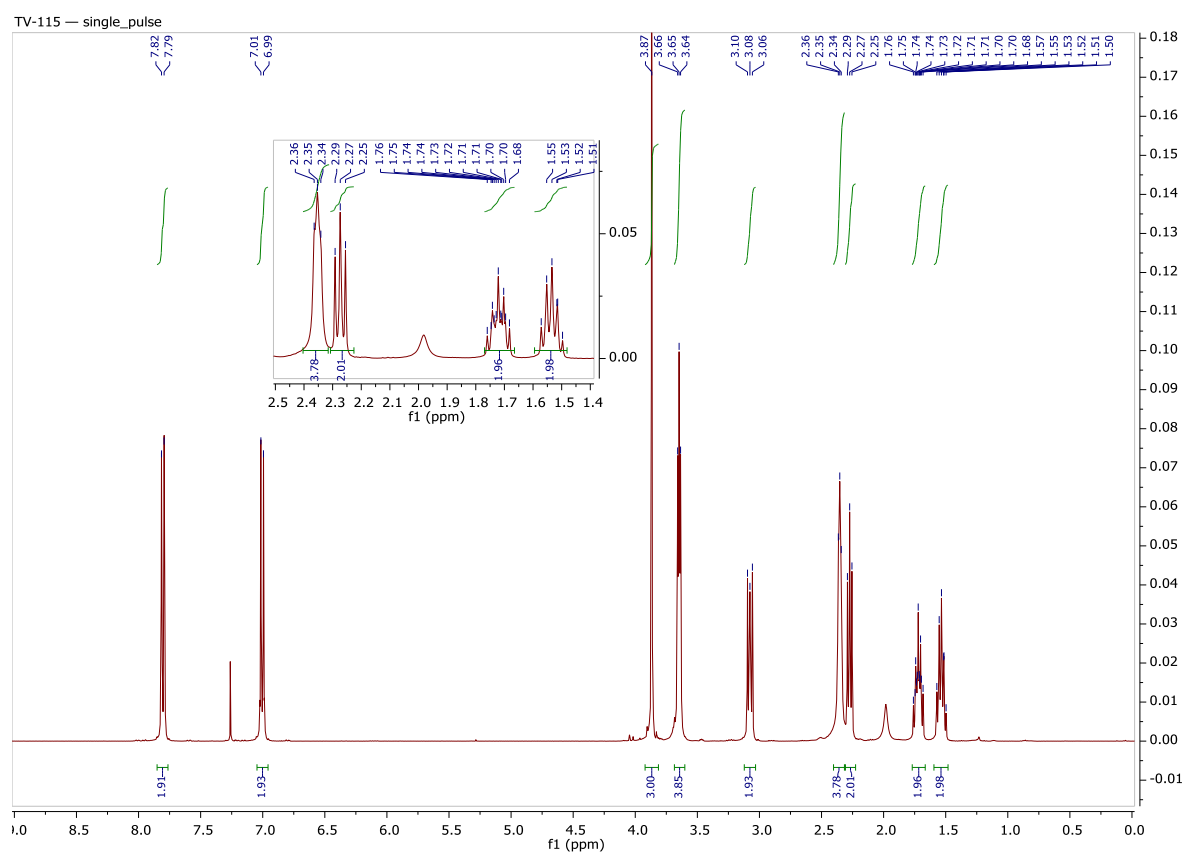


Figure S25. ^{13}C NMR of **12**.

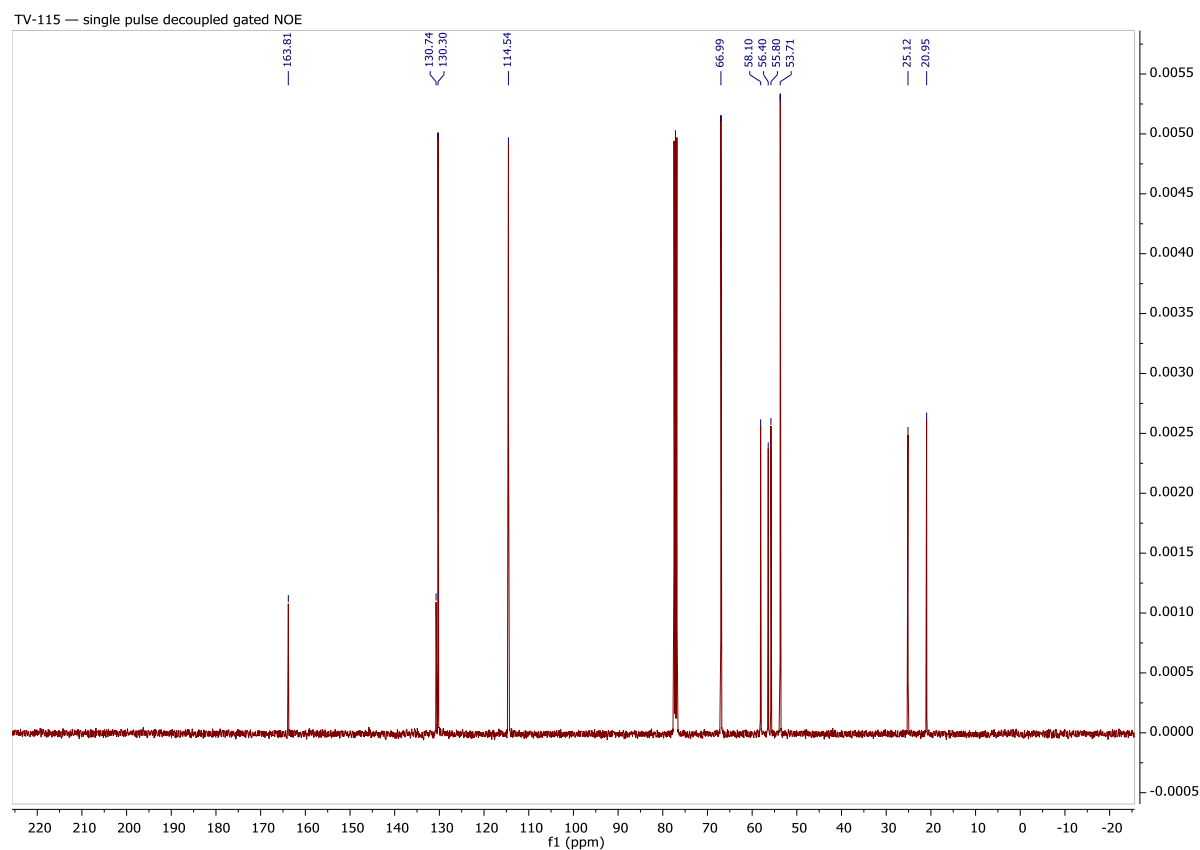
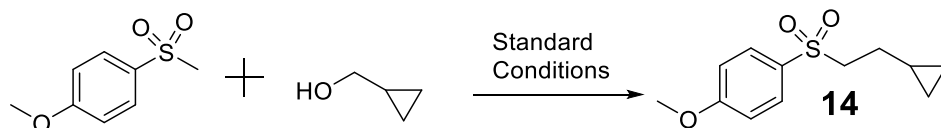
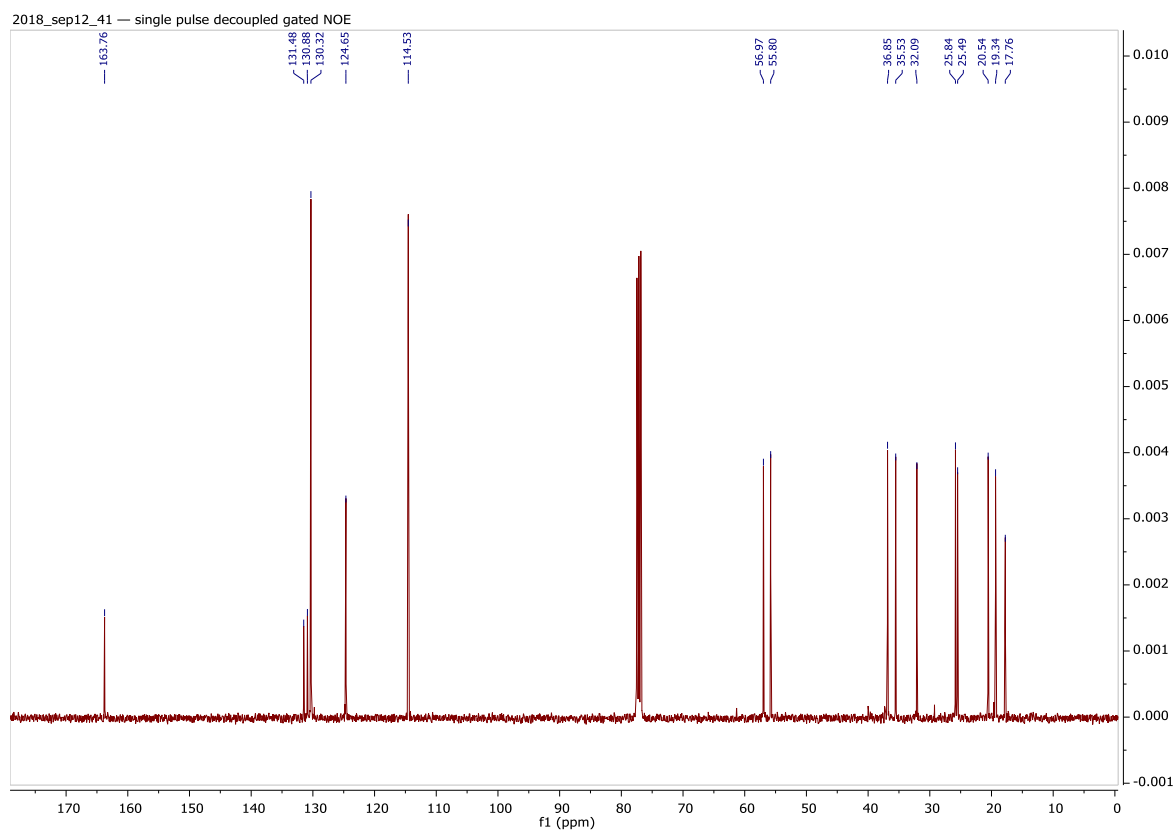


Figure S27. ^{13}C NMR of **13**.



Physical State: Colorless oil. Isolated Yield: 75%

^1H NMR (400 MHz, Chloroform-*d*) δ 7.81 (d, J = 8.9 Hz, 2H), 7.01 (d, J = 8.9 Hz, 2H), 3.88 (s, 3H), 3.24 – 3.05 (m, 2H), 1.63 – 1.52 (m, 2H), 0.76 – 0.59 (m, 1H), 0.51 – 0.36 (m, 2H), 0.09 – -0.05 (m, 2H). ^{13}C NMR (101 MHz, Chloroform-*d*) δ 163.74, 130.82, 130.28, 114.51, 56.67, 55.79, 28.12, 9.74, 4.74. HRMS: $[\text{C}_{12}\text{H}_{17}\text{O}_3\text{S}]^+$ Expected 241.0899; Obtained 241.0878.

Figure S28. ^1H NMR of **14**.

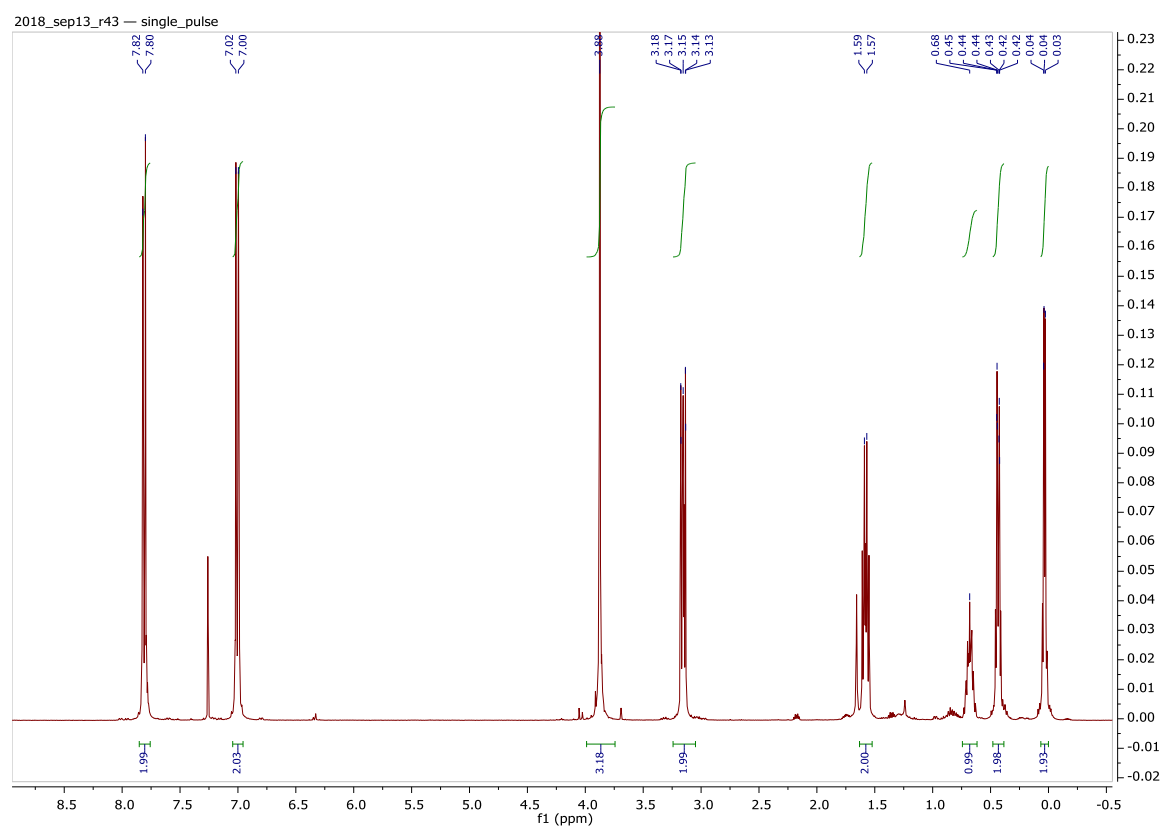
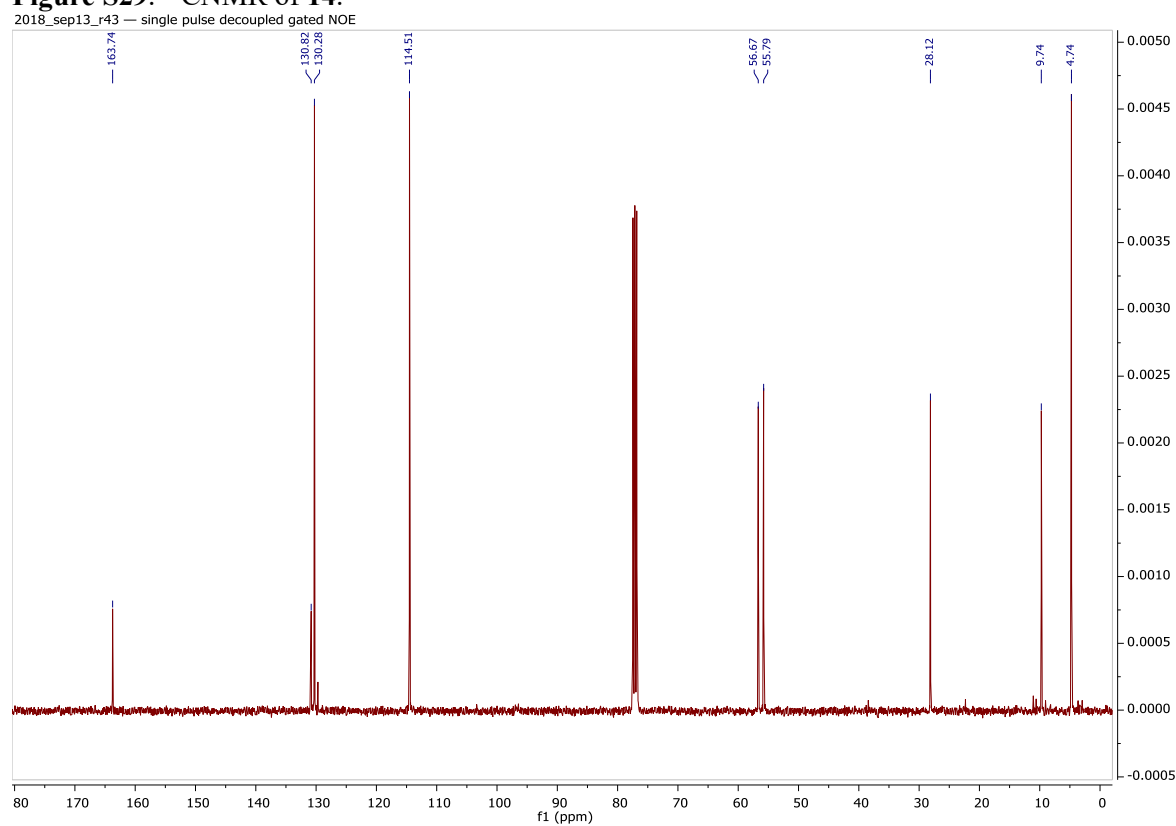
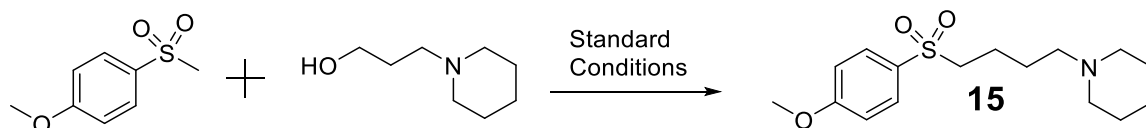


Figure S29. ^{13}C NMR of **14**.





Physical State: Tan oil. Darkens on air. Isolated Yield: 83%

^1H NMR (400 MHz, Chloroform-*d*) δ 7.80 (d, $J = 8.8$ Hz, 2H), 7.00 (d, $J = 8.8$ Hz, 2H), 3.87 (s, 3H), 3.11 – 3.04 (m, 2H), 2.60 (s, 1H), 2.32 (bs, 3H), 2.28 – 2.21 (m, 2H), 1.74 – 1.63 (m, 2H), 1.60 – 1.49 (m, 6H), 1.39 (p, $J = 5.9$ Hz, 2H). ^{13}C NMR (101 MHz, Chloroform-*d*) δ 163.78, 130.66, 130.32, 114.54, 58.48, 56.43, 55.80, 54.57, 25.81, 25.40, 24.33, 21.17. HRMS: $[\text{C}_{16}\text{H}_{26}\text{O}_3\text{S}_1\text{N}_1]^+$ Expected 312.1634; Obtained 312.1628.

Figure S30. ^1H NMR of **15**.

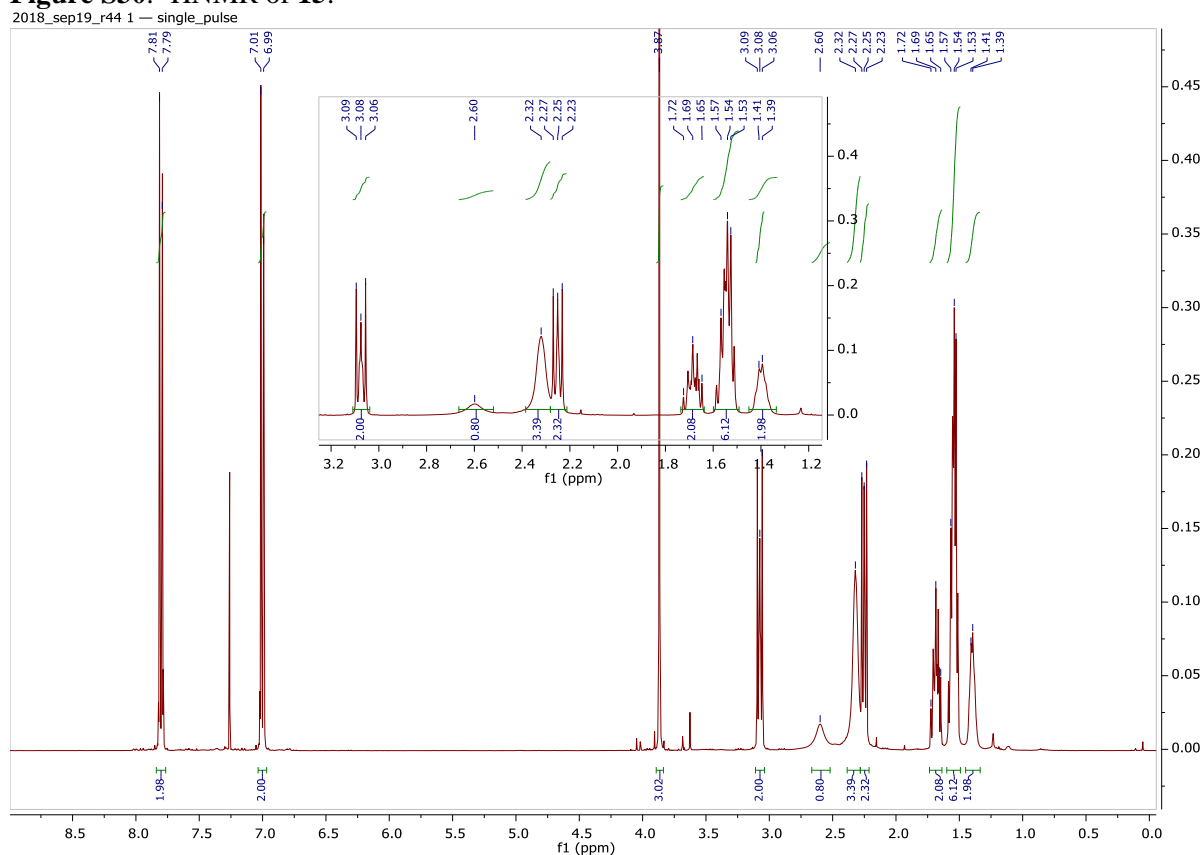
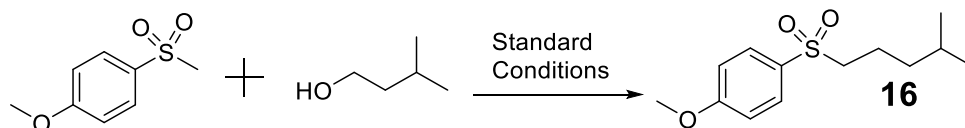
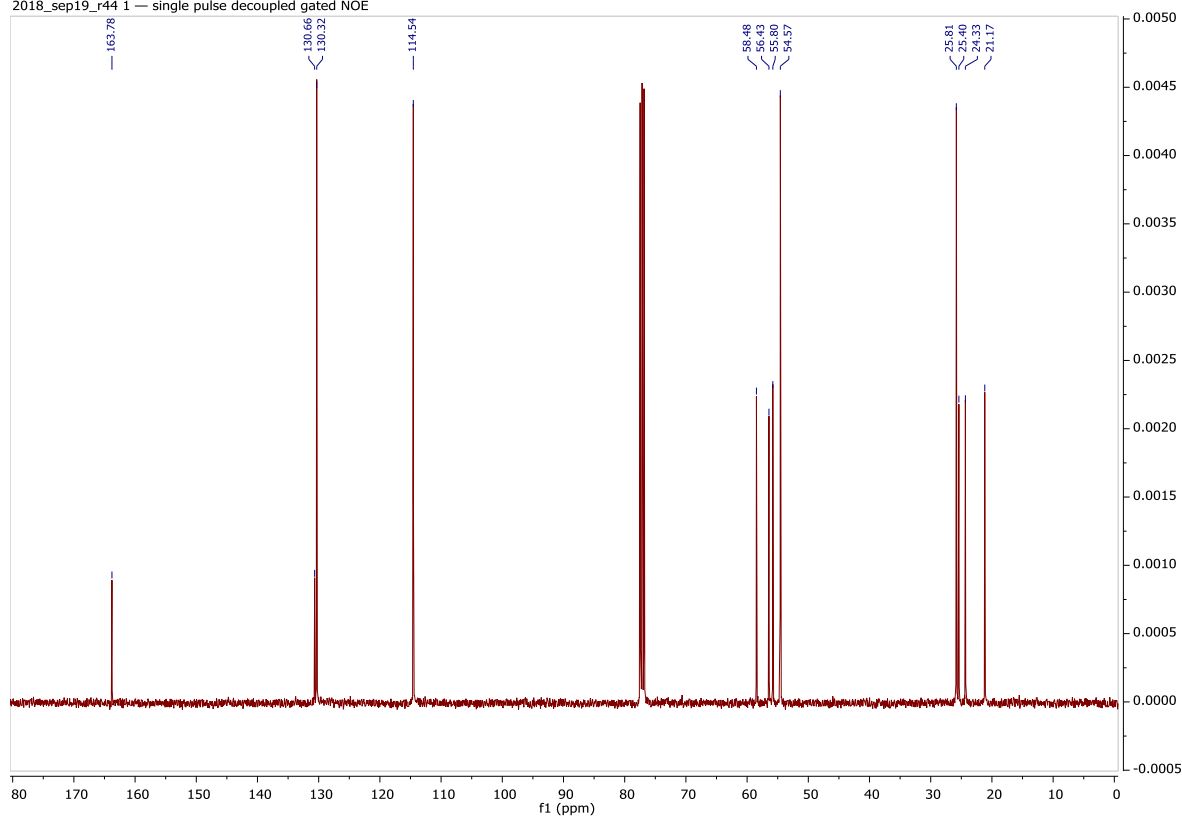


Figure S31. ^{13}C NMR of **15**.

2018_sep19_r44 1 — single pulse decoupled gated NOE



Physical State: Colorless solid. Isolated Yield: 76%

^1H NMR (400 MHz, Chloroform-*d*) δ 7.78 (d, J = 9.0, 2H), 6.98 (d, J = 9.0 Hz, 2H), 3.84 (s, 3H), 3.06 – 2.93 (m, 2H), 1.73 – 1.59 (m, 2H), 1.40 – 1.52 (m, 1H), 1.23 – 1.12 (m, 2H), 0.80 (d, J = 6.7 Hz, 6H). ^{13}C NMR (101 MHz, Chloroform-*d*) δ 163.69, 130.75, 130.22, 114.46, 56.80, 55.74, 37.31, 27.65, 22.33, 20.76. HRMS: $[\text{C}_{13}\text{H}_{21}\text{O}_3\text{S}]^+$ Expected 257.1212; Obtained 257.1206.

Figure S32. ^1H NMR of **16**.

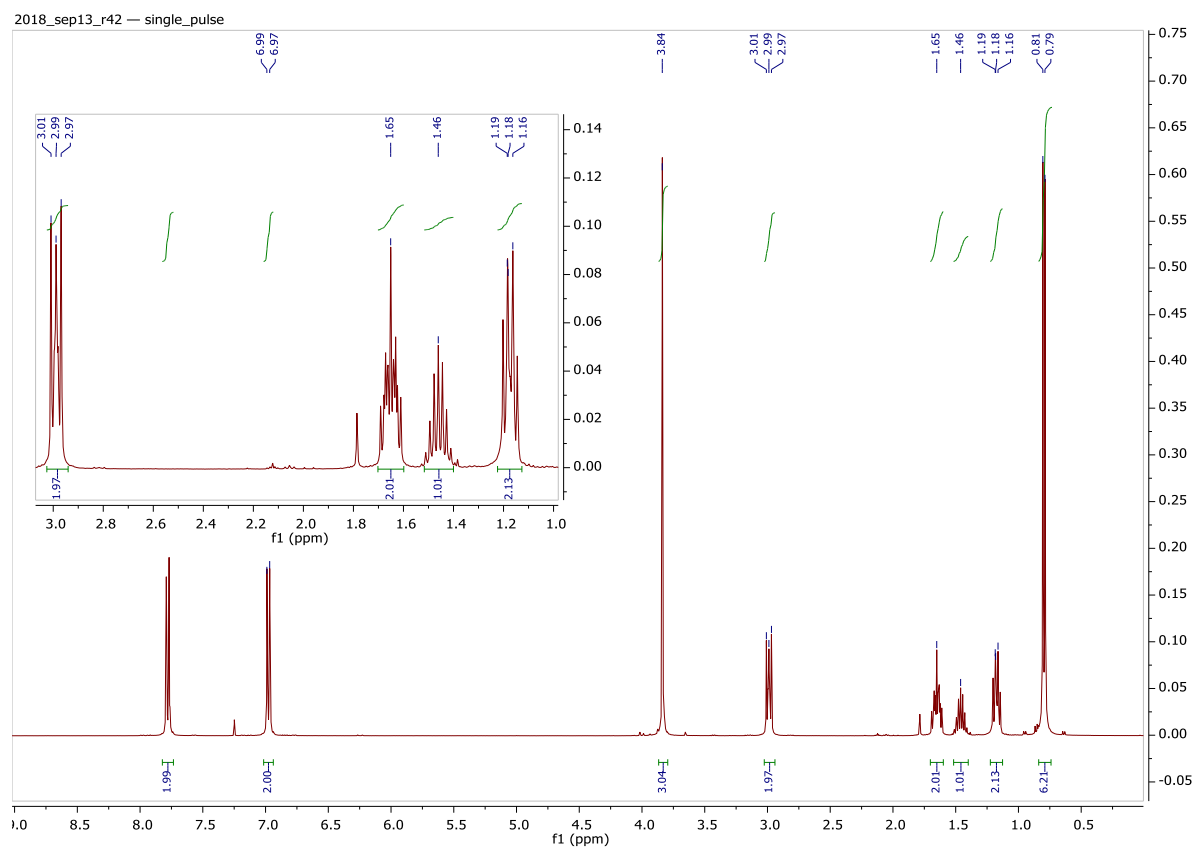
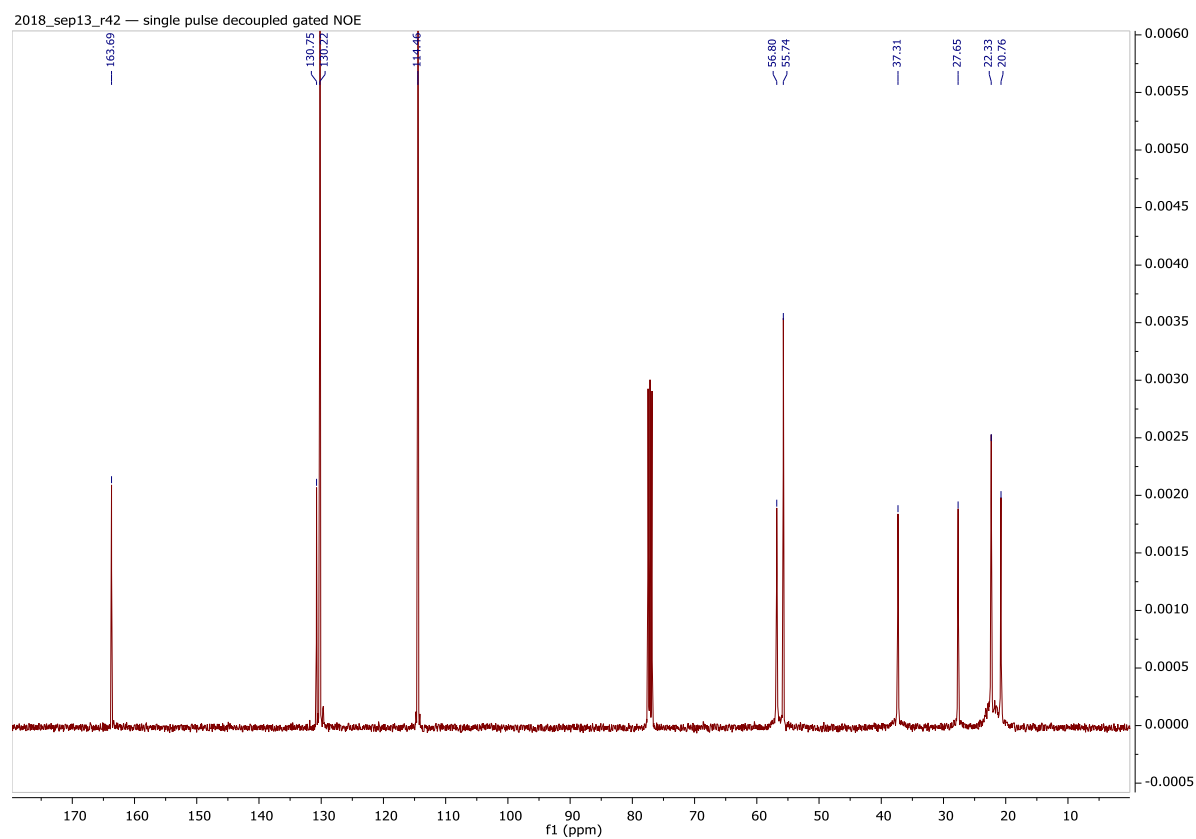
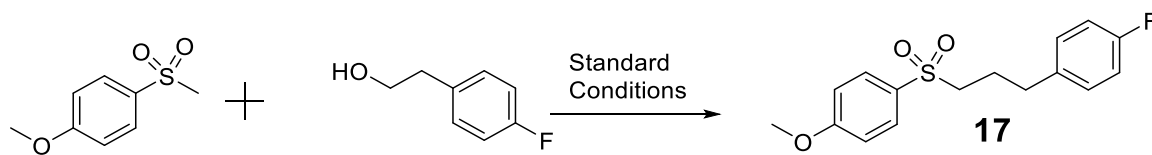


Figure S33. ^{13}C NMR of **16**.





Physical State: Colorless oil. Isolated Yield: 36%

^1H NMR (400 MHz, Chloroform- d) δ 7.78 (d, J = 9.0 Hz, 2H), 7.08 – 7.02 (m, 2H), 6.99 (d, J = 8.9 Hz, 2H), 6.93 (vt, J = 8.7 Hz, 2H), 3.87 (s, 3H), 3.05 – 2.99 (m, 2H), 2.65 (t, J = 7.5 Hz, 2H), 2.04 – 1.93 (m, 2H). ^{13}C NMR (101 MHz, Chloroform- d) δ 163.83, 161.60 (d, J_{CF} = 244.4 Hz), 135.70 (d, J_{CF} = 3.2 Hz), 130.64, 130.30, 129.88 (d, J_{CF} = 7.9 Hz), 115.48 (d, J_{CF} = 21.2 Hz), 114.57, 55.80, 55.69, 33.38, 24.60. HRMS: $[\text{C}_{16}\text{H}_{18}\text{O}_3\text{S}_1\text{F}_1; \text{M}+\text{H}]^+$ Expected 309.0961; Obtained 309.0961.

Figure S34. ^1H NMR of **17**.

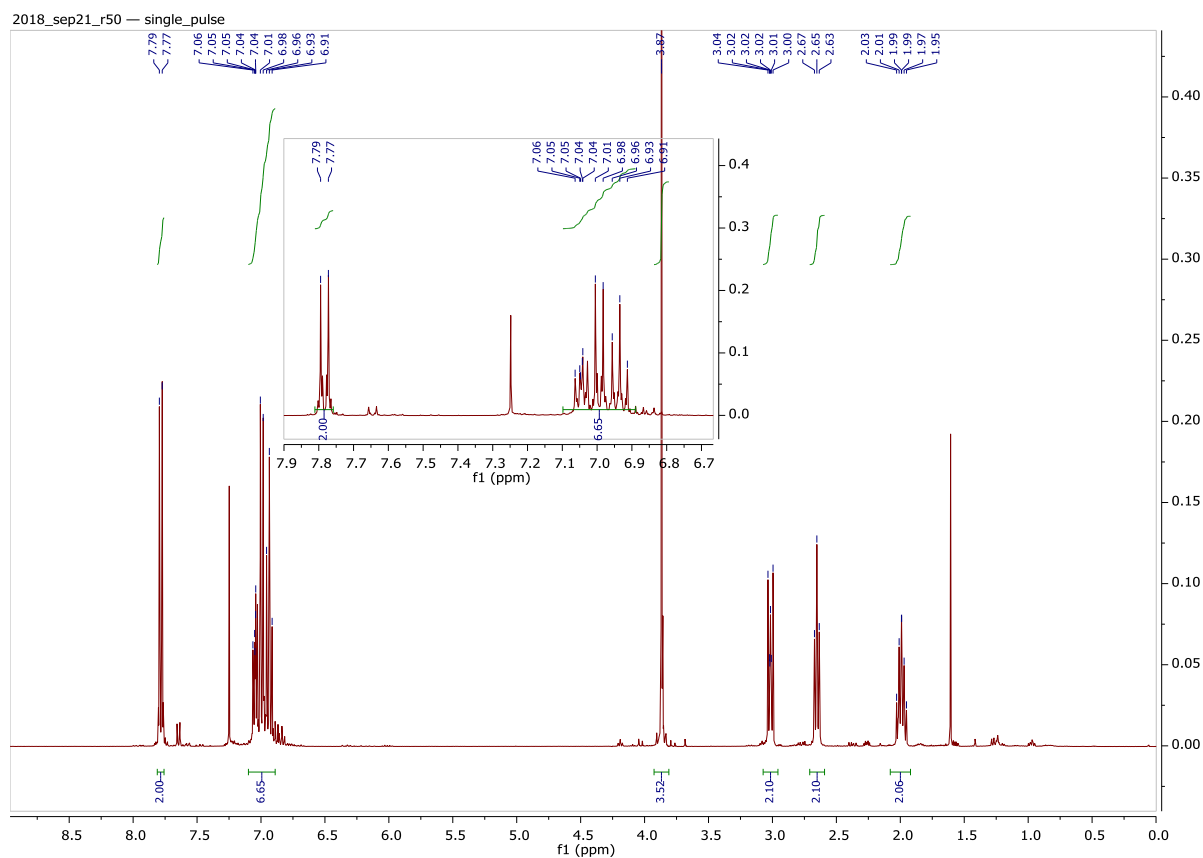
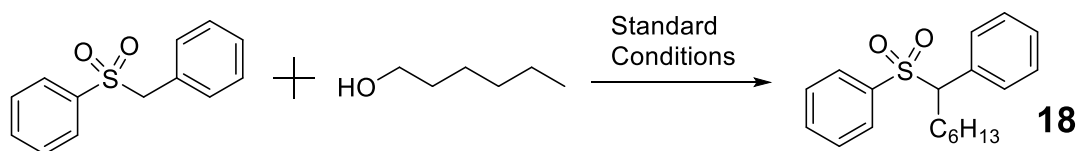
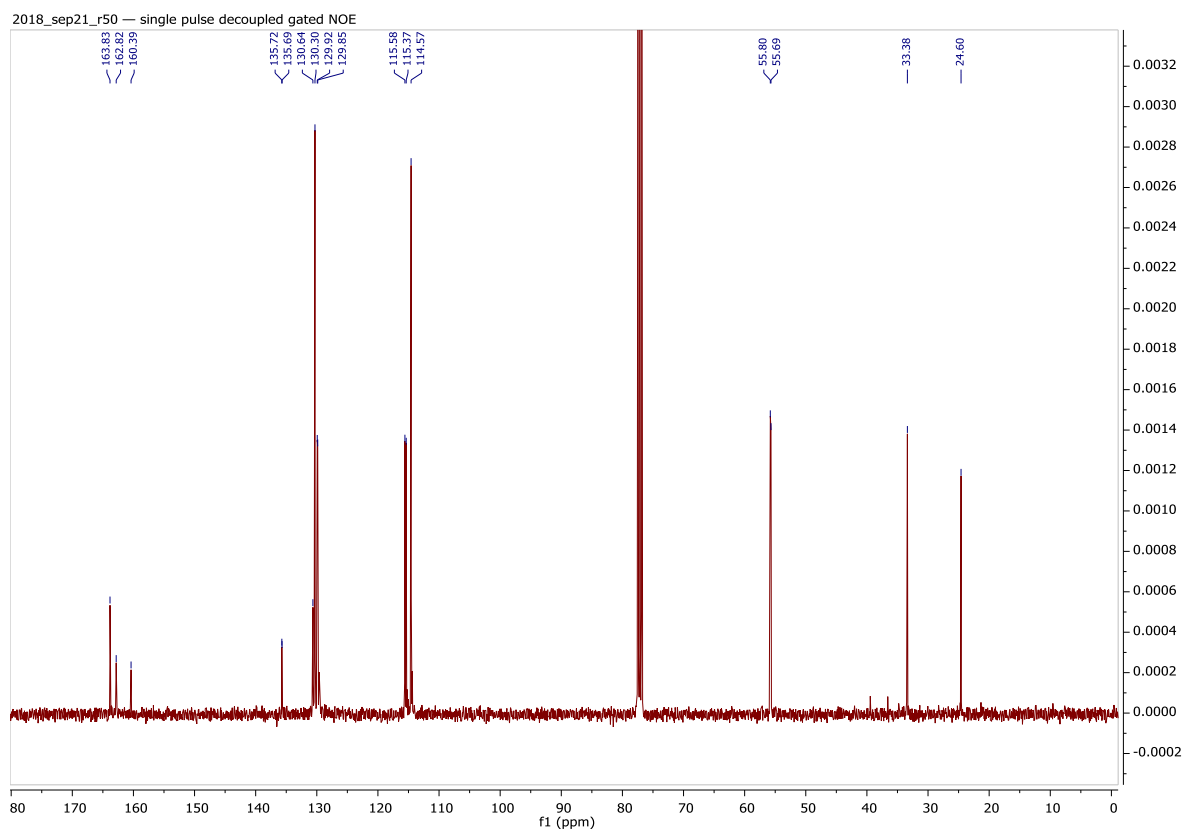


Figure S35. ^{13}C NMR of **17**.



Physical State: Clear oil that solidified on prolonged standing to a white solid. Isolated Yield: 79%

^1H NMR (400 MHz, Chloroform-*d*) δ 7.57 – 7.48 (m, 3H), 7.40 – 7.33 (m, 2H), 7.30 – 7.18 (m, 3H), 7.11 – 7.06 (m, 2H), 4.02 (dd, J = 11.6, 3.7 Hz, 1H), 2.41 (dtd, J = 13.3, 7.8, 3.6 Hz, 1H), 2.15 (ddt, J = 13.8, 11.8, 6.9 Hz, 1H), 1.35 – 1.07 (m, 8H), 0.82 (t, J = 6.9 Hz, 3H). ^{13}C NMR (101 MHz, Chloroform-*d*) δ 137.55, 133.49, 132.53, 129.98, 129.15, 128.81, 128.69, 128.57, 71.79, 31.51, 28.93, 27.31, 26.85, 22.61, 14.11. HRMS: [C₁₉H₂₅O₂S₁ ; M+H]⁺ Expected 317.1575; Obtained 317.1563.

Figure S36. ^1H NMR of **18**.

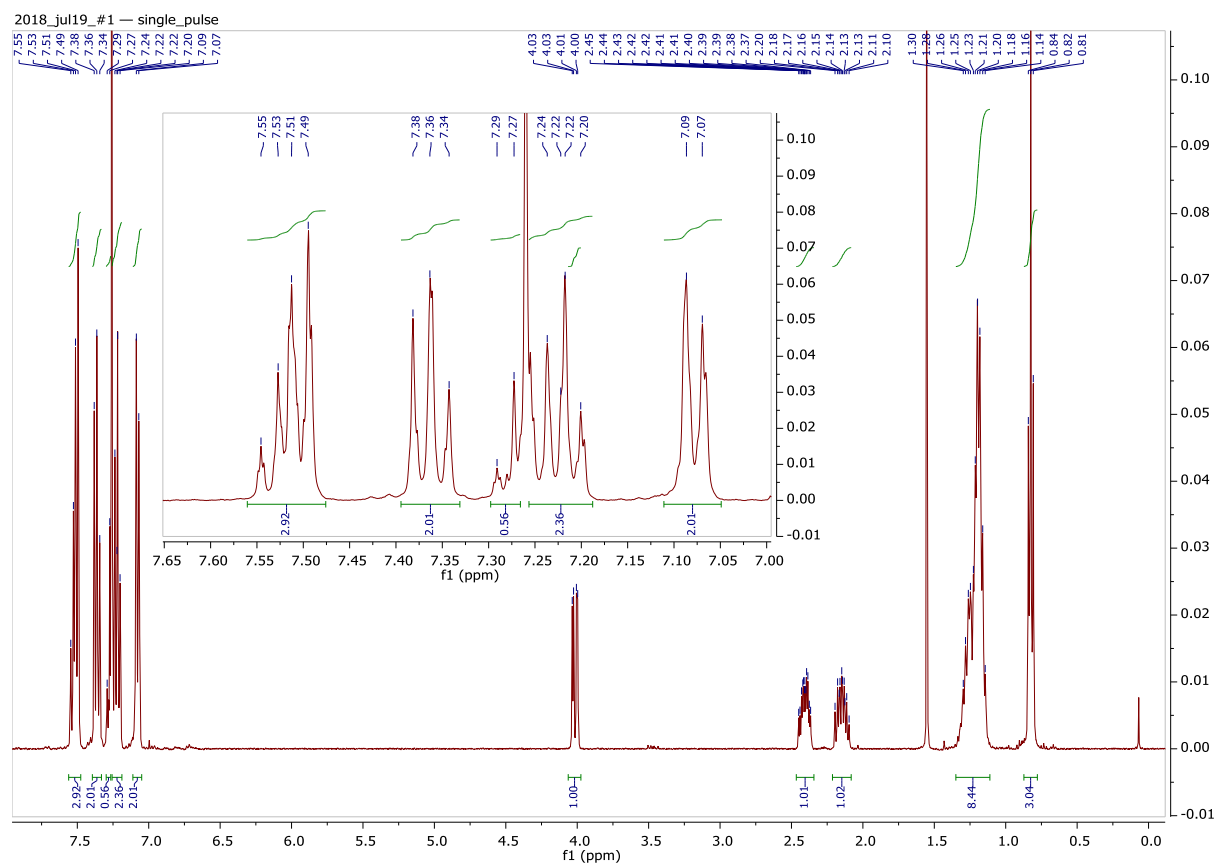
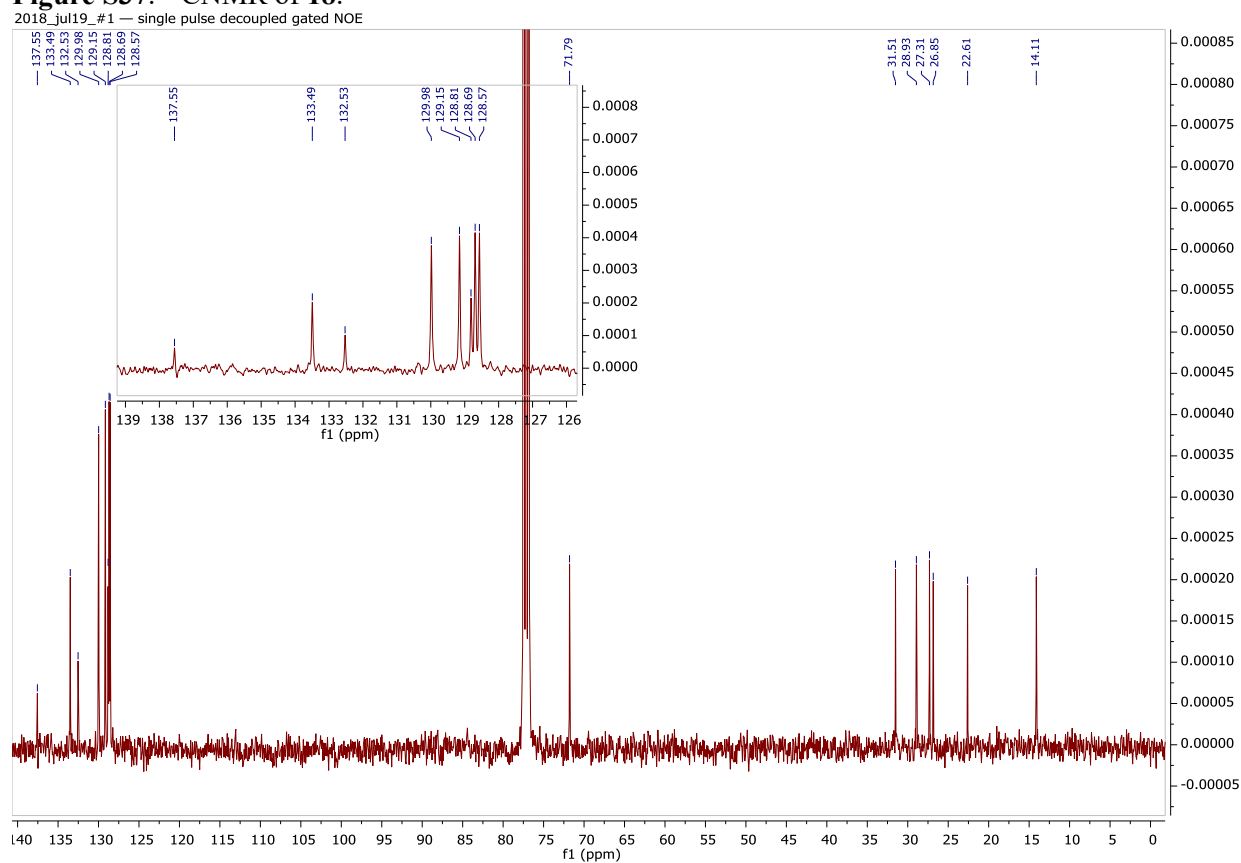
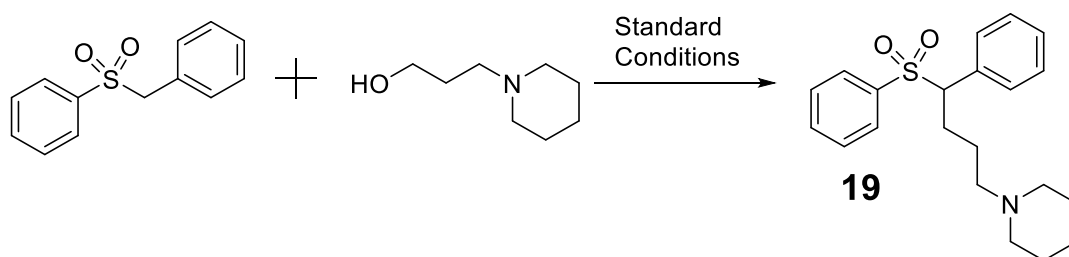


Figure S37. ^{13}C NMR of **18**.





Physical State: Light tan waxy solid. Isolated Yield: 62%

^1H NMR (400 MHz, Chloroform-*d*) δ 7.52 – 7.46 (m, 3H), 7.33 (dd, J = 8.5, 7.1 Hz, 2H), 7.27 – 7.14 (m, 3H), 7.08 – 7.04 (m, 2H), 4.08 (dd, J = 11.7, 3.7 Hz, 1H), 2.35 (ddt, J = 16.8, 8.2, 4.1 Hz, 1H), 2.27 – 2.08 (m, 7H), 1.43–1.50 (m, 4H), 1.40 – 1.29 (m, 4H). ^{13}C NMR (101 MHz, Chloroform-*d*) δ 137.44, 133.45, 132.23, 129.94, 129.05, 128.79, 128.64, 128.50, 71.43, 58.69, 54.60, 25.98, 25.63, 24.43, 24.17. HRMS: $[\text{C}_{21}\text{H}_{28}\text{O}_2\text{S}_1\text{N}_1; \text{M}+\text{H}]^+$ Expected 358.1841; Obtained 358.1876.

Figure S38. ^1H NMR of **19**.

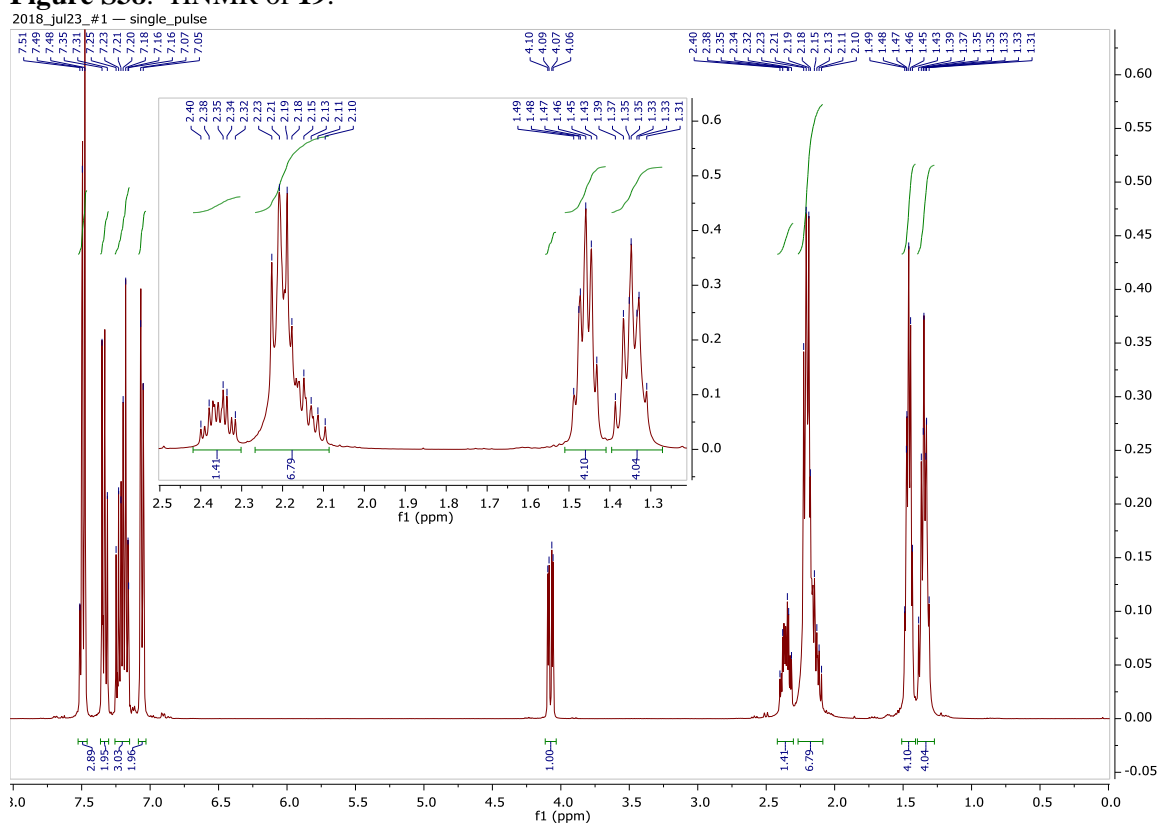
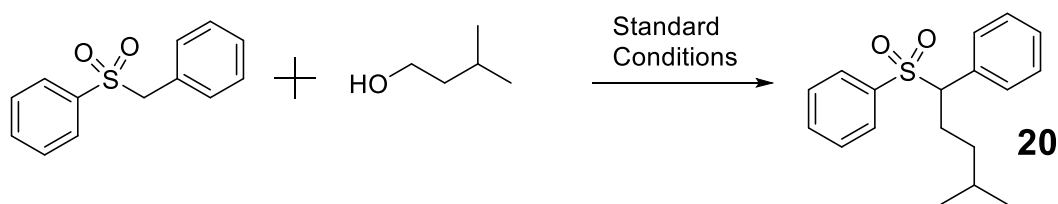
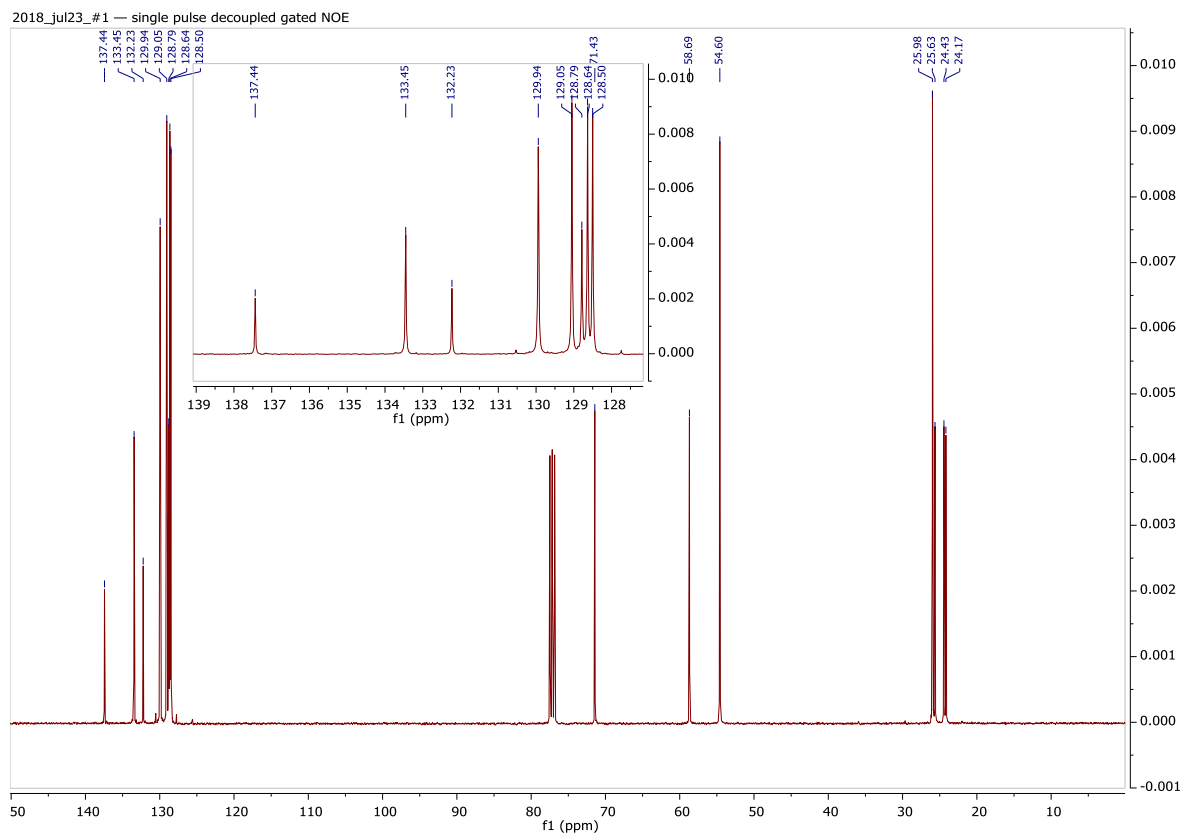


Figure S39. ^{13}C NMR of **19**.



Physical State: White solid. Isolated Yield: 82%

^1H NMR (400 MHz, Chloroform-*d*) δ 7.55 – 7.45 (m, 3H), 7.31-7.37 (m, 2H), 7.29 – 7.17 (m, 3H), 7.08 – 7.03 (m, 2H), 3.97 (dd, J = 11.7, 3.6 Hz, 1H), 2.42 (dddd, J = 13.2, 11.2, 5.8, 3.5 Hz, 1H), 2.13 (dtd, J = 13.4, 11.2, 4.7 Hz, 1H), 1.52 (dp, J = 13.4, 6.7 Hz, 1H), 1.15 – 1.05 (m, 1H), 1.04 – 0.94 (m, 1H), 0.81 (v.dd, 6H). ^{13}C NMR (101 MHz, Chloroform-*d*) δ 137.47, 133.48, 132.47, 129.92, 129.07, 128.78, 128.66, 128.54, 71.94, 35.87, 27.92, 25.19, 22.73, 22.09. HRMS: $[\text{C}_{18}\text{H}_{22}\text{O}_2\text{S}_1\text{Na}_1; \text{M}+\text{Na}]^+$ Expected 325.1238; Obtained 325.1245.

Figure S40. ^1H NMR of **20**.

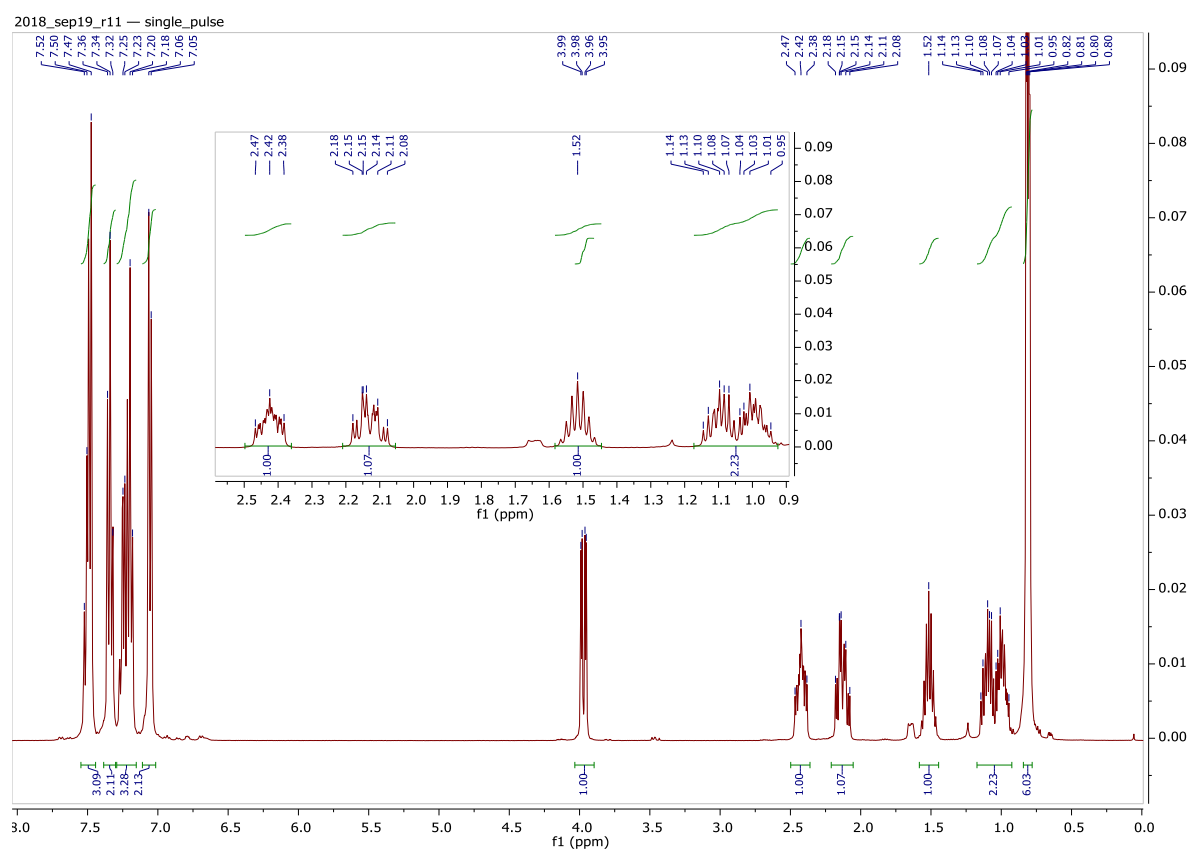
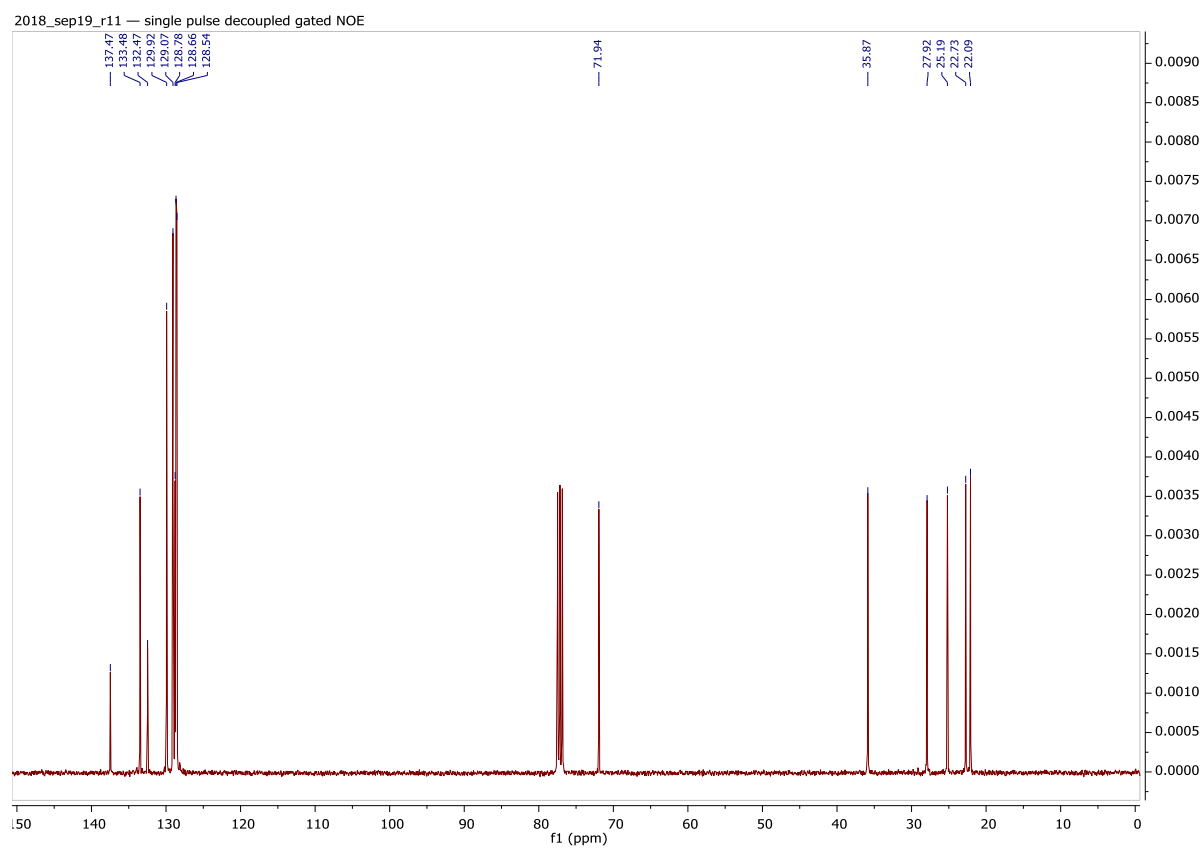
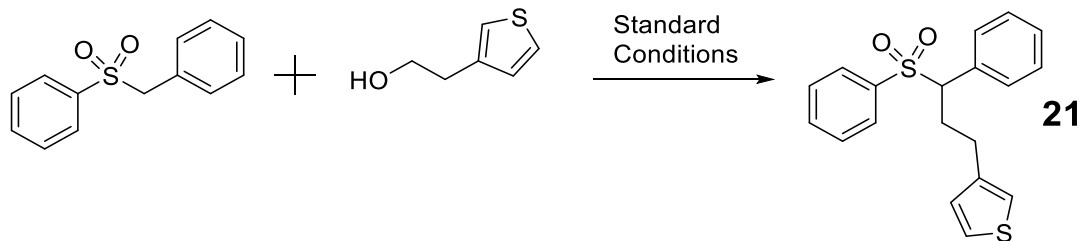


Figure S41. ^{13}C NMR of **20**.





Physical State: White solid. Isolated Yield: 17%

^1H NMR (400 MHz, Chloroform-*d*) δ 7.55 – 7.45 (m, 3H), 7.37 – 7.20 (m, 6H), 7.07 (d, J = 7.3 Hz, 2H), 6.82 (d, J = 4.1 Hz, 2H), 3.98 (dd, J = 11.0, 3.6 Hz, 1H), 2.81 – 2.58 (m, 2H), 2.53 – 2.39 (m, 2H). ^{13}C NMR (101 MHz, Chloroform-*d*) δ 140.31, 137.32, 133.58, 131.98, 130.09, 129.12, 129.01, 128.73, 128.70, 127.97, 125.97, 121.05, 70.60, 28.08, 27.07. HRMS: $[\text{C}_{19}\text{H}_{18}\text{O}_2\text{S}_2\text{Na}]^+$ Expected 365.0646; Obtained 365.0661.

Figure S42. ^1H NMR of **21**.

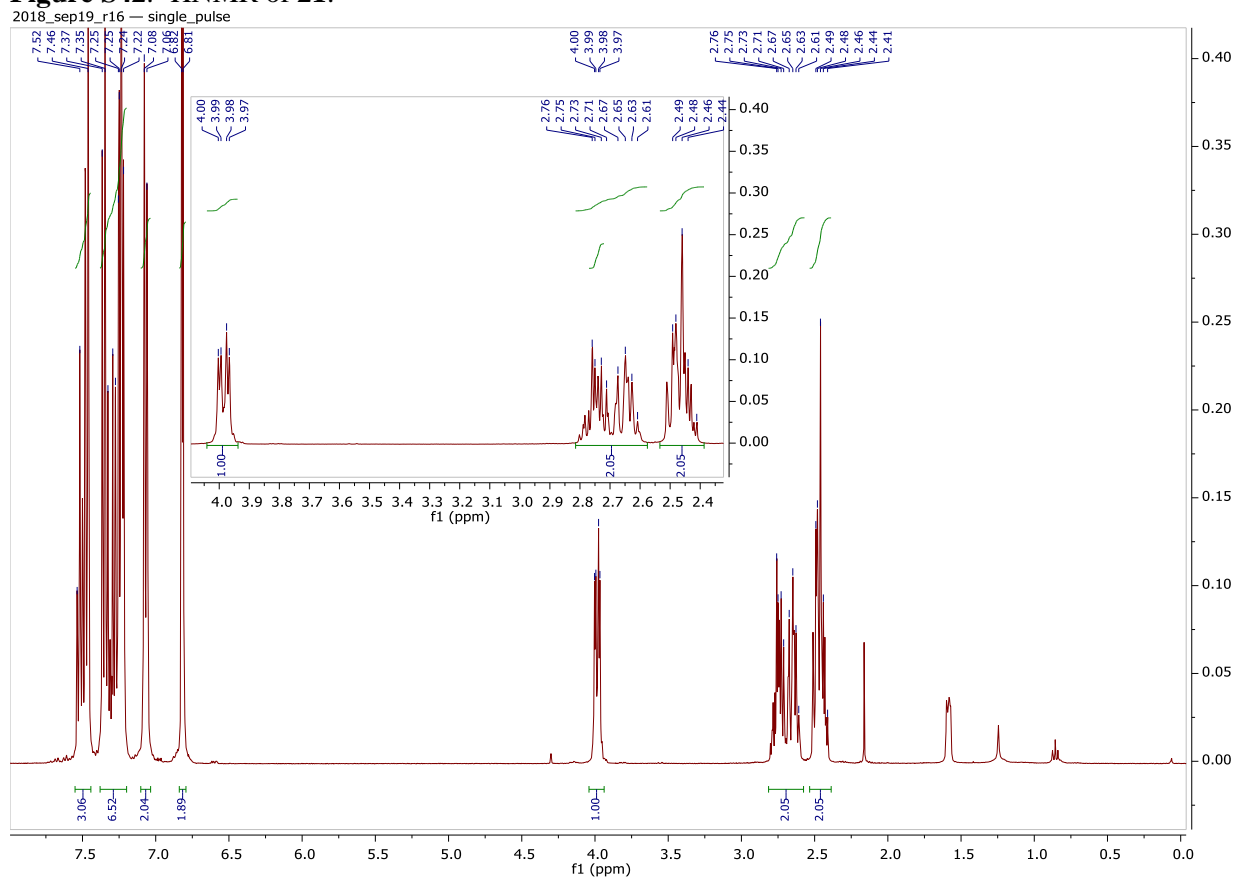
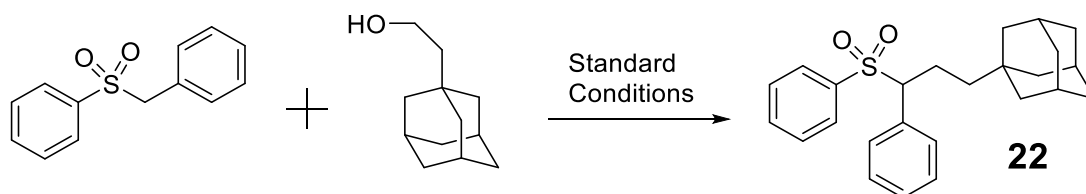
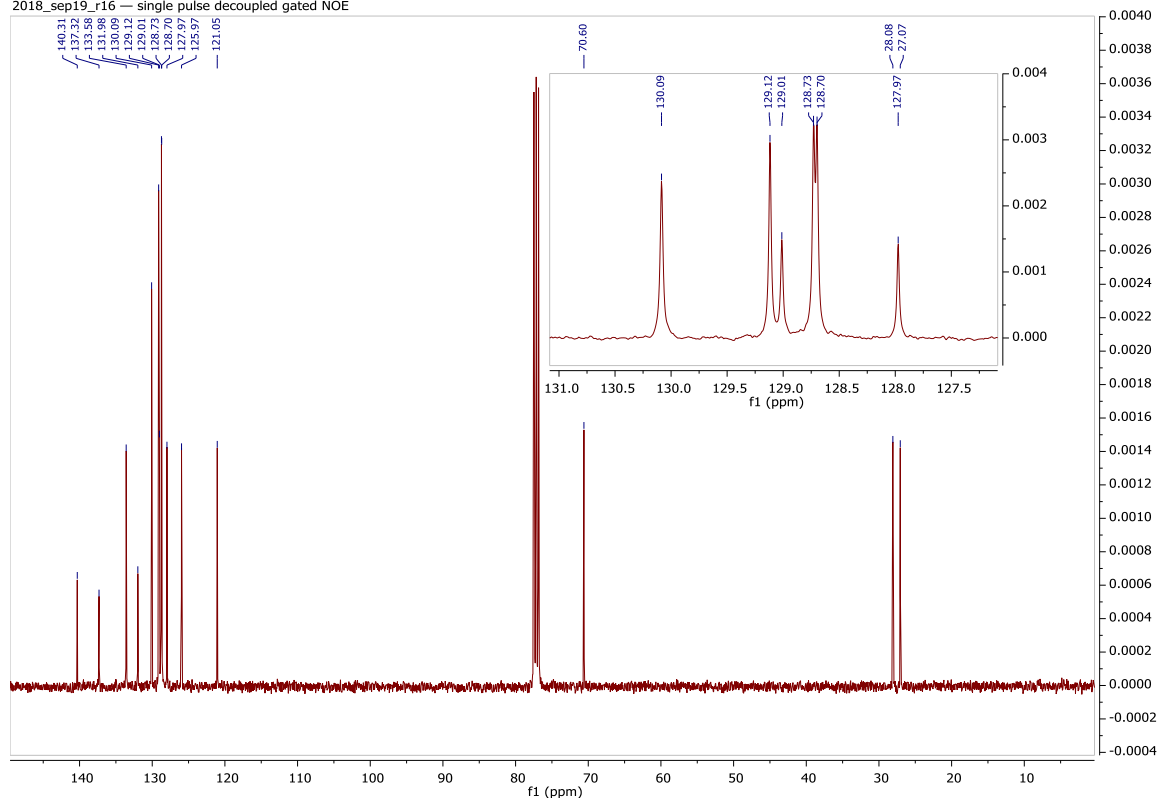


Figure S43. ^{13}C NMR of **21**.

2018_sep19_r16 — single pulse decoupled gated NOE



Physical State: White crystalline solid. Isolated Yield: 72%

^1H NMR (600 MHz, Chloroform-*d*) δ 7.40 (t, J = 7.4 Hz, 1H), 7.37 (d, J = 7.5 Hz, 2H), 7.24 (t, J = 7.7 Hz, 2H), 7.15 (t, J = 7.3 Hz, 1H), 7.09 (t, J = 7.5 Hz, 2H), 6.93 (d, J = 7.6 Hz, 2H), 3.81 (dd, J = 11.7, 3.4 Hz, 1H), 2.33 (tt, J = 13.0, 4.1 Hz, 1H), 2.00 (qd, J = 12.5, 4.0 Hz, 1H), 1.80 (s, 3H), 1.56 (d, J = 12.3 Hz, 3H), 1.47 (d, J = 12.4 Hz, 3H), 1.31 (t, J = 9.6 Hz, 6H), 0.87 (td, J = 13.0, 4.7 Hz, 1H), 0.73 (td, J = 13.0, 4.1 Hz, 1H). ^{13}C NMR (151 MHz, Chloroform-*d*) δ 137.61, 133.44, 132.60, 129.96, 129.08, 128.75, 128.64, 128.52, 72.53, 42.26, 41.38, 37.18, 32.40, 28.71, 20.59. HRMS: $[\text{C}_{25}\text{H}_{30}\text{O}_2\text{S}_1\text{Na}_1]^+$ Expected 417.1864; Obtained 417.1875.

Figure S44. ^1H NMR of **22**.

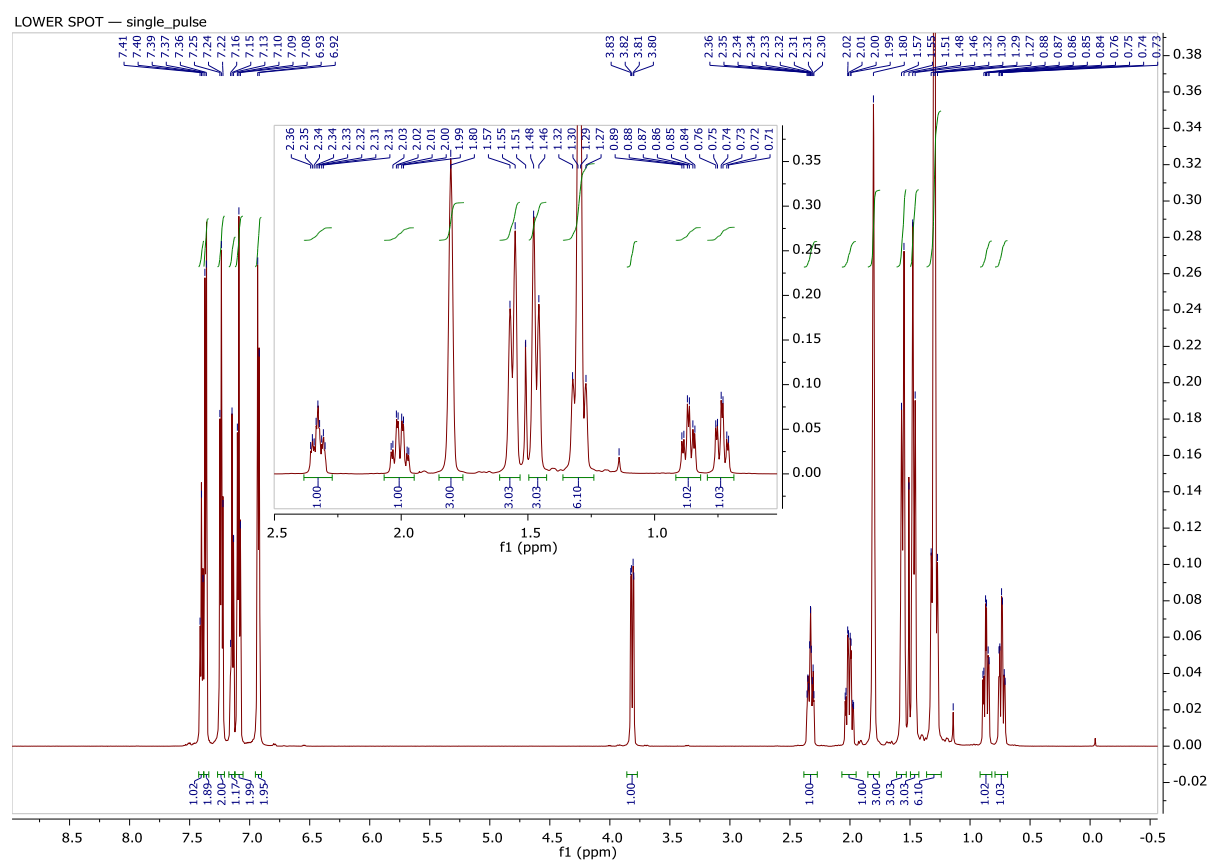
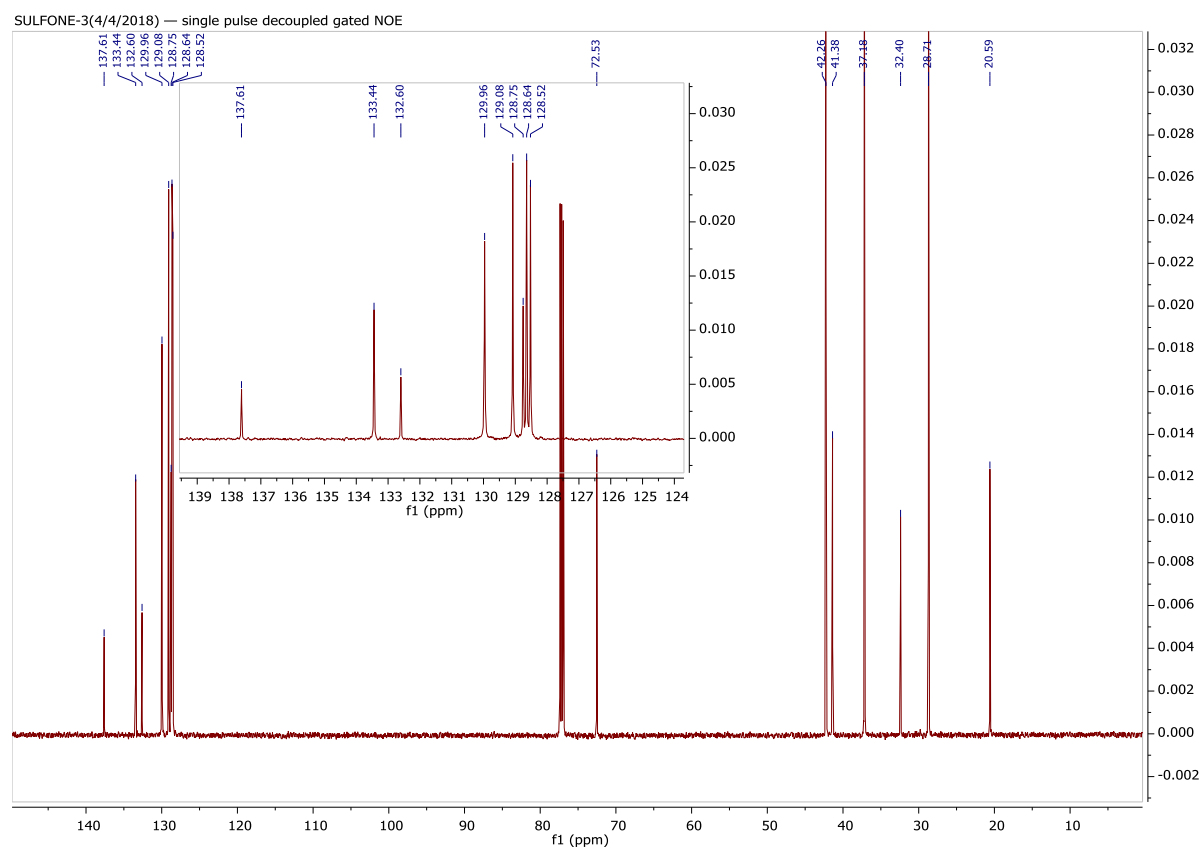
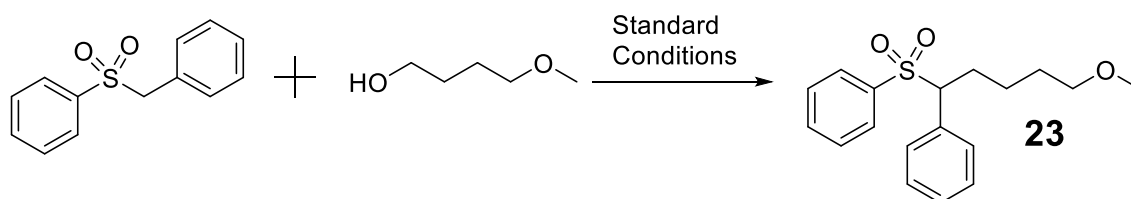


Figure S45. ^{13}C NMR of **22**.





Physical State: White crystalline solid. Isolated Yield: 67%

^1H NMR (400 MHz, Chloroform-*d*) δ 7.56 – 7.45 (m, 3H), 7.40 – 7.30 (m, 2H), 7.31 – 7.15 (m, 3H), 7.06 (d, J = 6.8 Hz, 2H), 4.01 (dd, J = 11.6, 3.7 Hz, 1H), 3.26 (td, J = 6.4, 1.7 Hz, 2H), 3.23 (s, 3H), 2.41 (dtd, J = 16.9, 8.3, 7.8, 3.7 Hz, 1H), 2.26 – 2.08 (m, 1H), 1.54 (tq, J = 13.7, 6.9 Hz, 2H), 1.26 (h, J = 7.1 Hz, 2H). ^{13}C NMR (101 MHz, Chloroform-*d*) δ 137.49, 133.52, 132.32, 129.97, 129.12, 128.86, 128.70, 128.60, 72.25, 71.67, 58.64, 29.26, 27.20, 23.66. HRMS: $[\text{C}_{18}\text{H}_{23}\text{O}_3\text{S}_1; \text{M}+\text{H}]^+$ Expected 319.1368; Obtained 319.1359.

Figure S46. ^1H NMR of **23**.

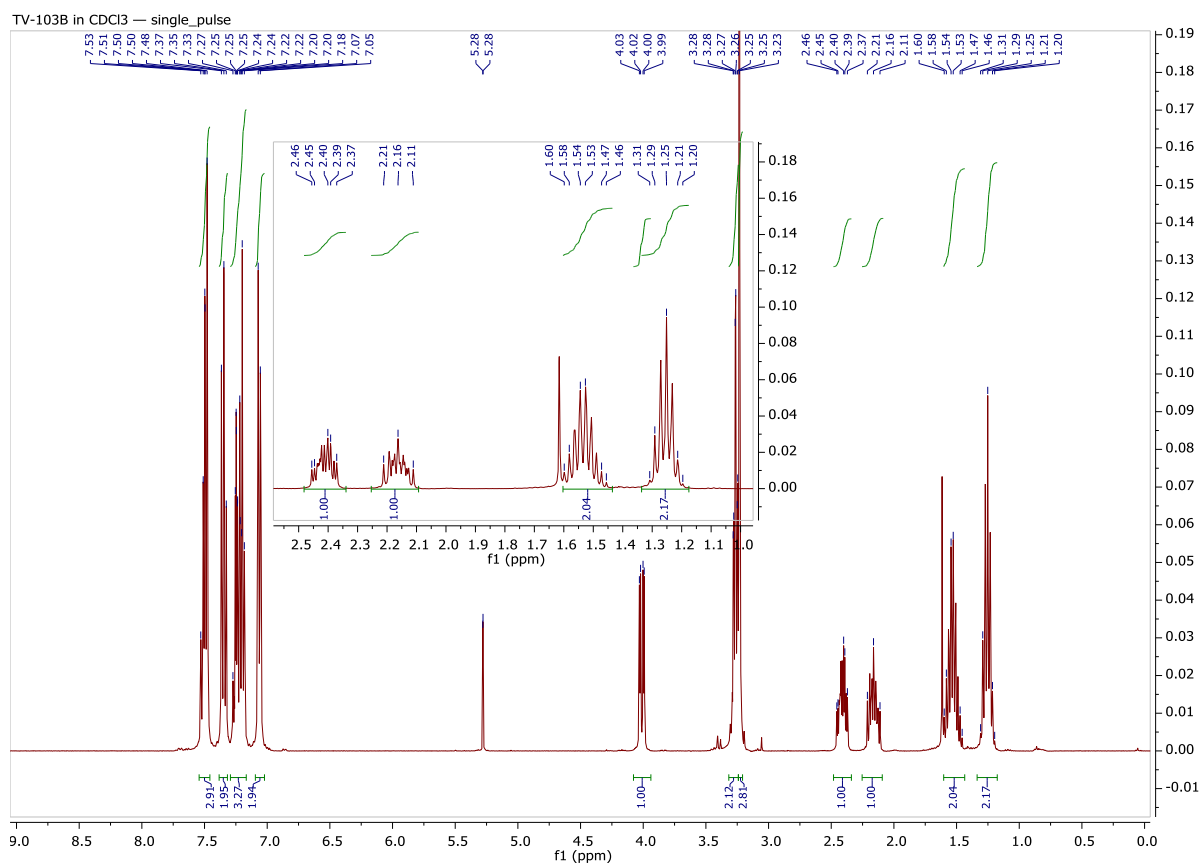
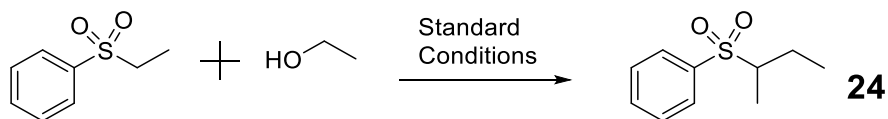
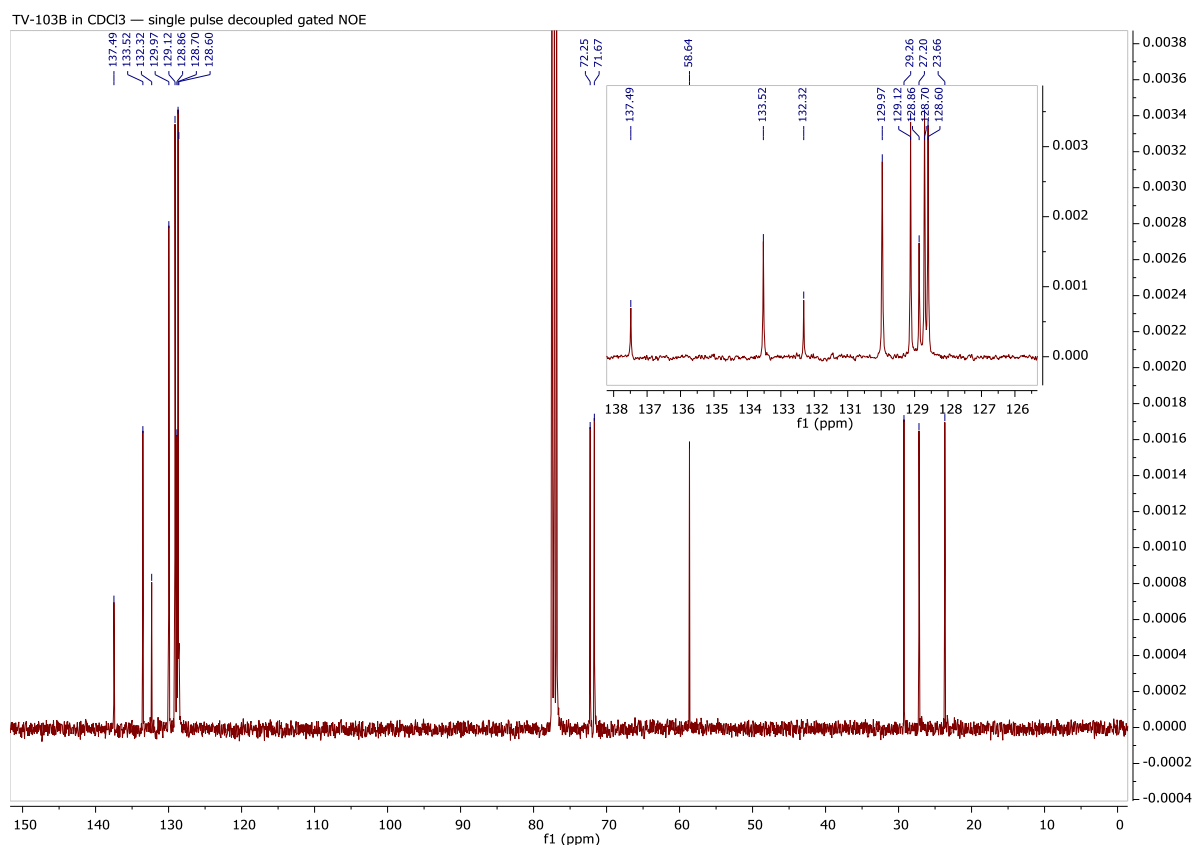


Figure S47. ^{13}C NMR of **23**.



Physical State: Colorless liquid. Isolated Yield: 69%

^1H NMR (600 MHz, $\text{Chloroform-}d$) δ 7.88 (d, $J = 7.4$ Hz, 2H), 7.65 (t, $J = 7.4$ Hz, 1H), 7.56 (vt, $J = 7.8$ Hz, 2H), 2.95 (dq, $J = 10.5, 6.9, 3.6$ Hz, 1H), 1.97 – 2.05 (m, 1H), 1.48 – 1.38 (m, 1H), 1.26 (d, $J = 6.9$ Hz, 3H), 0.97 (t, $J = 7.5$ Hz, 3H). ^{13}C NMR (151 MHz, $\text{Chloroform-}d$) δ 137.55, 133.67, 129.18, 129.14, 61.67, 22.62, 12.70, 11.28. HRMS: $[\text{C}_{10}\text{H}_{14}\text{O}_2\text{S}_1\text{Na}_1; \text{M}+\text{Na}]^+$ Expected 221.0612; Obtained 221.0616.

Figure S48. ^1H NMR of **24**.

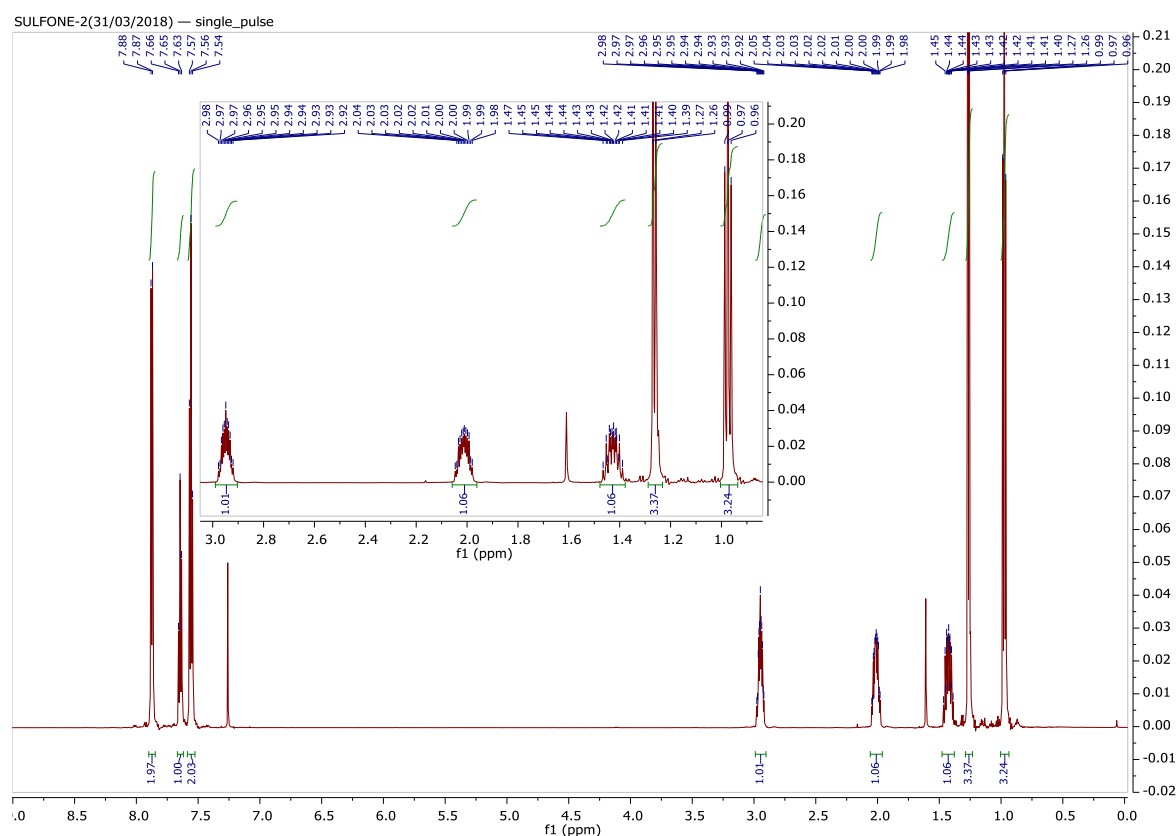
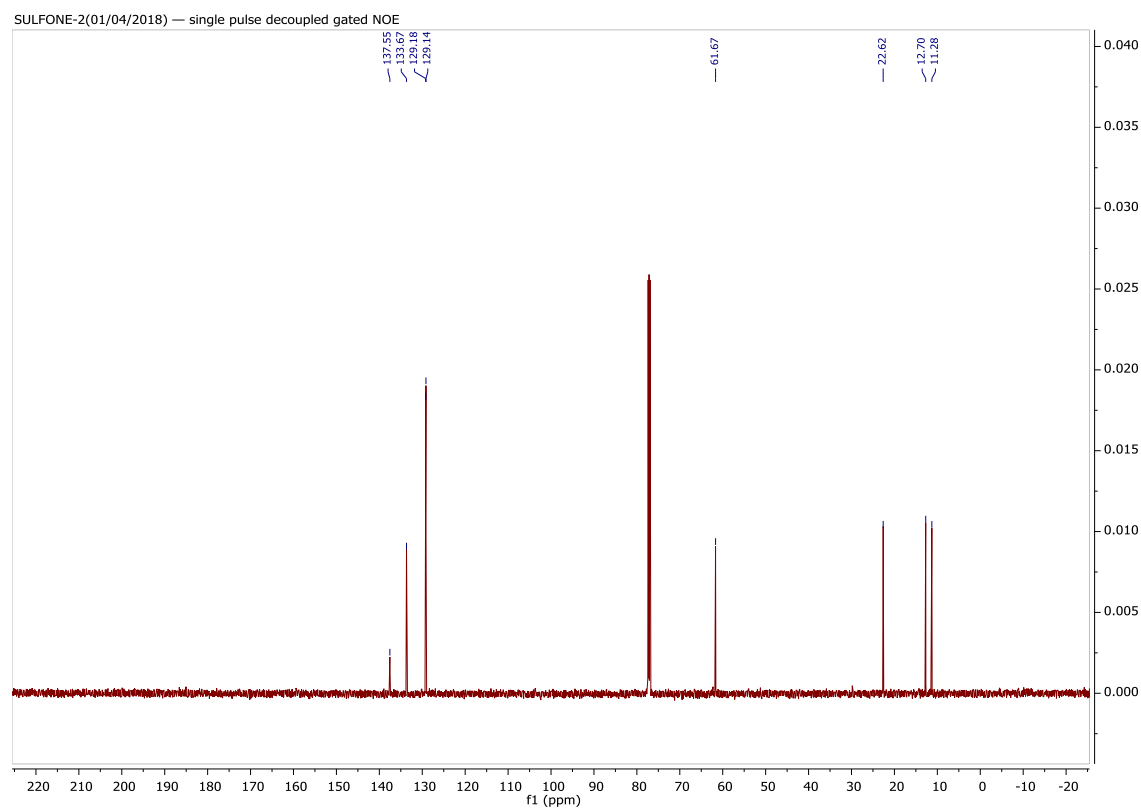
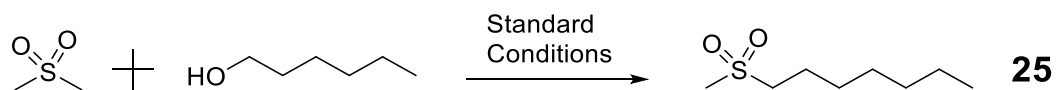


Figure S49. ^{13}C NMR of **24**.





Physical State: Viscous, colorless oil. Isolated Yield: 71%

^1H NMR (600 MHz, Chloroform-*d*) δ 3.03 – 2.97 (m, 2H), 2.89 (s, 3H), 1.89 – 1.80 (m, 2H), 1.48 – 1.40 (m, 2H), 1.37 – 1.22 (m, 6H), 0.88 (t, $J = 6.9$ Hz, 3H). ^{13}C NMR (151 MHz, Chloroform-*d*) δ 55.01, 40.54, 31.55, 28.84, 28.49, 22.64, 22.59, 14.14. HRMS: $[\text{C}_8\text{H}_{18}\text{O}_2\text{S}_1\text{Na}_1; \text{M}+\text{Na}]^+$ Expected 201.0925; Obtained 201.0918.

Figure S50. ^1H NMR of **25**.

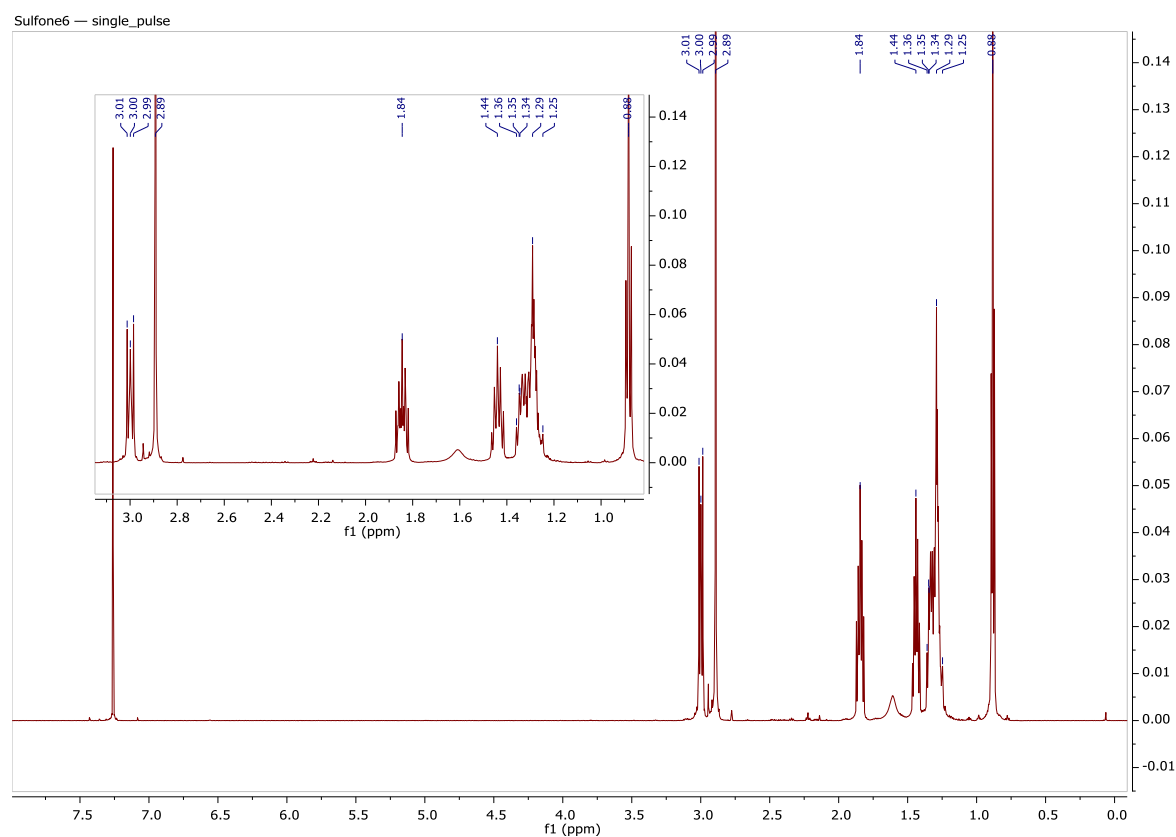
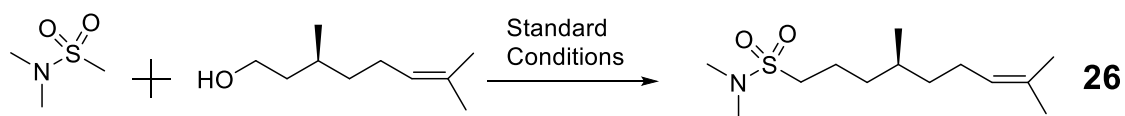
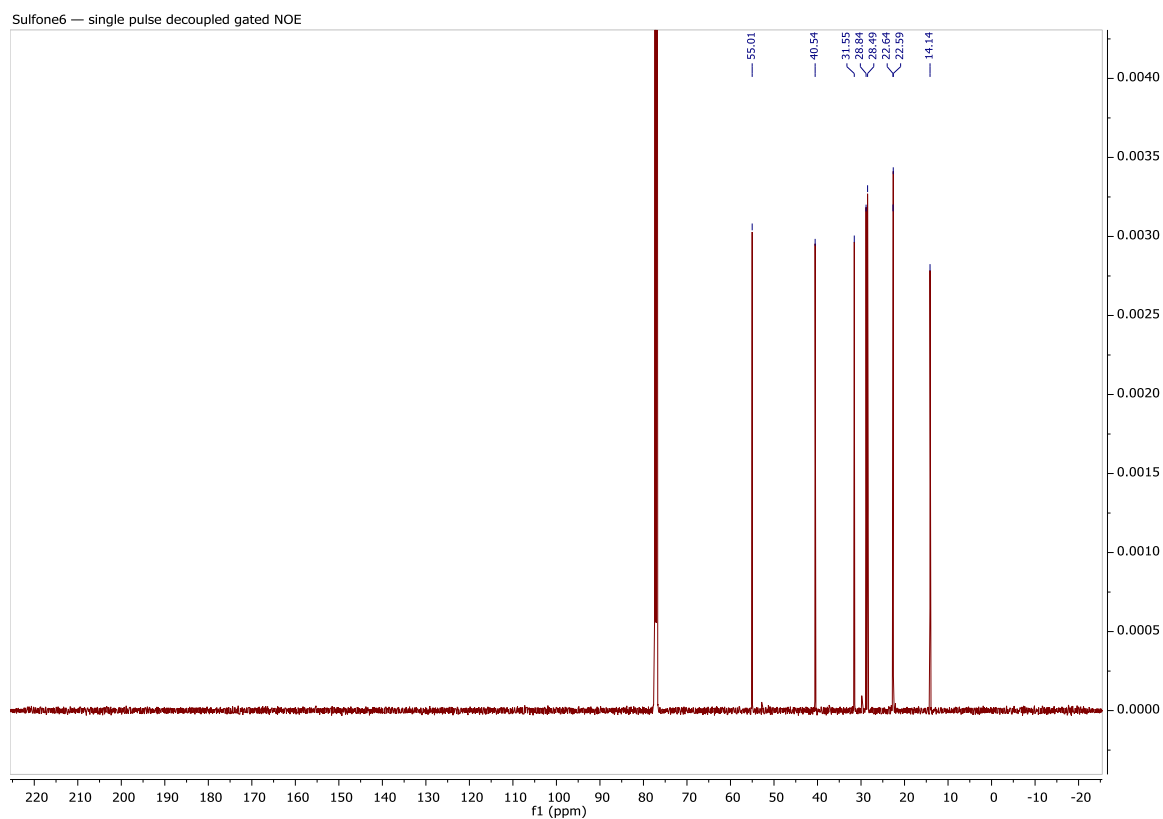


Figure S51. ^{13}C NMR of **25**.



Physical State: Colorless oil. Isolated Yield: 95%

^1H NMR (600 MHz, Chloroform-*d*) δ 5.07 (tp, $J = 7.1, 1.4$ Hz, 1H), 2.91 – 2.83 (m, 2H), 2.87 (s, 6H), 2.03 – 1.89 (m, 2H), 1.88 – 1.81 (m, 1H), 1.80 – 1.72 (m, 1H), 1.67 (s, 3H), 1.59 (s, 3H), 1.47 – 1.36 (m, 2H), 1.32 (dddd, $J = 13.3, 9.5, 6.5, 5.2$ Hz, 1H), 1.27 – 1.20 (m, 1H), 1.15 (dddd, $J = 13.5, 9.4, 7.7, 5.9$ Hz, 1H), 0.89 (d, $J = 6.6$ Hz, 3H). ^{13}C NMR (101 MHz, Chloroform-*d*) δ 131.48, 124.70, 48.61, 37.64, 36.92, 35.85, 32.20, 25.84, 25.55, 20.82, 19.41, 17.78. HRMS: $[\text{C}_{13}\text{H}_{27}\text{N}_1\text{O}_2\text{S}_1; \text{M}+\text{H}]^+$ Expected 262.1841; Obtained 262.1820.

Figure S52. ^1H NMR of **26**.

tv118 — single_pulse

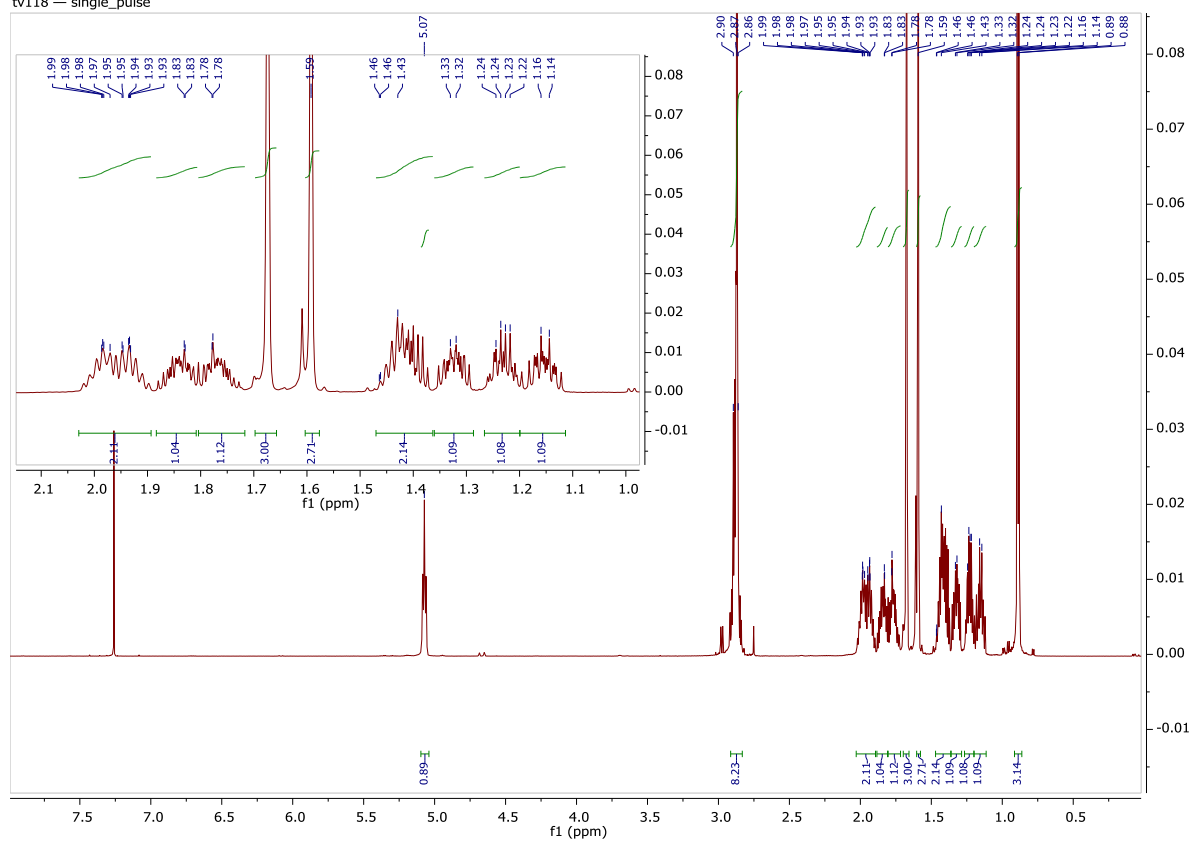


Figure S53. ^{13}C NMR of **26**.

TV-118citro — single pulse decoupled gated NOE

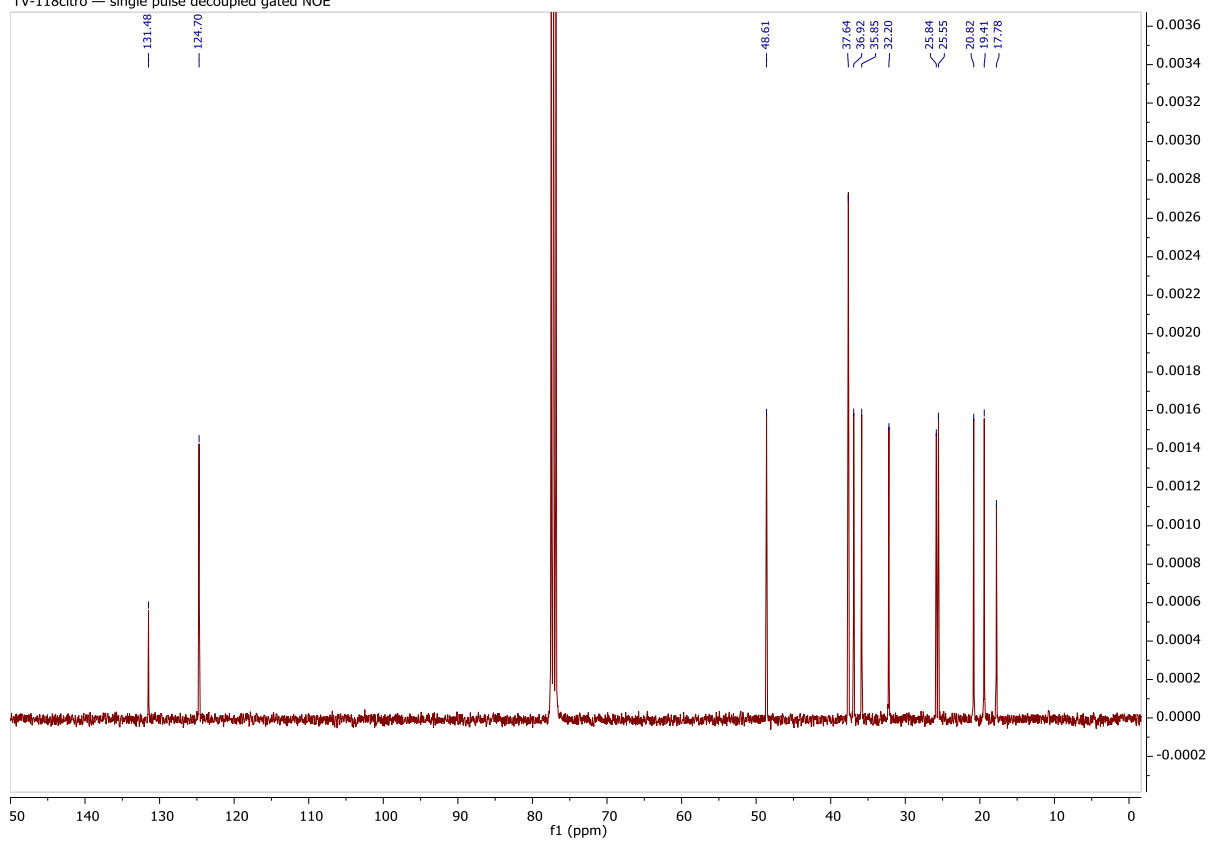
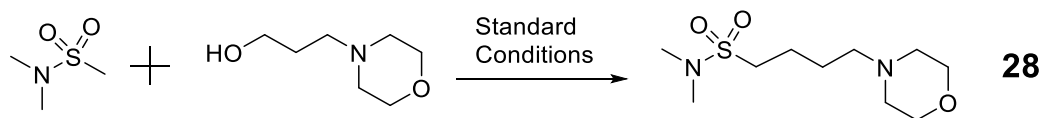
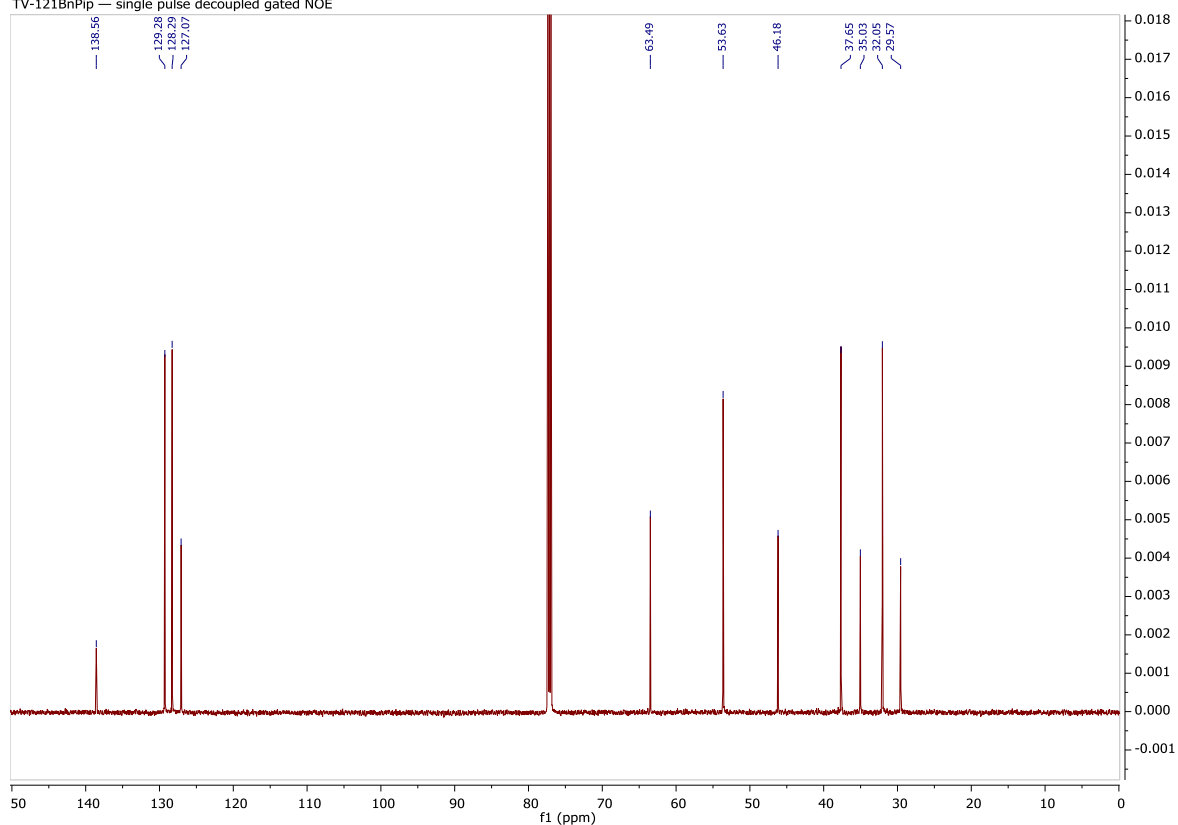


Figure S55. ^{13}C NMR of **27**.

TV-121BnPip — single pulse decoupled gated NOE



Physical State: Colorless oil. Isolated Yield: 85%

^1H NMR (400 MHz, Chloroform- d) δ 3.67 (t, J = 4.0 Hz, 4H), 2.97 – 2.90 (m, 2H), 2.85 (s, 6H), 2.40 (bs, 4H), 2.36 – 2.30 (m, 2H), 1.83 (dddd, J = 12.1, 9.3, 5.4, 1.6 Hz, 2H), 1.55 – 1.63 (m, 2H). ^{13}C NMR (101 MHz, Chloroform- d) δ 67.00, 58.19, 53.73, 47.91, 37.59, 25.32, 21.18. HRMS: $[\text{C}_{10}\text{H}_{23}\text{O}_3\text{N}_2\text{S}]^+$; Expected 251.1430; Obtained 251.1406.

Figure S56. ^1H NMR of **28**.

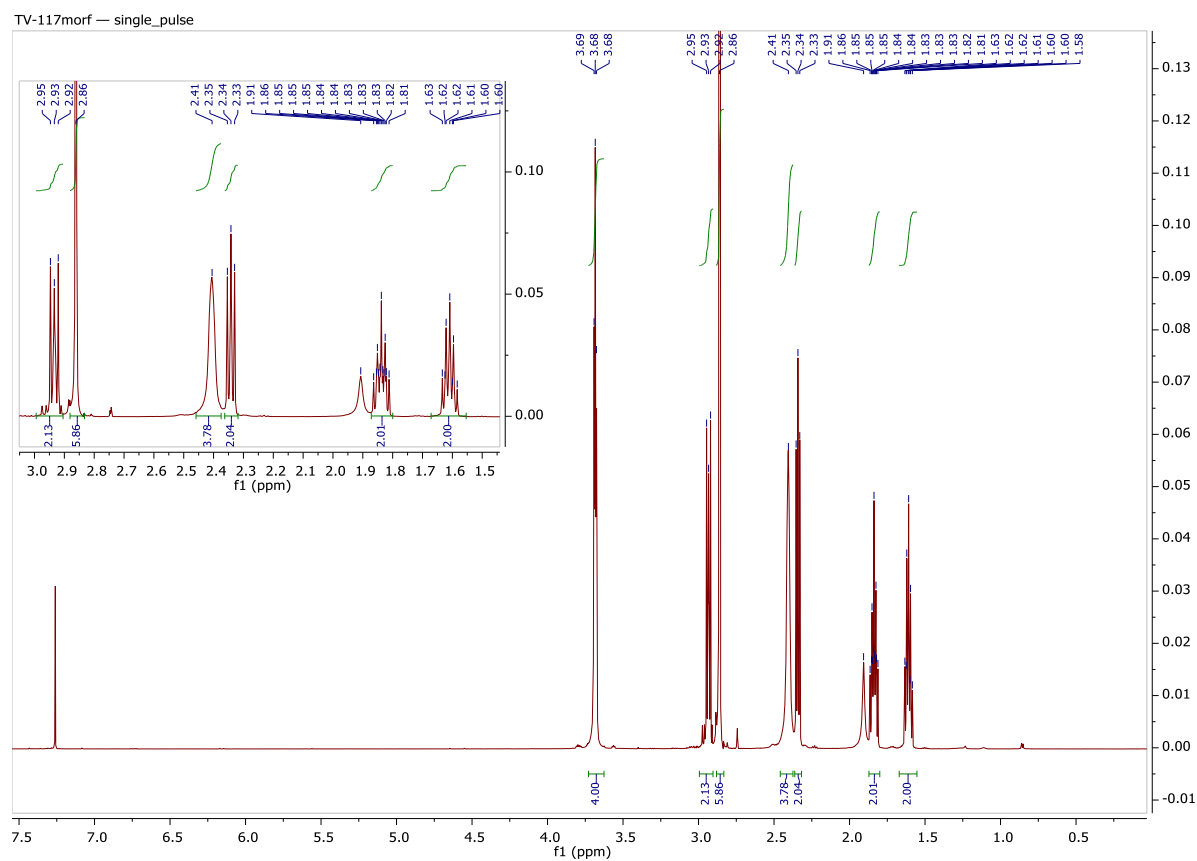
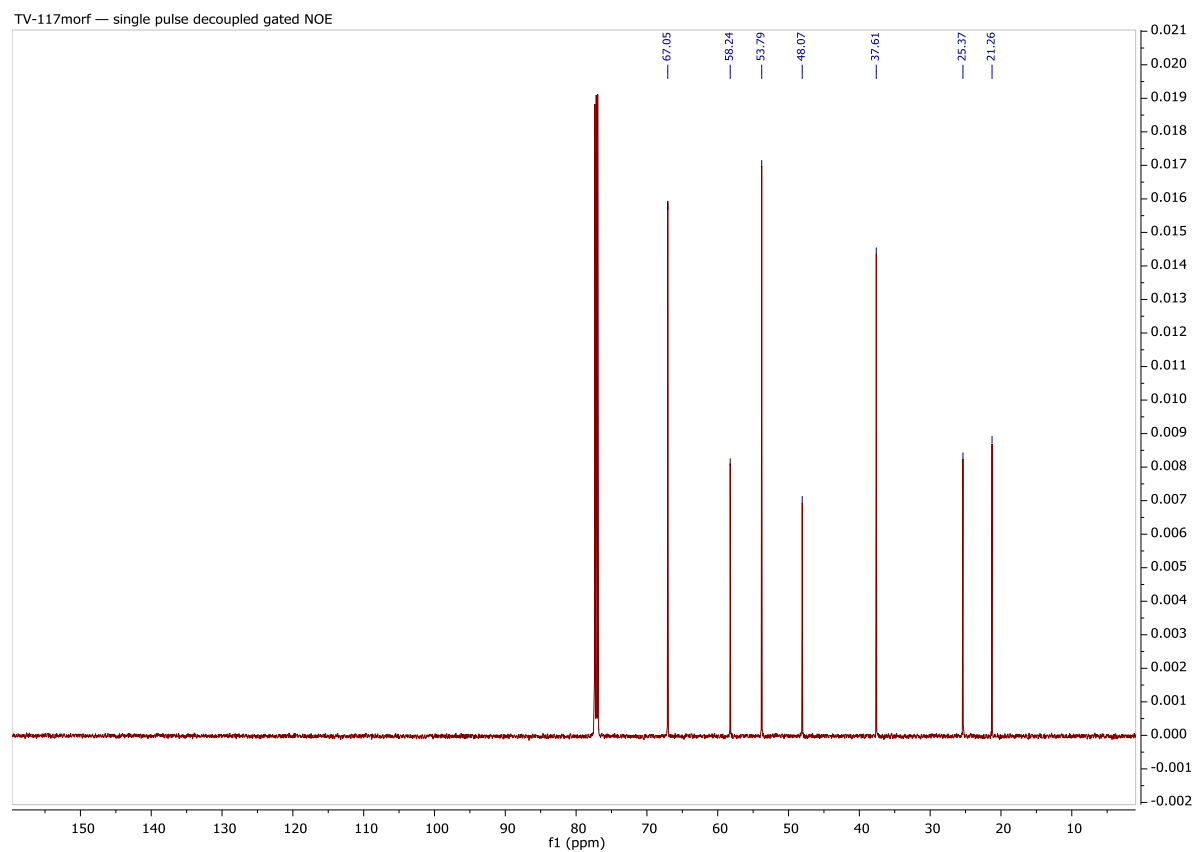
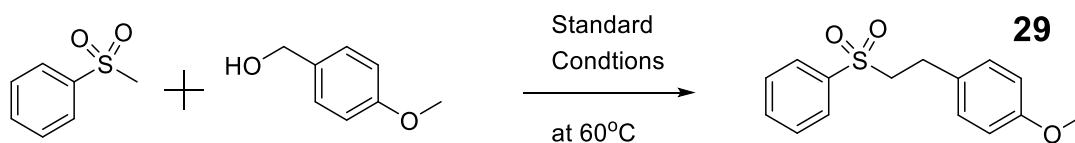


Figure S57. ^{13}C NMR of **28**.





Physical State: White crystalline solid. Isolated Yield: 78%

^1H NMR (400 MHz, Chloroform- d) δ 7.93 (d, J = 7.2 Hz, 2H), 7.67 (d, J = 7.2 Hz, 1H), 7.57 (t, J = 7.2 Hz, 2H), 7.02 (d, J = 8.7 Hz, 2H), 6.79 (d, J = 8.7 Hz, 2H), 3.75 (s, 3H), 3.38 – 3.27 (m, 2H), 3.03 – 2.93 (m, 2H). ^{13}C NMR (101 MHz, Chloroform- d) δ 158.61, 139.16, 133.87, 129.47, 129.44, 129.39, 128.16, 114.29, 57.84, 55.36, 27.98. HRMS: $[\text{C}_{15}\text{H}_{17}\text{O}_3\text{S}_1; \text{M}+\text{H}]^+$ Expected 277.0899; Obtained 277.0890.

Figure S58. ^1H NMR of **29**.

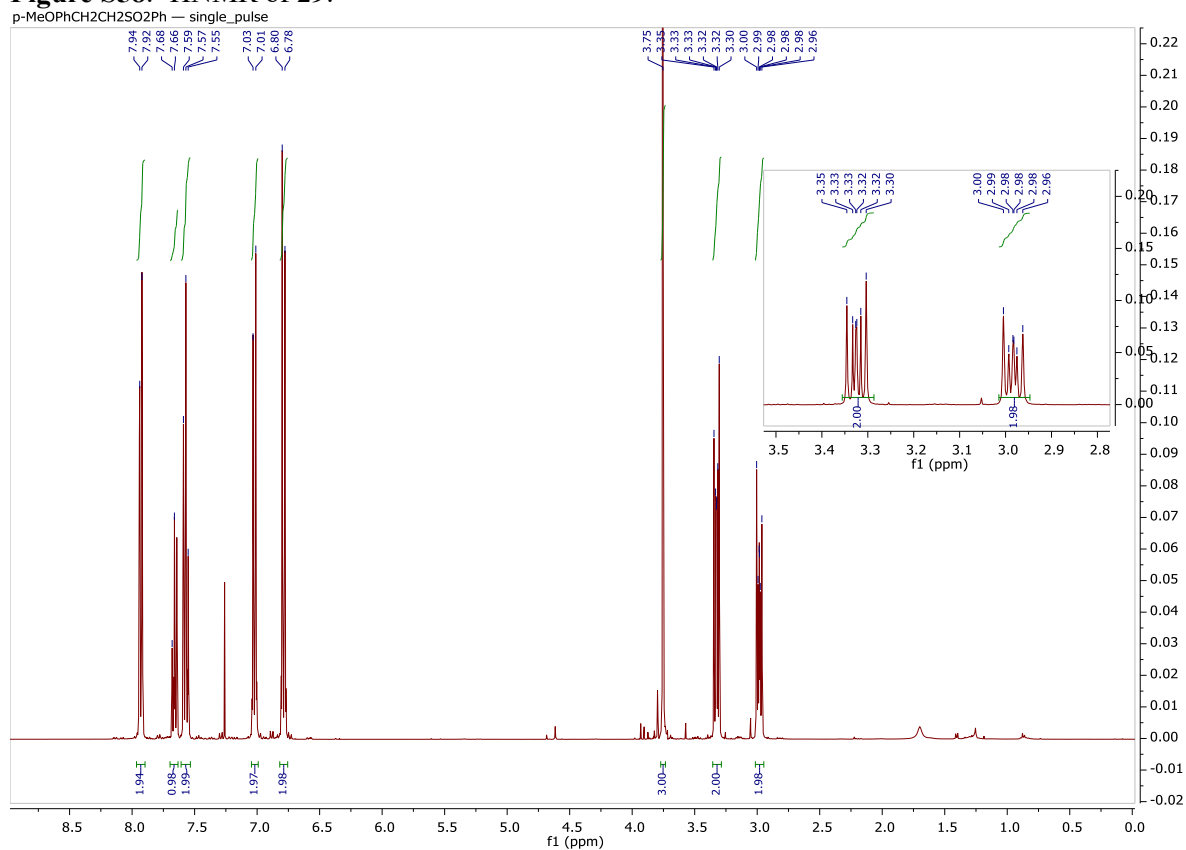
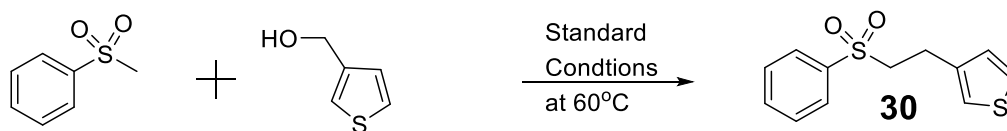
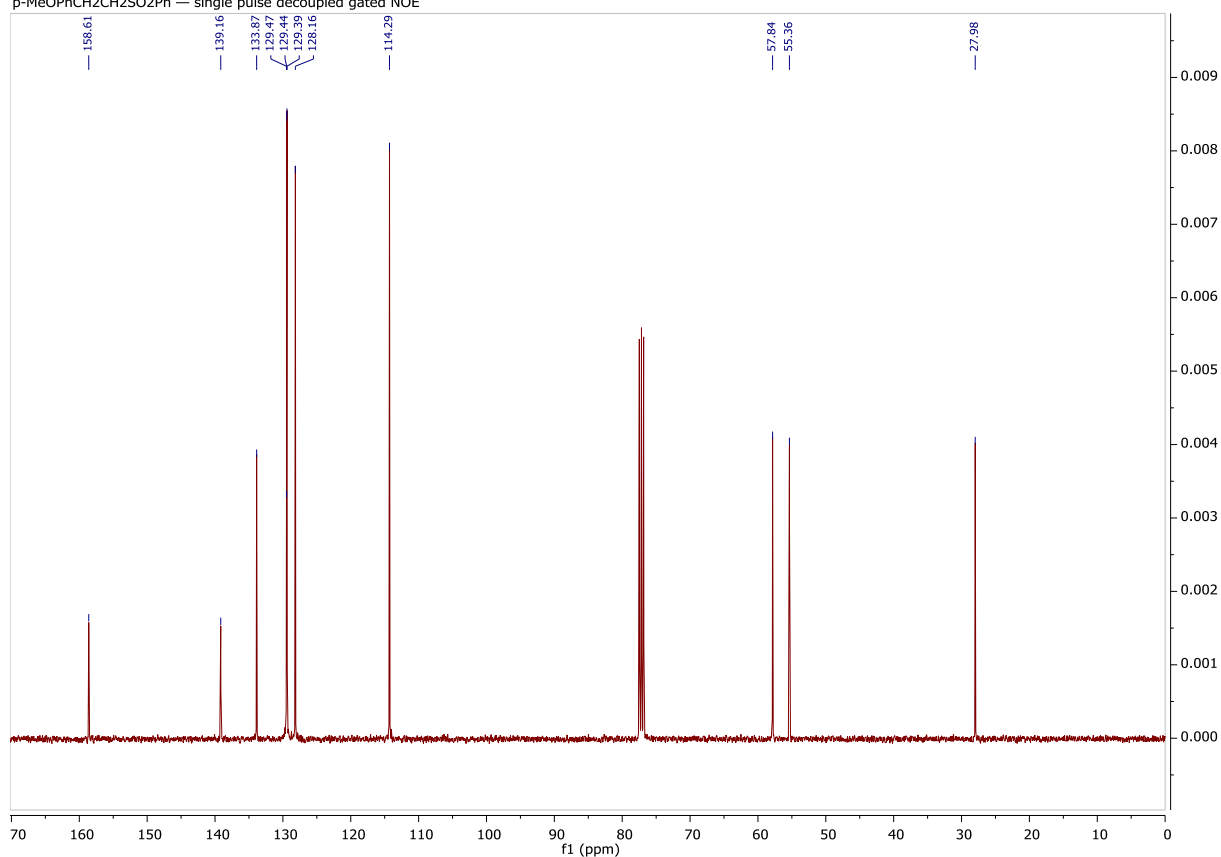


Figure S59. ^{13}C NMR of **29**.

p-MeOPhCH₂CH₂SO₂Ph — single pulse decoupled gated NOE

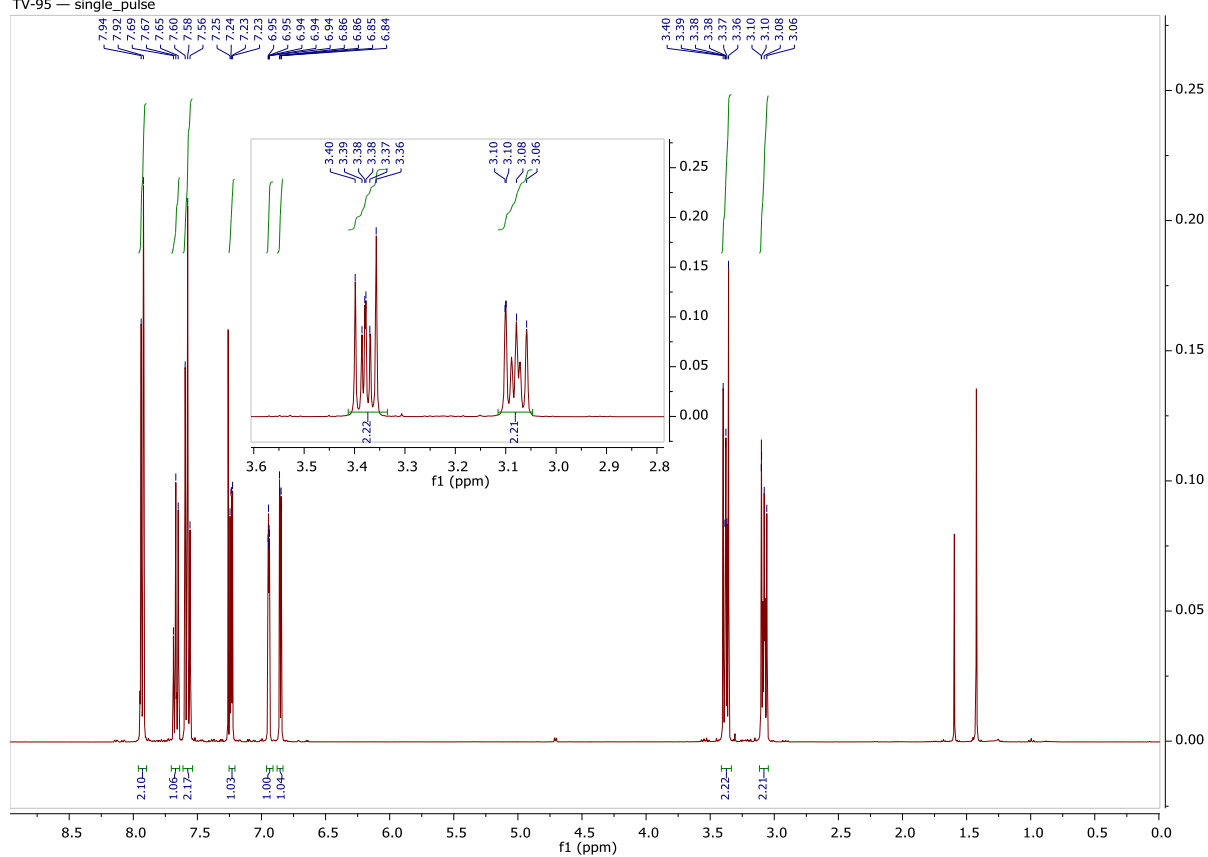


Physical State: White crystalline solid. Isolated Yield: 44%

^1H NMR (400 MHz, Chloroform-*d*) δ 7.93 (d, J = 7.4 Hz, 2H), 7.67 (t, J = 7.4 Hz, 1H), 7.58 (t, J = 7.4 Hz, 2H), 7.24 (dd, J = 5.0, 2.9 Hz, 1H), 6.98 – 6.91 (m, 1H), 6.85 (dd, J = 5.0, 1.4 Hz, 1H), 3.43 – 3.33 (m, 2H), 3.14 – 3.02 (m, 2H). ^{13}C NMR (101 MHz, Chloroform-*d*) δ 139.09, 137.59, 133.95, 129.49, 128.22, 127.61, 126.49, 121.64, 56.83, 23.56. HRMS: $[\text{C}_{12}\text{H}_{13}\text{O}_2\text{S}_2; \text{M}+\text{H}]^+$ Expected 253.0357; Obtained 253.0346.

Figure S60. ^1H NMR of **30**.

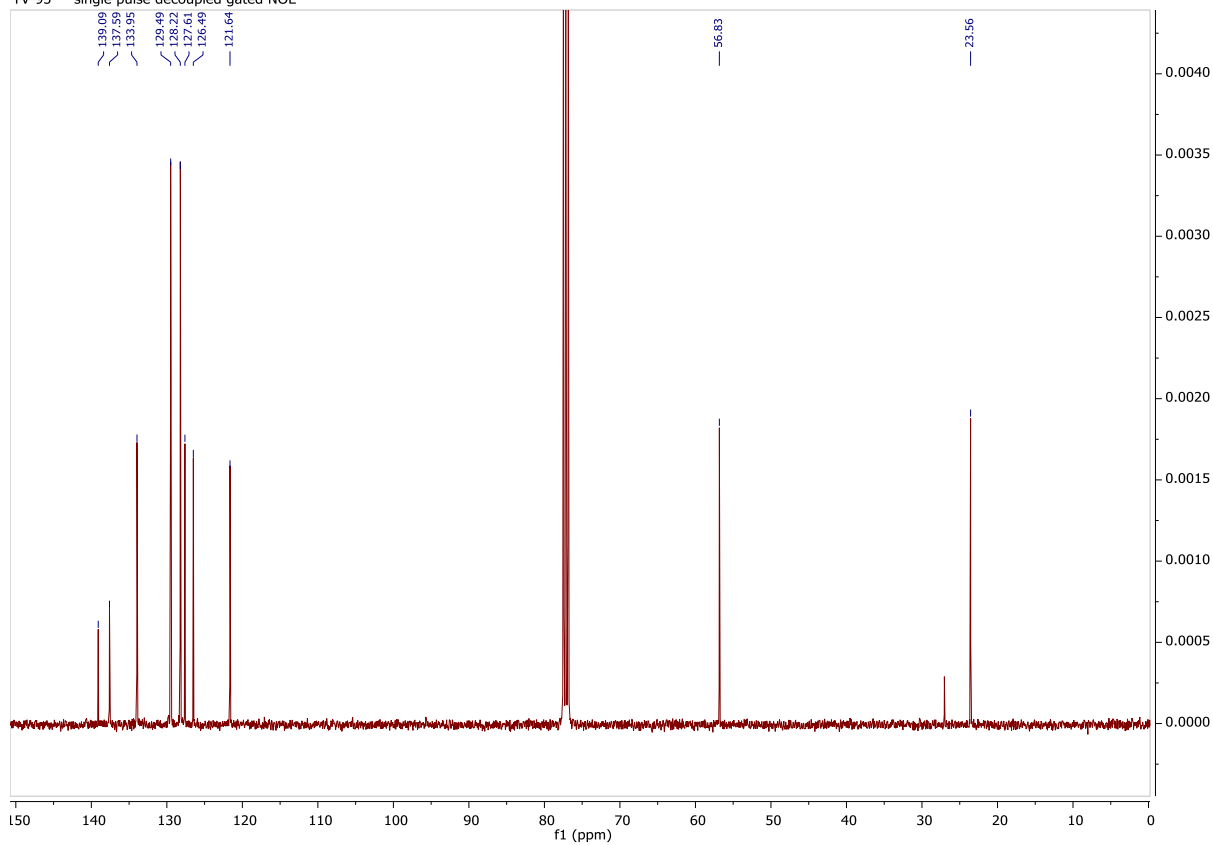
TV-95 — single_pulse



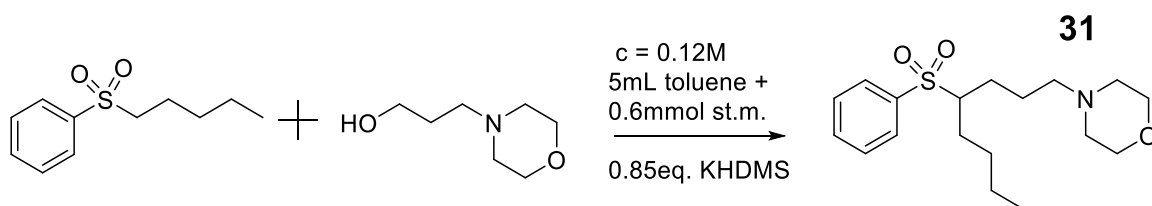
Cyclohexane impurity observed at 1.43ppm (water 1.56ppm)

Figure S61. ^{13}C NMR of **30**.

TV-95 — single_pulse decoupled gated NOE



Cyclohexane impurity observed at 26.9ppm



Physical State: A pale yellow oil. Isolated Yield: 39% (37%Y obtained at 0.060M conc.)

^1H NMR (400 MHz, Chloroform-*d*) δ 7.88 (d, J = 7.1 Hz, 2H), 7.65 (t, J = 7.4 Hz, 1H), 7.56 (t, J = 7.5 Hz, 2H), 3.70 – 3.61 (m, 4H), 2.94 (ddd, J = 10.5, 6.5, 3.9 Hz, 1H), 2.37 (bs, 4H), 2.27 (t, J = 7.0 Hz, 2H), 1.83 (td, J = 15.3, 14.8, 3.6 Hz, 2H), 1.71 – 1.49 (m, 4H), 1.35–1.45 (m, 1H), 1.33 – 1.18 (m, 3H), 0.84 (t, J = 7.2 Hz, 3H). ^{13}C NMR (151 MHz, Chloroform-*d*) δ 138.25, 133.61, 129.18, 128.86, 67.00, 64.30, 58.48, 53.72, 28.89, 27.63, 25.65, 23.63, 22.61, 13.81. HRMS: $[\text{C}_{18}\text{H}_{30}\text{O}_3\text{S}_1\text{N}_1; \text{M}+\text{H}]^+$ Expected 340.1947; Obtained 340.1937.

Figure S62. ^1H NMR of **31**.

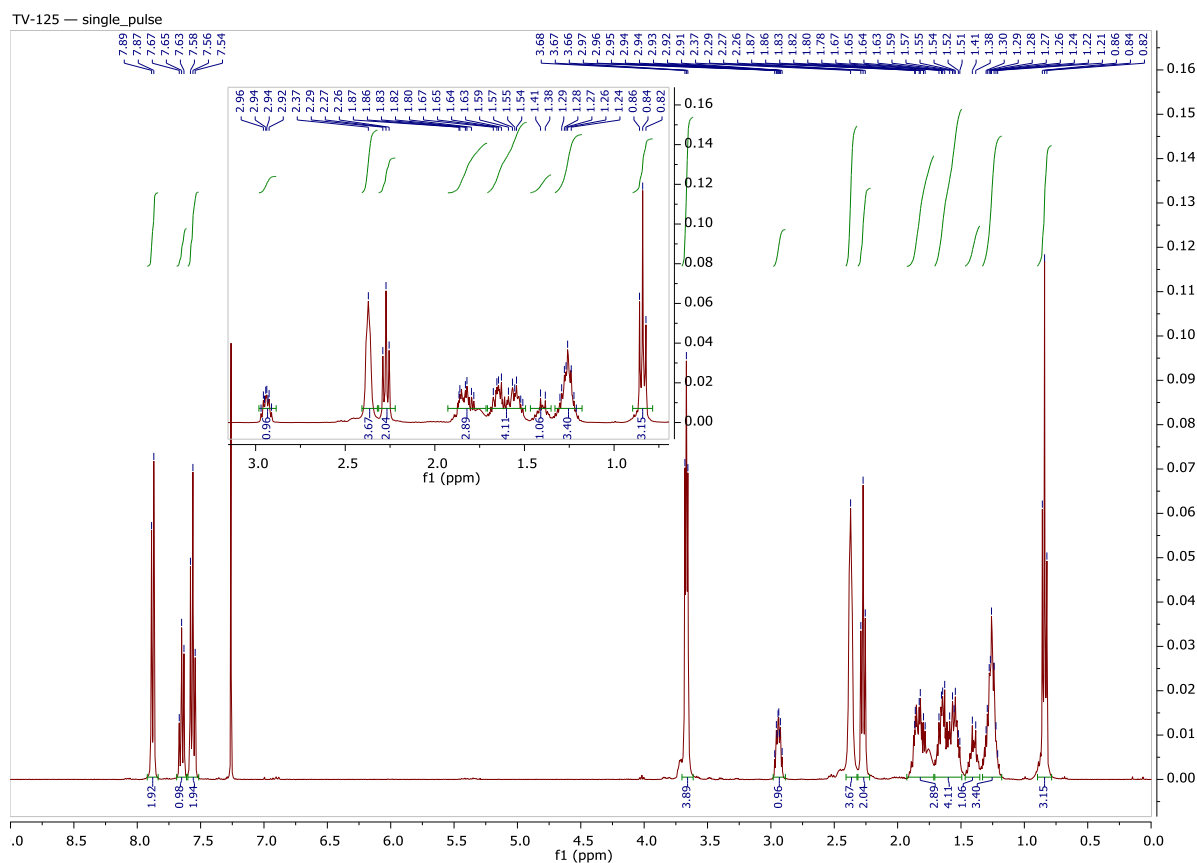
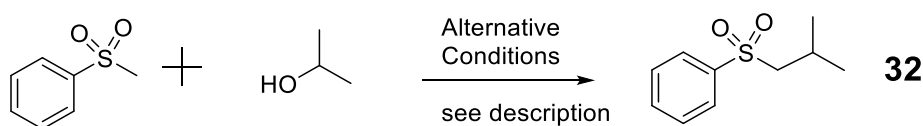
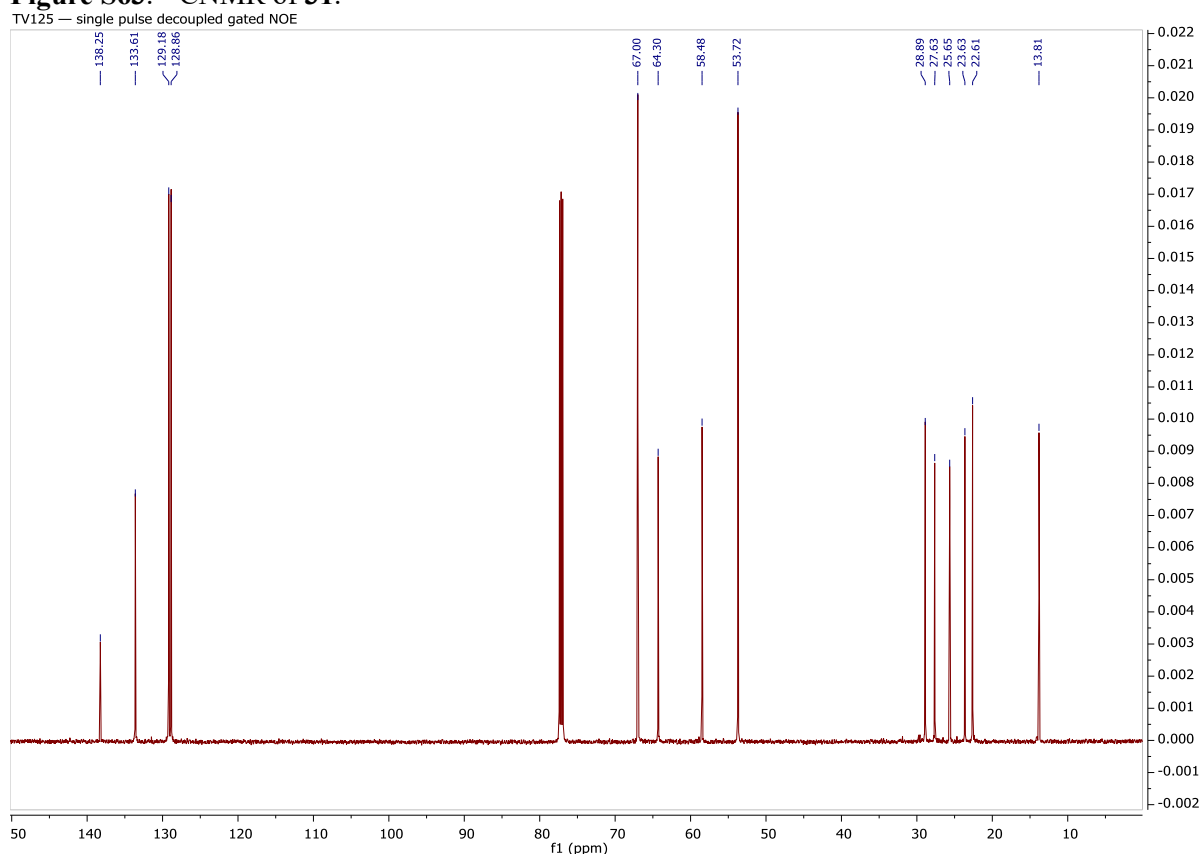


Figure S63. ^{13}C NMR of **31**.



Physical State: Clear liquid. Isolated Yield: 42%

Reaction performed with 2 eq. of KHMDS at 100°C for 24 h. 10eq. of isopropanol were used and the amount of isopropanol to toluene was 1:1 v/v.

At 1 eq. of KHMDS and/or lower amounts (3 eq., 1 eq.) of isopropanol, the yield did not exceed 10% by GC. At 3 eq. of KHMDS, the isolated yield was higher (48%), but there was an extra 5% of cyclopropane impurity which proved impossible to separate.

^1H NMR (600 MHz, Chloroform-*d*) δ 7.91 (d, J = 8.3 Hz, 2H), 7.4 (t, J = 7.6 Hz 1H), 7.56 (t, J = 7.6 Hz, 2H), 2.98 (d, J = 6.8 Hz, 2H), 2.22 (sep, J = 6.8 Hz, 1H), 1.05 (d, J = 6.8 Hz, 6H). ^{13}C NMR (151 MHz, Chloroform-*d*) δ 140.33, 133.65, 129.39, 127.94, 64.09, 24.20, 22.84. HRMS: $[\text{C}_{10}\text{H}_{15}\text{O}_2\text{S}]^+$; Expected 199.0793; Obtained 199.0785.

Figure S64. ^1H NMR of **32**.

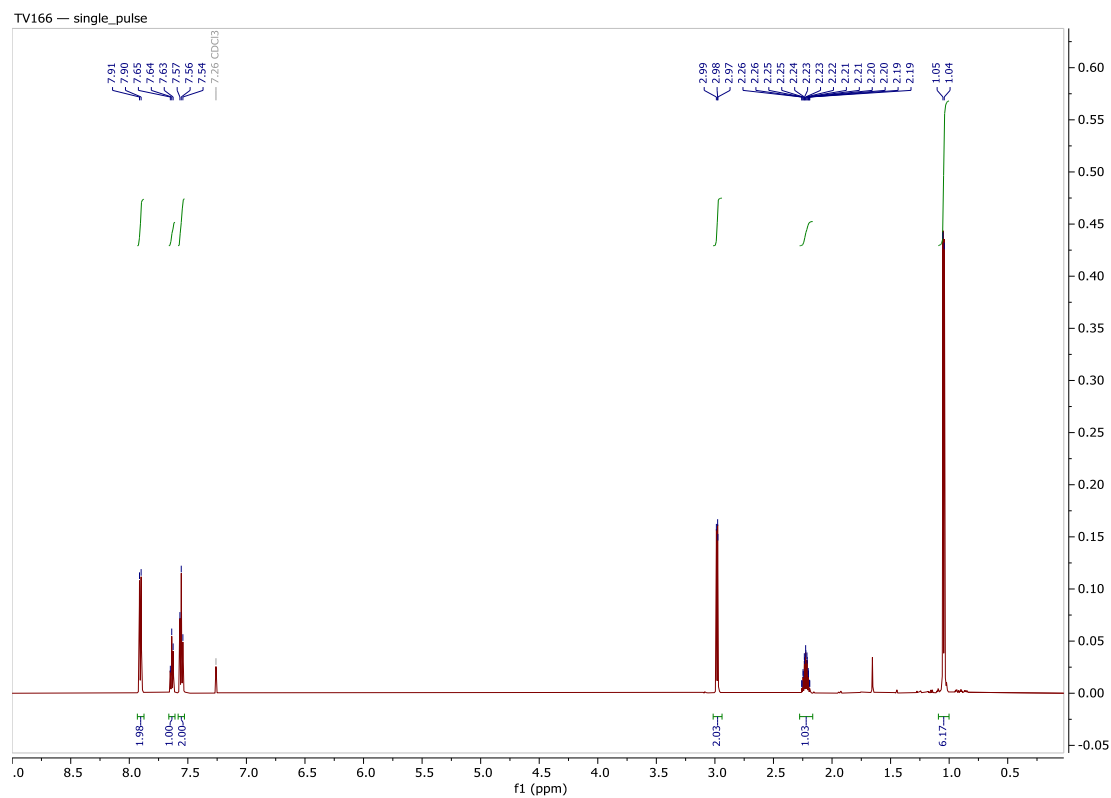
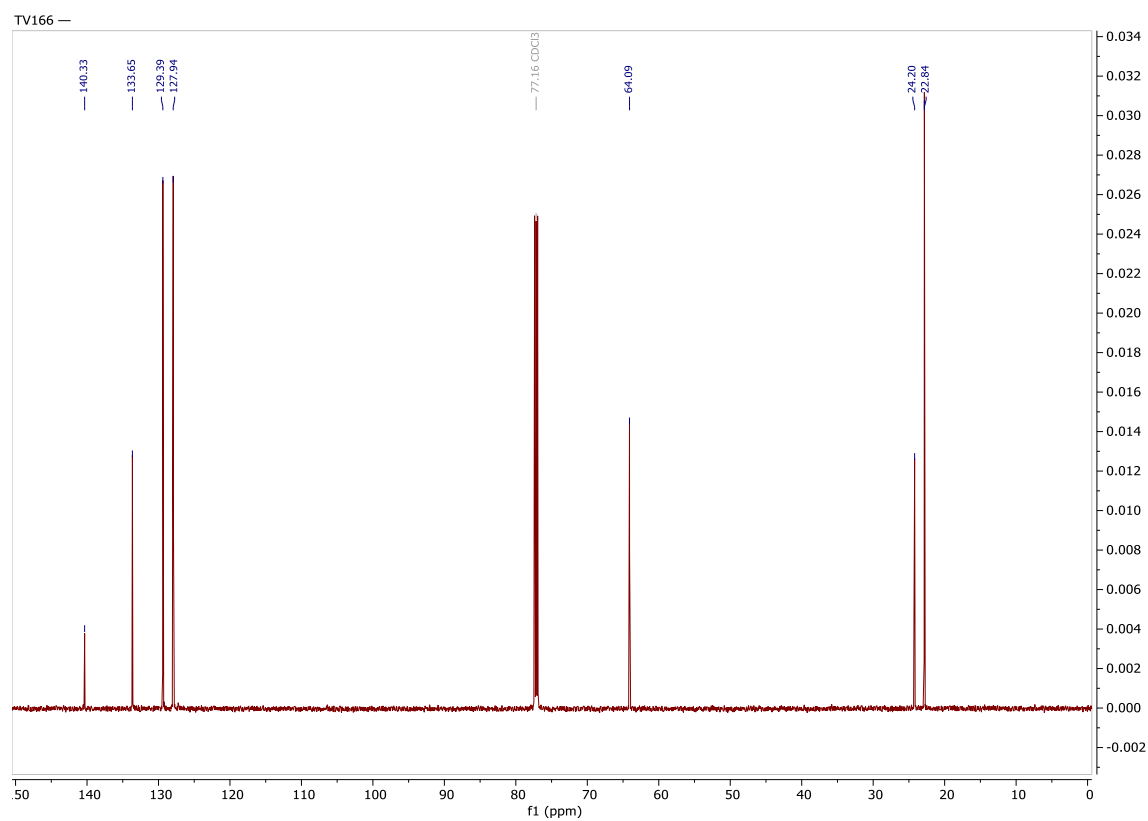


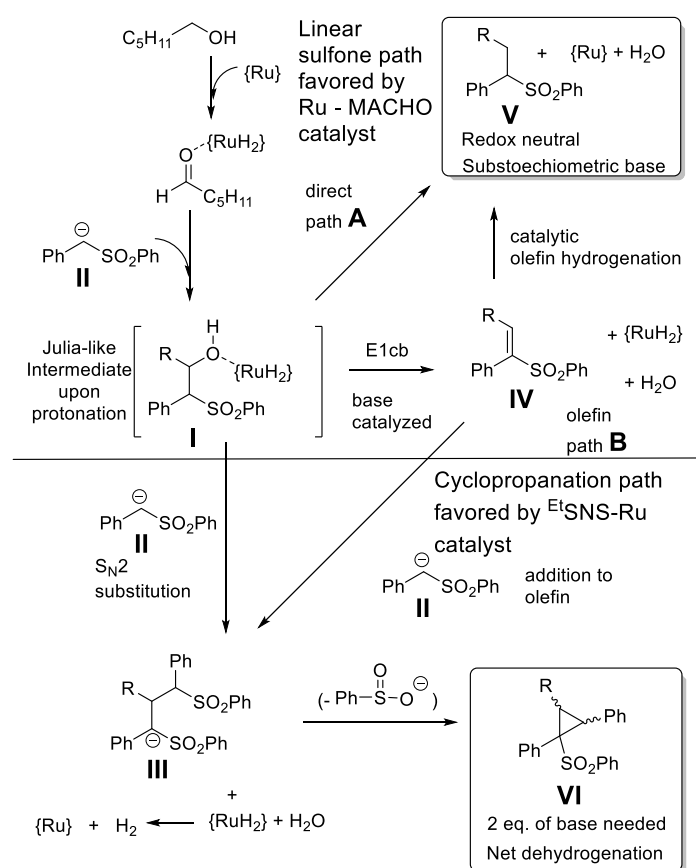
Figure S65. ^{13}C NMR of **32**.



Mechanistic Discussion

1. Introduction

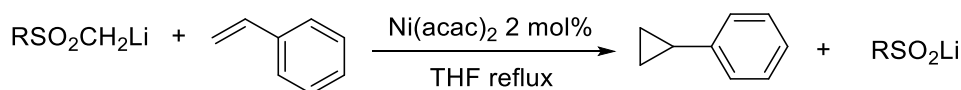
The general mechanism outlined in Scheme S1 was established based on stoichiometric reactions performed in the previous publication on the synthesis of cyclopropanes.^{S1} At least for cyclopropanation, it was supported with a number of stoichiometric and olefin spiking catalytic experiment, which are reproduced below with permission from reference S1, copyright (2018) ACS as a slightly modified Schemes S3, which is related to the mechanism. We have also supplemented the mechanistic reactions from the previous publication (Scheme S3) with a number of new experiments (Schemes S4-6) that are more specific to the linear sulfone reaction. The previous results did not show that **IV** formed in the cyclopropanation reaction, so it was not considered initially as a viable intermediate. However, based on the new experiments and comparison with previous results, we came to the conclusion that in contrast to the cyclopropanation reaction where we believe direct substitution occurs, the linear sulfone reaction proceeds via a vinyl sulfone via a ‘hydrogen borrowing’ mechanism (Path B).



Scheme S1. Proposed Mechanism

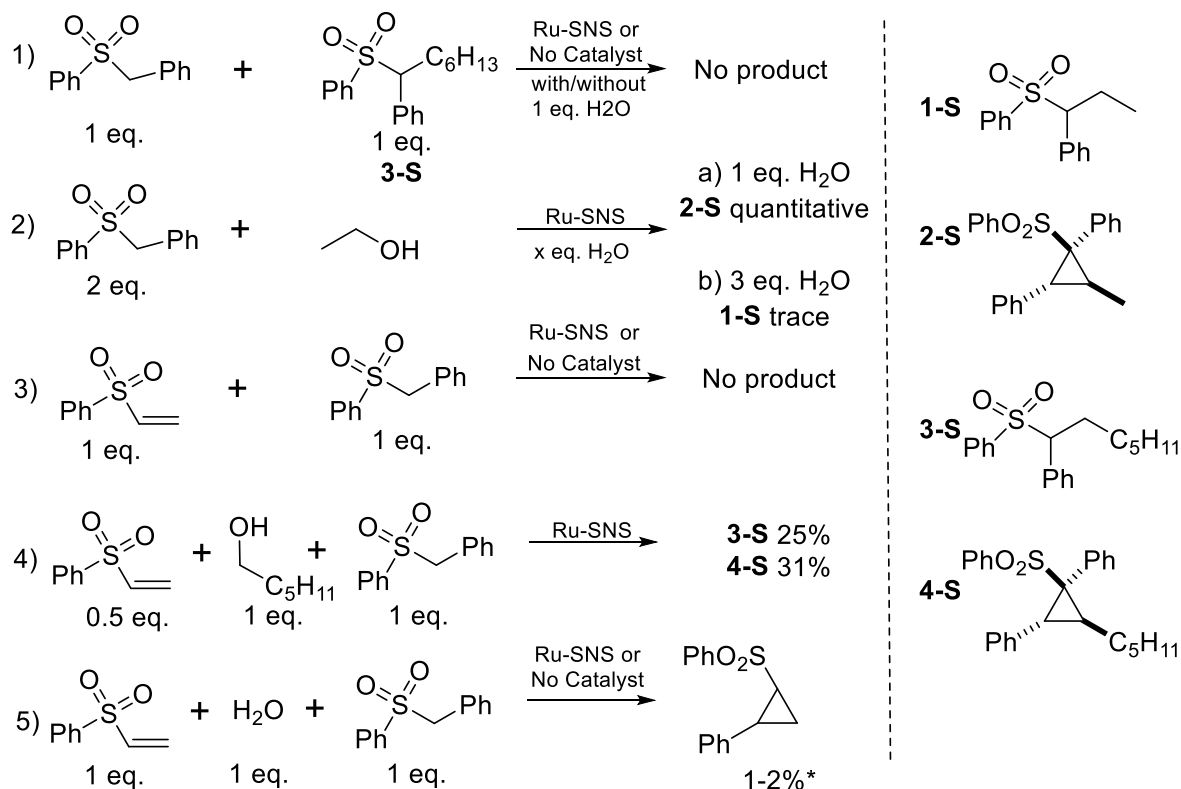
In the previous publication, the Gusev catalyst used was shown to selectively give cyclopropane (bottom half of Scheme S1). Cyclopropanation was shown to occur without catalyst in the case of formaldehyde, suggesting that the ruthenium complex only acted as a dehydrogenation catalyst. Elimination from the Julia-like intermediate **I** could lead to an olefin which adds a carbene equivalent to give cyclopropane. However, in the absence of a traditional carbene equivalent such as would be provided by a Corey-Chaykovsky reagent,^{S2} and the known stability of Julia olefination intermediates towards elimination in strongly basic environments (butyl lithium is used to produce them)^{S3} we wanted to have more solid proof of double bond intermediacy and carried out a number of mechanistic reactions. Interestingly, sulfone anionic addition to olefins, where the sulfur moiety leaves as a sulfinate, was also reported by Julia (the ‘Julia olefination’ chemist) in 1991, but it required nickel catalysis in refluxing THF, and only worked well for tert-butyl methyl sulfone, and did not work for phenyl methyl

sulfone (Scheme S2).^{S4} To the best of our knowledge, besides our reported cyclopropanation result, we have not found subsequent reports that used sulfones as carbene sources.



Scheme S2. Julia reported nickel catalyzed addition of sulfones to olefins.

2. Previous mechanistic experiments in the cyclopropanation report



Scheme S3. Mechanistic investigation reactions into cyclopropanation from the previous report

The reaction to form either the cyclopropane or the linear sulfone adducts does not proceed in the absence of a potassium cation containing base. Sodium and lithium versions of KHMDS gave 0% of the product and a lot of starting material remained unconverted. The Gusev dehydrogenation catalyst is active for dehydrogenative alcohol to ester coupling at much lower temperatures than the 120°C used in the previous report, as reported earlier by Gusev. Large amounts of byproducts **1-S** and **3-S** were isolated in the initial pre-screening experiments that were performed at lower temperatures that could be used for later mechanistic studies.

We treated isolated **3-S** with one equivalent of base and sulfone under the catalytic reaction conditions with and without catalyst and in the presence or absence of 1 eq. of water, as water forms as a product of the cyclopropanation reaction (Scheme S3, reaction 1). In all cases, the linear sulfone was unreactive. This suggests that once the linear sulfone is formed, the reverse reaction to form the olefin **IV** or the Julia intermediate **I** does not occur. Also the linear sulfone cannot be used to synthesize cyclopropane. A large amount of water seriously retarded the reaction (Scheme S3, reaction 2), either by quenching base equivalents or by altering the coordination environment around the potassium, which was earlier shown to be essential. Adding molecular sieves to the reaction did not have an effect on yield. There was also no addition of the sulfone anion to stoichiometric vinyl sulfone under the reaction conditions, suggesting that it is an unlikely intermediate. A catalytic reaction with hexanol under a flow of argon

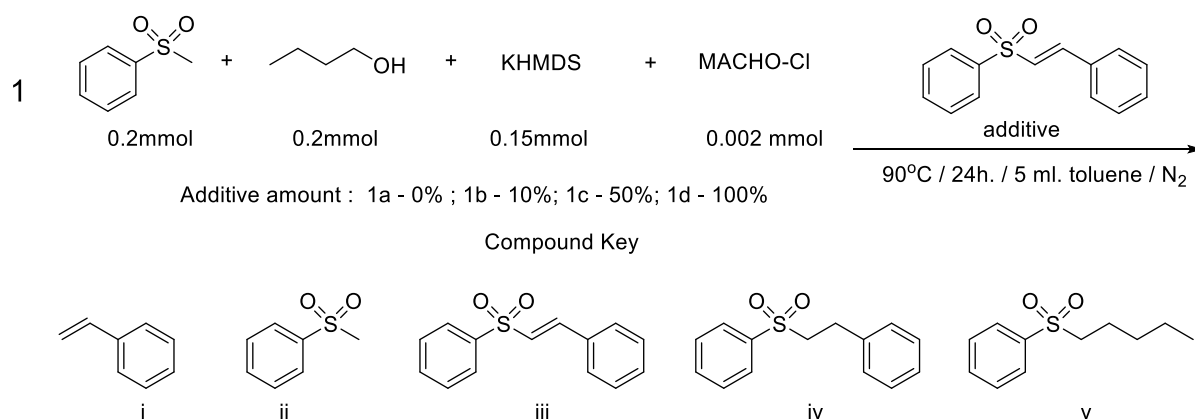
(open system) that would allow generated H₂ to escape did not alter the yields or selectivity of the reaction, also arguing against the olefin being an important intermediate. Spiking a normal catalytic reaction with vinyl phenyl sulfone led to lower yields and selectivity (reaction 4). Finally, adding water to the vinyl phenyl sulfone did finally lead to trace cyclopropane (reaction 5), suggesting that only after reforming Julia-like intermediate **I**, was cyclopropanation possible as this product was not seen in the absence of water (reaction 3).

Based on these factors, we tend to favor the direct transformation of intermediate **I** to **III** in the cyclopropanation reaction. However, the other pathway cannot be conclusively ruled out, as it is possible that the vinyl sulfone is formed in minute amounts at a steady rate and behaves differently under those circumstances. Large amounts of vinyl sulfone could isomerize under the reaction conditions before they can react with a carbene equivalent.

3. Current mechanistic investigation

The linear sulfone formation occurs via the same pathway through intermediate **I**, but the catalyst subsequently reacts either with intermediate **I** directly, or it hydrogenates an olefin formed by elimination via a ‘borrowing hydrogen’ methodology. The reaction conditions that favor linear sulfone synthesis, mainly lower temperature and the different catalyst used, mean that we cannot discount an olefin like **IV** as an intermediate.

In order to probe the possible mechanism, we carried out vinyl sulfone spiking reactions under the conditions relevant to linear sulfone synthesis with MACHO catalyst for three different vinyl sulfones. The results were compared by qualitative GC/MS integration in the presence of mesitylene internal standard. The first vinyl sulfone was the relatively activated phenyl styryl sulfone which models an intermediate that would be obtained during the synthesis of products such as **29** and **30**.



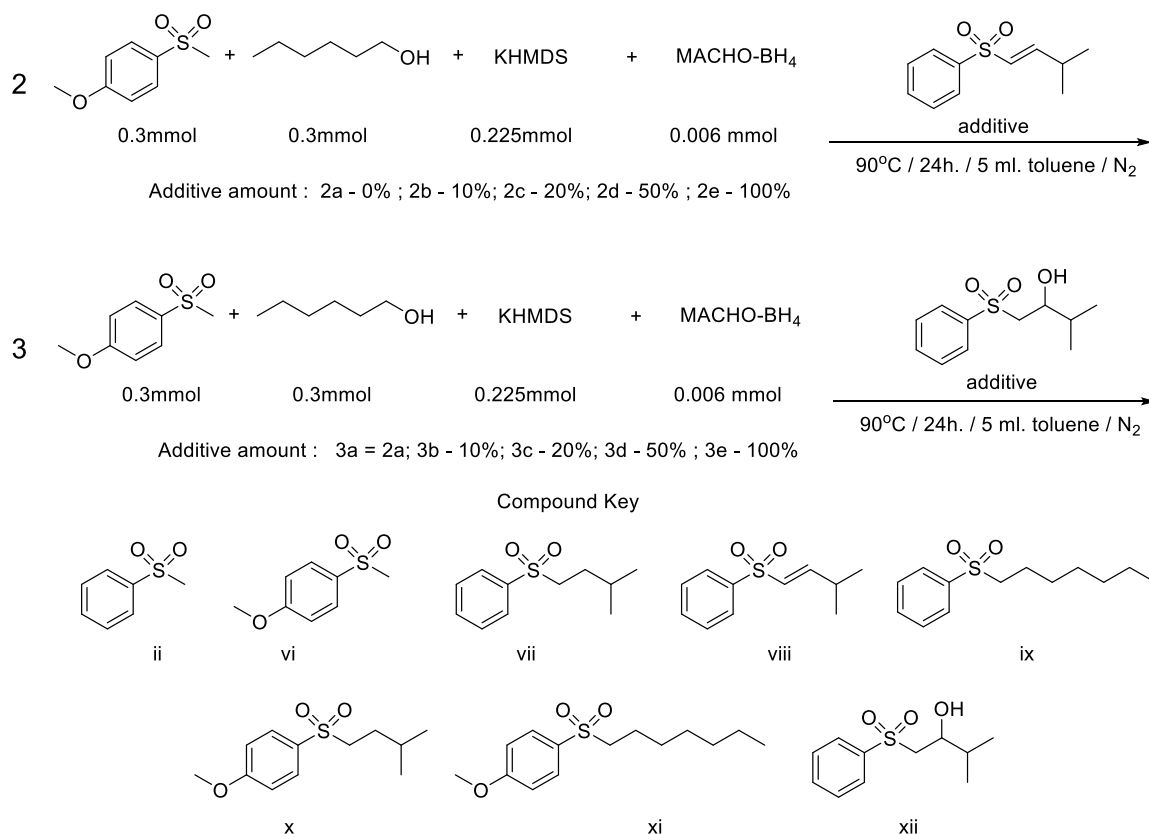
Scheme S4. Catalytic reaction spiking with phenyl styryl sulfone

The control reaction (1a) showed almost full conversion to the linear product **v** with only a trace peak of starting material **ii** remaining. Adding a small amount, 10mol%, of additive lowers the yield by a comparable amount and a peak of styrene **i** is seen, the product of decomposition of **iii**. As the latter decomposes, if competes for base, lowering the overall yield of **v**. At 50% additive, the yield of **v** is greatly reduced and small peak of **iv**, which is hydrogenated additive, starts to appear. There is also a lot more styrene and unreacted **ii**. Finally, at 100 mol% additive, there is only a trace of **v** that can be seen and about ~20-30% of **iv** can be observed. There is also less styrene. In all reactions, we do not observe any **iii** remaining, suggesting that it is very sensitive to the reaction conditions. We also did not observe any cyclopropane beyond the expected very small trace background peak produced in reaction 1a.

Based on these results, it can be argued that the vinyl sulfone is a viable intermediate that is hydrogenated during the course of the reaction. It is also unstable under the reaction conditions, as the

yield of **iv** at 100mol% of **iii** added is a lot less than the peak of regular product **v** at 0 or 10mol% of **iii** added. If the catalyst remains bound to the Julia-like intermediate **I** and hydrogenation occurs shortly after, it could explain the high yields of linear sulfones in our reactions despite the apparent instability of **iii**, since the catalyst would not be found in close association to **iii**.

In order to probe intermediate that are directly relevant to most of our substrates (i.e. similar to compound **5**) we synthesized a vinyl sulfone and a β hydroxy sulfone from isobutyraldehyde and spiked a catalytic reaction with differing amounts of each additive.



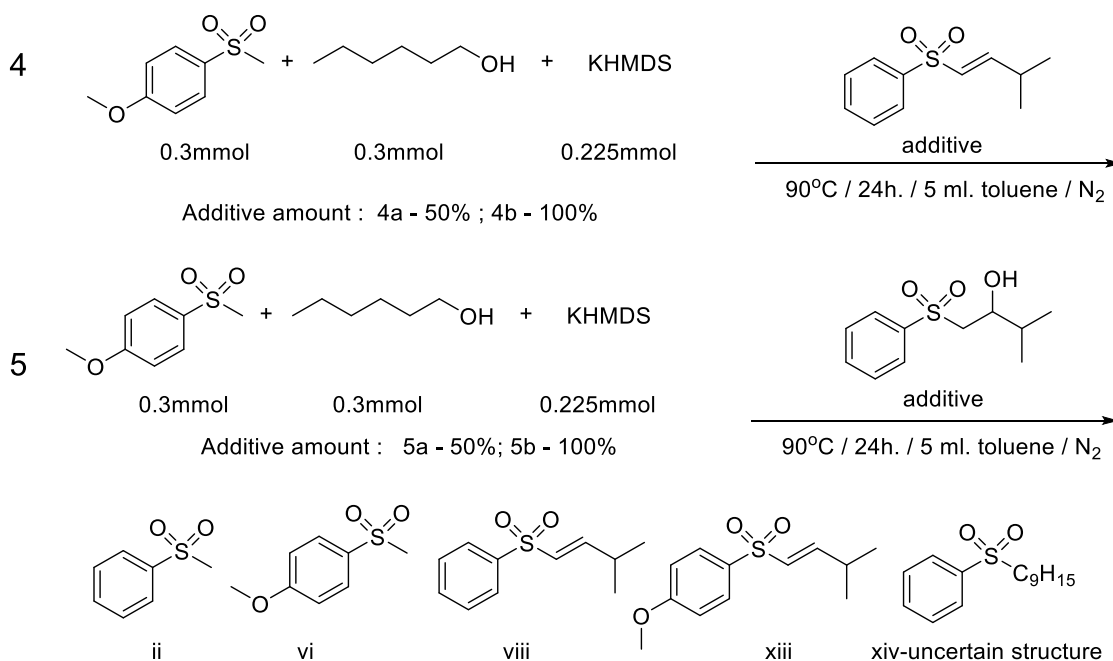
Scheme S5. Catalytic reaction spiking with vinyl an β hydroxy sulfone based on isobutyraldehyde

The first set of experiments were carried out with the vinyl sulfone as in reaction 1. The control experiment showed full conversion to the expected sulfone **xi**, with only a trace amount of unreacted **vi** remaining. At 10 mol% additive, we could see a very small peak of hydrogenated **vii** that was similar in size to unreacted **vi**. At 20 mol%, the amount of **vii** was slightly greater (reaction 2c), while the amount of **vii** decreased only slightly. At 50 mol% of **viii** added (reaction 2d), the peaks of unreacted **vi** and hydrogenated **vii** were much bigger, with the yield of **xi** being only ~70% of its amount in reaction 2a. At 100 mol% additive (reaction 2e), the peaks of **vi** and **vii** are equal in intensity to **xi**. For the first time, trace **viii** that remains after the end of reaction is now also seen. Even at this large amount of additive however, a significant amount (~30-40%) of linear product **xi** is still formed.

If the olefin forms in the reaction, it would be the result of water elimination from intermediate **I**. Therefore, we decided to test the β hydroxy sulfone **xii** directly as an additive under the reaction conditions and compare it to the reactivity seen with olefin **viii**. With reaction set 3, already at 10 mol% of **xii**, we could see trace peaks of **ix** and **x** start to appear. Interestingly, these products come from the decomposition of **xii** towards the aldehyde and anionic sulfone. The sulfone **ii** and **vi** and butyraldehyde are now present in the reaction and the sulfones can react with hexanal and butyraldehyde to give these new scrambling products. At 20 mol% additive (reaction 3c), the peaks of **ix** and **x** are bigger and there is a lot more unreacted **vi**. This trend is continued at 50 mol% additive (reaction 3d), but there are also

now small peaks of **ii** and **vii** that start to appear. The latter product comes from the hydrogenation of olefin **viii** and seems to suggest that **viii** can be formed under the reaction conditions, presumably by elimination from **xii**. There is also a lot less of normal product **xi** (~10-20%). Finally, at 100 mol% of additive **xii**, there is a lot more unreacted **vi** and the peak of **xi** is very small (~2-3%). There is a large peak of **ii**, suggesting a robust reverse reaction, and a large peak of **ix** that is 20x bigger than **xi**. Interestingly the peak of methoxy sulfone based **x** is also small (~2-3%), meaning that it reacts slower than phenyl methyl sulfone obtained via the reverse reaction. For the first time, the peak of **viii** is seen, but it is also a very small product on par with hydrogenated **vii** (both ~1-2%).

Finally, we performed a control reaction with spiking the β hydroxy alcohol sulfone and the vinyl sulfone obtained from isobutyraldehyde without catalyst. Control reactions previously showed no conversion without the catalyst, but they were not performed in the presence of these spiked reagents (Scheme S6).



Scheme S6. Control reaction spiking with vinyl an β hydroxy sulfone based on isobutyraldehyde

None of the reactions showed any reactivity of the sulfone with hexanol. At 50 mol% of the vinyl sulfone additive (reaction 4a), we did not observe much conversion of **vi**, and just a small peak of **xiv**, which appears to be the decomposition product of a reaction of two molecules of **viii**, was obtained, while the peak of **viii** could not be seen. The product **xiv** matches the mass of a molecule that contains two double bonds and appears to come from a second isobutyr-olefin addition to **viii**. At 100 mol% additive (reaction 4b), there is still lots of unreacted **vi**, but the decomposition peak **xiv** is about 3 times bigger. Also there is a small peak of **ii** that comes from the loss of a butene equivalent (likely during the formation of **xiv**) and a trace amount of unreacted **viii** is now seen.

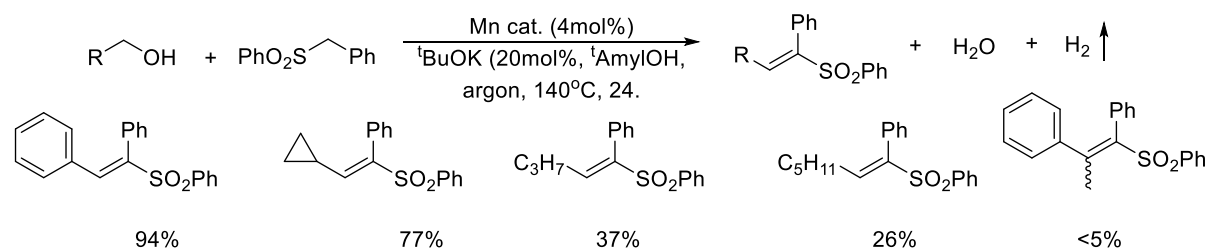
With β hydroxy sulfone additive at 50 mol% (reaction 5a), there is a large peak of unreacted **vi** and a small peak of phenyl methyl sulfone **ii**, which comes from the reverse nucleophilic addition reaction from the additive to give isobutyraldehyde and **ii**. At 100 mol%, the picture is very different. While we still see a big peak of unreacted **vi**, there are three other peaks at about $\sim 2/3^{\text{rd}}$ of the intensity of **vi**. They are compounds **ii**, **viii**, and **xiii**. The last one comes from the decomposition of the additive (i.e. reversible nucleophilic addition) and the subsequent reaction of **vi** with isobutyraldehyde produced by this decomposition, followed by an elimination to give the olefin **xiii**. These olefin signals are a lot stronger than anything seen in reaction 4 where olefin was the actual additive. The only difference between reactions 4 and 5 is that the latter has a water molecule that is produced during the course of

the reaction and it can presumably neutralize base and make the reaction conditions milder. Besides confirming that the first step in Scheme S1 is reversible, it's hard to use this experiment as proof of an olefin intermediate as with only 50% additive we didn't see any olefin. The olefin would be formed in minute amounts during the actual reaction as well. Cyclopropane is also not observed during these control reactions, but this is likely due to the lower temperature utilized than that normally required for cyclopropanation formation.

4. Conclusions on Mechanism

Based on the above spiking experiments that demonstrate that the olefin can be hydrogenated under the reaction conditions, and that it can form from the hydroxy intermediate, we favor the pathway that goes through olefin intermediate **IV**. We can also conclude that the formation of intermediate **I** is reversible, while olefin **IV** cannot be converted back into the Julia-like intermediate.

A recent paper by the Maji group is directly relevant to our mechanistic discussion. It shows that vinyl sulfones can form via manganese catalyzed coupling of phenyl benzyl sulfones and alcohols.^{S5} Manganese is not capable of hydrogenating the vinyl sulfone product, so the vinyl sulfone is isolated at the end of the reaction, even though the temperature is 50°C higher than that used in our protocol. In our reaction 4 (spiking with vinyl sulfone in the absence of catalyst) we saw extensive decomposition of the vinyl sulfone, but we also used a much larger amount of base and our vinyl sulfone was doubly substituted as opposed to the tri-substituted ones that would be formed from phenyl benzyl sulfone in Maji's results.



Scheme S7. Manganese catalyzed synthesis of vinyl sulfones

While a tri substituted vinyl sulfone is more stable toward side reactions such as polymerization in a highly basic medium, it is an analogue of hypothetical vinyl sulfone intermediates for our products **18-24** (phenyl benzyl sulfone and aliphatic alcohol), where we don't detect any vinyl sulfone side products by GC/MS. Most of Maji's reported products are from benzylic alcohols, with only the cyclopropyl methanol substrate giving high yield in one of the three aliphatic alcohol examples. The vinyl sulfones derived from butanol and hexanol are obtained in low yields (Scheme S7) and have NMRs contaminated by side products (likely a cis/trans isomer, especially for the product derived from hexanol). This is in contrast with our high yields of linear sulfones from these same alcohols at a lower temperature. Compound **18** (79% isolated yield) is a direct analogue of the hexyl vinyl sulfone obtained in Scheme S7. It may be that for Maji, alkyl vinyl sulfones also decompose at higher temperatures with 20 mol% base. Cyclopropanation at this high temperature is also a likely side reaction.

In our case we showed that it is possible to see olefins under the reaction conditions (see especially reaction 5, Scheme S6). Our putative dihydride Ru intermediate bound to intermediate **I** could also rapidly hydrogenate **IV** after elimination, explaining our higher relative yields to Maji's alkyl alcohol examples. Maji's results further lend credence to the vinyl sulfone intermediate hypothesis, but the conditions and catalyst do not directly overlap. Ultimately, we cannot rule out the direct transformation of **I** to **V**. However, the balance of evidence leads us to favor the olefin pathway for linear sulfone formation via a 'hydrogen borrowing' pathway, perhaps with a Ru dihydride complex closely associated with such an olefin intermediate, in contrast to a direct substitution pathway earlier suggested for cyclopropane formation.

Substrates that did not work or worked poorly

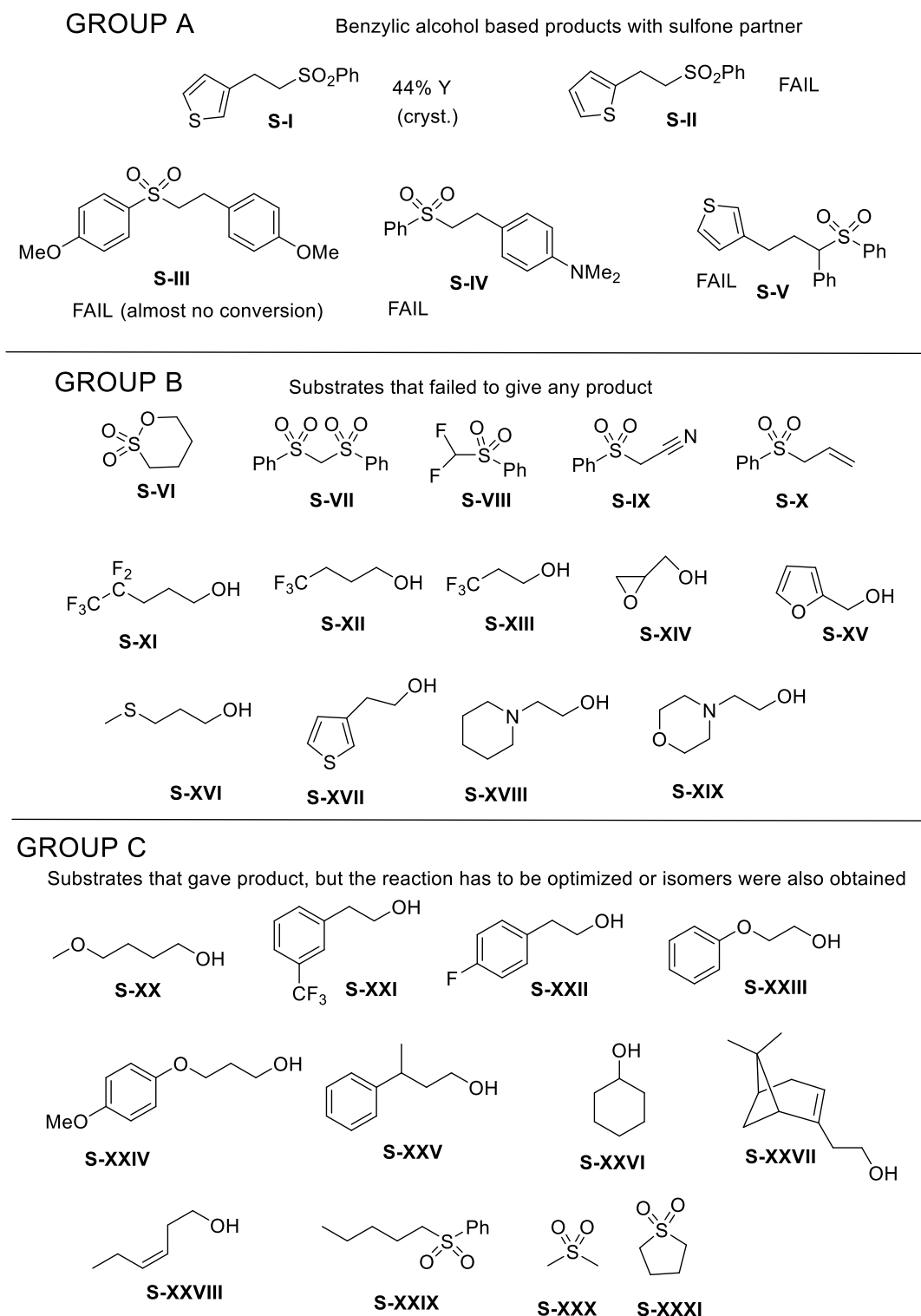


Figure S66. Challenging substrates

In general, we performed all reactions on a 0.2mmol trial scale with mesitylene internal standard to obtain a GC yield and judge the general outcome of the reaction in terms of conversion and byproducts, before proceeding to attempt to isolate the product on a larger scale. Figure S64 is a condensed summary of substrates that either did not work, or were not attempted on larger scale due to low yields or challenging admixtures.

Group A

Although benzylic alcohols were discussed in the main text, and we obtained a good isolated yield in the coupling of phenyl methyl sulfone and para-methoxy benzyl alcohol, in general the reaction did not perform well, with most substrates eliminating to give styrenes, and we got a good amount of styrene byproduct even in the best case scenario of compound **29**. In contrast to the expected poor reactivity with electron poor benzyl alcohols there were some other trends that we could not explain based on having success with compound **29** and **S-I** (compound **30**). Compound **S-II** was expected to perform even better than **S-I**, but we did not observe any product. This could be due to a thiophene electron pair interfering with the catalyst when the benzyl alcohol is in the 2 position on the ring. An electron rich sulfone failed to react to give **S-III**, while another electron rich benzyl alcohol **S-IV** also did not react. Phenyl benzyl sulfone failed to react in our only official trial with it to give **S-V**, and we couldn't identify any products by GC/MS. However, in some exploratory reaction, we often saw styrenes form between benzyl alcohols and phenyl benzyl sulfone.

Group B

This group failed to give any product. A too low pK_a (**S-VII**) generally does not lead to either linear sulfone or cyclopropane product. Alcohol (and sulfone) coupling partners with fluorines generally do not work. In compounds **6** and **17**, which do contain fluorines, these atoms are far away from the hydroxy moiety, but the isolated yields are still much lower in contrast to other substrates. This may be due to catalyst deactivation by CF bond activation or due to unfavorable interactions between the potassium and fluorine compounds in a transition state. Furan and epoxide decomposed under the reaction conditions (**S-XIV** and **S-XV**). We are not sure why compound **S-XVI** failed to give product, but it is probably for the same reason as compound **S-II** (Group A). Finally, compounds **S-XVII** to **S-XIX** where there is a heteroatom on the β carbon were already expected not to react at all from the cyclopropane work, in contrast to substitution at the γ carbon where we get very high yields.

Group C

Compound **S-XX** was obtained in a similar qualitative yield to the latter two fluorinated alcohols pictured when coupling the alcohol with an aryl methyl sulfone; the latter two alcohols eventually gave compounds **6** and **17**, but we expected a higher yield for the ether based **S-XX**. We did obtain a high yield with **S-XX** with a benzyl phenyl sulfone coupling partner, compound **23**, but the reaction with other sulfones has to be further optimized. **S-XXIII** has a β carbon heteroatom substituent (see compounds that failed in Group B), but on the other hand it is a relatively inert ether functionality. Overall, this compound gave ~20-30% yield with phenyl methyl sulfone under the standard reaction conditions. Similar reactivity was observed for compound **S-XXIV**. Both of these reactions would have to be optimized further before attempting them on larger scale. Compound **XXV** is similar to butyraldehyde, but slightly bulkier, explaining the sub 50% GC yield and our decision not to pursue it on larger scale.

Secondary alcohols such as isopropanol are a very important substrate class, however they are a lot bulkier than even isobutyraldehyde. With isopropanol, an initial experiment where we attempted to see if secondary alcohols worked, we managed to obtain ~10% linear sulfone with methoxyphenyl methyl sulfone as a coupling partner under the standard reaction conditions after 24 hours of reaction time. Eventually, after coming back at a reviewer's request, we managed to reach a 42% isolated yield with phenyl methyl sulfone (see conditions for compound **32**). We appeared to obtain bigger yields with sulfonamide as a coupling partner, but it's more difficult to isolate these products (no UV absorption). Another secondary alcohol that we tried at the time was cyclohexanol **S-XXVI**. It appeared to react better than isopropanol, but we could not make its solutions as concentrated and used only a 3x molar excess. GC suggested ~50% yield with 2 eq. of KHMDS, however there was also the corresponding vinyl sulfone present in minor amounts (~5%) and we decided we would not be able to cleanly isolate our desired product. Isopropanol was left as the only official secondary alcohol example. It may be possible to optimize this reaction further with much longer reaction times or with a different catalyst.

S-XXVII and **S-XXVIII** were attempts to see if olefins that could potentially isomerize would give product. Ru complexes are known for olefin chain scrambling. It does not occur as readily for a more substituted olefin at low temperatures, such as product **13**. Accordingly, less substituted hexene **S-XXVIII** gave a number of isomers that are difficult to separate by chromatography. Likewise, nopol **S-XXVII** gave three isomers with the sulfonamide coupling partner. Although conversion was quantitative, the ratio of isomers was 85:8:7, with 2D NMR experiments suggesting that the double bond migrates to the exo position in the major isomer, likely due to the favorable conjugation stabilizing effect in the intermediate aldehyde. Purification of this product was not pursued.

Sulfone **S-XXIX** gave low amounts of products with various alcohols. We isolated compound **31** (Figure 3) in 39% yield, but the sub 50% yields are disappointing. We expected to further modify most of our linear sulfones in order to show the versatility of the method in building up sulfones selectively from two different alcohol moieties. Considering the cheap prices of the starting sulfone and alcohol materials, obtaining functionalized product **31** in two steps in overall 28% isolated yield is acceptable. The double addition product was always the minor one in our optimization procedures (Tables S2-S5), and it's likely harsher conditions are required for efficient addition of a second alcohol to a secondary alkyl sulfone. However, optimizing these conditions without suffering from significant cyclopropane byproduct formation is beyond the scope of the current work.

Dimethyl sulfone **S-XXX** actually gave good yields of product, but it was not selective for double over mono addition unless a large excess of alcohol was used, and in that case the double addition (one alcohol each on both methyl groups) product was obtained. We did not consider it more interesting than the mono product since the latter would allow for functionalizing the other methyl with a different alcohol. It is possible to isolate the mono addition product by chromatography due to significant polarity differences with the double addition product, but ultimately this was not pursued since the yield is too greatly impacted. Finally, sulfolane **S-XXXI** does react to give the normal addition product in ~50% yield with alkyl alcohols, however there are many byproducts and it's not a clean reaction. The major byproduct is the result of sulfolane decomposition to butadiene after addition of the alcohol and addition of a butadiene equivalent. While this reaction is interesting in itself, this byproduct is relatively minor (~20%), and there are many other unidentified decomposition byproducts.

References

- S1. Jenkins, T. C.; Fayzullin, R. R.; Khaskin, E. Three-Component [1 + 1 + 1] Cyclopropanation with Ruthenium(II). *Organometallics* **2018**, 37, 2609-2617.
- S2. Corey, E. J.; Chaykovsky, M., *J. Am. Chem. Soc.* **1965**, 87, 1353-64.
- S3. Baudin, J. B.; Hareau, G.; Julia, S. A.; Ruel, O. A direct synthesis of olefins by the reaction of carbonyl compounds with lithio derivatives of 2-[alkyl- or 2'-alkenyl- or benzylsulfonyl]benzothiazoles. *Tetrahedron Lett.* **1991**, 32, 1175-8
- S4. Gai, Y.; Julia, M.; Verpeaux, J. N., Nickel-catalyzed cyclopropanation of alkenes via methylene transfer from lithiated *tert*-butyl methyl sulfone. *Synlett* **1991**, 56-7.
- S5. Waiba, S.; Barman, M. K.; Maji, B. Manganese-Catalyzed Acceptorless Dehydrogenative Coupling of Alcohols With Sulfones: A Tool To Access Highly Substituted Vinyl Sulfones. *J. Org. Chem.* **2019**, 84, 973-982.